Engineering AAV-2 Targeting Vectors:

A New Insertion Site and

scFv Driven Vectors

vorgelegt von

Jorge Miguel Martins Bouças

aus Lissabon, Portugal

Köln, August 2008

Berichterstatter/in:

Prof. Dr. Manolis Pasparakis

Prof. Dr. Herbert Pfister

PD Dr. Hildegard Büning

Tag der mündlichen Prüfung: 28. Oktober 2008

Eidesstattliche Erklaerung

Ich versichere, daß ich die von mir vorgelegte Dissertation selbständig angefertigt, die benutzen Quellen und Hilfsmittel vollständig angegeben und die Stellen der Arbeit – schließlich Tabellen, Karten und Abbildungen -, die anderen Werken in Wortlaut oder dem Sinn nach entnommen sind, in jedem Einzelfall als Entlehnung kenntlich gemacht habe; daß diese Dissertation noch keiner anderen Fakultät oder Universität zur Prüfung vorgelegen hat; daß sie – abgesehen von unten angegebenen Teilpublikationen – noch nicht veröffentlicht worden ist sowie, daß ich eine solche Veröffentlichung vor Abschluß des Promotionsverfahrens nicht vornehmen werde. Die Bestimmungen dieser Promotionsordnung sind mir bekannt.

Köln, 19. August 2008   Jorge Miguel Martins Bouças

I thank PD Dr. Hildegard Büning for accepting me in her group, for constant and valuable scientific advice and for personal support during these years.

I would like to thank Prof. Dr. Michael Hallek for opening me the doors to the group of PD Dr. Büning and creating the opportunity that led to the realization of this work.

Also, I thank Prof. Manolis Pasparakis for supporting my thesis.

All this work would have not been as successful and exciting without the collaboration of all my friends and colleagues of the Büning group and of the University of Cologne.

A especial thank goes to Prof. Dr. Hinrich Abken, Prof. Dr. Dagma Moersdorf, Prof. Dr. Ulrike Protzer, Dr. Andreas Hombach, Dr. Sibille Quadt-Humme, Dr. David Kofler, Dr. Luca Perabo, Dr. Kerstin Lux, Dr. Marianna Hössel, Dr. Caro Kopecky, Dr. Venkateswara Rao Simhadri, Dr. Marcus Chmielewski, Dr. Natascha Schuhmann, Stefanie Stahnke, Hanna Janicki, Stefan Maersch, Anke Huber, Silke Uhrig, Tobias Riet, Heike Köhler, Martin Zuther and Patrick Schmidt for stimulating discussions and practical help.

I thank all those that so kindly received me in Cologne with open arms.

Finally I thank my mother and my cousins for continuous support over a life span. I thank to all those that during the last decade treated me as brother and especially to who, without any obligation, treated me as a son.

I especially thank Mareike for the extraordinary help, understanding and patience, along the years involving this work.

Die vorliegende Arbeit wurde in der Zeit von August 2005 bis August 2008 an der Klinik I für Innere Medizin der Medizinische Fakultät der Universität zu Köln unter der Anleitung von PD Dr. Hildegard Büning verfasst.

Im Verlaufe dieser Arbeit wurden folgende Veröffentlichungen angefertigt:

Perabo L. Goldnau D., White K., Endell J., **Boucas J.**, Humme S., Work L.M., Janicki H., Hallek M., Backer A.H. and Buning H. (2006). Heparan sulfate proteoglycan binding properties of adeno-associated virus retargeting mutants and consequences for their in vivo tropism. *J Virol* 80(14), 7265-9.

PCT/EP2008/004368; Buning H., Lux K., Nieland J., **Boucas J.**, Ritter M., Hoerer M., (2008) Mutated structural protein of a parvovirus. World Intellectual Property Organization

Perabo L., **Boucas J.**, Coutelle O., Hallek M. and Buning H. 2008. Engineering of viral capsids to evade the host immune system. *In* R. Herzog (ed.), Immunology of Gene Therapy. John Wiley & Sons. *In press.*

Boucas J., Lux K., Huber A., Schievenbusch S., Perabo L., Quadt-Humme S., Odenthal M., Hallek M., Buning H. (2008). Engineering AAV-2 based targeting vectors using a new insertion site – 453 – and single point mutations. *J Gene Med, under review.*

Boucas J., Hombach A., Hallek M., Abken H. and Buning H. (2008). Construction of scFv-VP2 directed AAV-2 vectors. *Manuscript in preparation.*

During all those years of experimentation and research, I never once made a discovery. All my work was deductive, and the results I achieved were those of invention, pure and simple.

Thomas Edison

To my mother

Zusammenfassung

Die Gentherapie ist eine alternative Strategie zur Behandlung von Gendefekten und malignen Erkrankungen, die als therapeutisches Agens eine Nukleinsäure verwendet. Essentiell für den Erfolg vieler gentherapeutischer Ansätze ist ein effizienter und Zell-spezifischer Gentransfer. Hierzu werden Zell-spezifische Vektoren, sogenannte *Targeting*-Vektoren, benötigt.

Für das in dieser Arbeit verwendete Vektorsystem, das auf dem nicht-pathogenen Serotyp 2 des Adeno-Assoziierten Virus (AAV-2) beruht, wird bevorzugt das direkte oder genetische *targeting* verwendet. Hierbei werden Peptidliganden in das AAV-Kapsid eingefügt, die dann die Interaktion mit dem gewünschten zellulären Rezeptor vermitteln. Als besonders geeignete für die Insertion und Präsentation von Peptidliganden hat sich hierbei die Aminosäureposition 587 (sowie die benachbarte Position, 588) erwiesen. In Ermangelung einer 3D-Struktur wurde zu ihrer Identifizierung ein Sequenz-Alignment mit einem verwandten Parvovirus, dem Canine Parvovirus (CPV) von dem entsprechende Strukturinformationen vorlagen, durchgeführt.

In der vorliegenden Arbeit wurde zum ersten Mal die nun vorhandene 3D-Struktur des AAV-2-Kapsid verwendet, um eine neue Klasse von Insertionsmutanten zu generieren. *In silico*-Analysen ermöglichten die Identifizierung der Aminosäureposition 453 als eine mögliche Insertionsstelle, die aufgrund ihrer deutlich besser exponierten Lage eine effizientere Interaktion zwischen einem hier inserierten Liganden und seinem Rezeptor ermöglichen sollte. Dies wurde mit Hilfe des Modell-Liganden RGD4C (ACDC<u>RGD</u>CDFCA), der an $\alpha V\beta 3$ und $\alpha V\beta 5$ Integrine bindet, untersucht. Hierzu wurde der Modell-Ligand genetisch in die Kapsidposition 453, 587 oder in beide Positionen gleichzeitig eingefügt. Da eine Insertion in Aminosäureposition 453 – im Gegensatz zu einer Insertion in 587 - nicht mit der Bindung des AAV-2-Kapsid an seinen Primärrezeptor Heparansulfatproteoglykan (HSPG) interferiert, wurde parallel ein zweiter Mutantensatz generiert, bei dem die Insertionsmutanten zusätzlich zwei Aminosäuresubstitutionen (R585A und R588A) enthielten. Diese Aminosäuresubstitutionen (A2) führen zum Verlust der Bindungsfähigkeit des Kapsids an HSPG.

Alle Mutanten konnten effizient hergestellt werden und waren mit Ausnahme der Doppelinsertionsmutanten zur effizienten Transduktion von HeLa-Zellen

(permissiv für AAV2) befähigt. Interessanterweise scheint die „Unfähigkeit" zur Transduktion, die für die Doppelinsertionsmutanten beobachtet werden konnte, nicht in einer „Unfähigkeit" zur Zell- oder Rezeptorbindung begründet zu sein, da sowohl eine Zellbindung als auch die Rezeptorbindung nachgewiesen werden konnte. In einem im Rahmen dieser Arbeit entwickelten ELISA konnte gezeigt werden, dass alle Insertionsmutanten die Fähigkeit zur Bindung des Zielrezeptors aufweisen. Interessanterweise, zeigten alle Mutanten, die zusätzlich zur Insertion die A2-Mutation trugen, eine deutlich effizientere Rezeptorbindung als die „reinen" Insertionsmutanten. Die effizienteste Mutante war r-RGD4C-453-A2 mit Peptidinsertion in der „neuen" Insertionsstelle und zusätzlicher A2-Mutation. Diese Mutante war zudem deutlich effizienter als rAAV-2 (mit unmodifiziertem Kapsid) und als die übrigen Mutanten in der Transduktion der HSPG-defizienten Zelllinie CHO psA-745. Kompetitionsexperimente mit löslichen Peptiden sowie mit Heparin (lösliches Analogon des HSPG) auf verschiedenen Zelllinien sowie auf primären HUVEC (Human Umbilical Vein Endothelial cells) zeigten, dass der inserierte Ligand die Zelltransduktion vermittelt, wenn die natürliche (HSPG-) Rezeptorbindung verhindert wird. Die in Maus durchgeführte Bioverteilungsstudie machte deutlich, dass – nach Eliminierung der HSPG-Bindung – die Bioverteilung von Targetingvektoren, die eine Insertion in Position 453 oder 587 tragen, allein vom inserierten Liganden bestimmt wird.

Die Insertion eines alternativen Peptids (NGRI) in 453 führte zur Generierung des AAV-Targetingvektors r-NGRI-453, mit dem HeLa-Zellen effizienter transduziert werden konnten als durch rAAV-2. Mit diesem Peptid konnten zudem infektiöse Doppelinsertionsmutanten hergestellt werden. Ein Peptid, dass durch AAV *Peptide display* für die Position 587 selektioniert worden war, konnte zwar erfolgreich in die Position 453 eingebaut werden; der entsprechende Vektor wies aber keine verbesserte Transduktionseffizienz auf. Zusätzlich wurde mit Hilfe der *NCBI Concerved domain database* zu 453 im AAV-2 Kapsid homologe Positionen in anderen Parvoviren identifiziert, um die Anwendungsmöglichkeiten der in dieser Arbeit identifizierten und optimierten Insertionsstelle zu erweitern.

Somit konnte in diesem Teil der Arbeit gezeigt werden, dass sich die Aminosäureposition 453 zur Insertion von Tropismus-modulierenden Peptidliganden eignet. Doppelinsertionsmutanten (Peptidliganden in Position 453 und 587) können ebenfalls generiert werden. Ihre Infektionsfähigkeit scheint jedoch peptidabhängig zu

sein. Ein weiterer interessanter Befund ist die deutliche Verbesserung der Rezeptorbindungsfähigkeit durch Kombination von RGD4C-Insertion und A2-Mutation. Dies stellt das erste Beispiel für die Bedeutung von Punktmutationen zur Optimierung von *Targeting*-Vektoren dar. Auf diesem Hintergrund wird die Wichtigkeit von evolutionären Ansätzen und *high throughput*-Selektionen für die Vektorentwicklung noch einmal deutlich. In diesen Ansätzen werden aus Bibliotheken von Kapsidmutanten für die jeweilige Anwendung optimierte Mutanten selektioniert.

Die sich mehrenden Berichte über die hohe Spezifität von Antikörperfragmente (*single-chain* Antikörper; scFv) motivierte das zweite Projekt dieser Arbeit. Da scFv aufgrund ihrer Größe ungeeignet für eine Insertion innerhalb von AAV-Kapsidproteinen z.B. an Position 453 oder 587 sind, wurde in dieser Arbeit der Versuch unternommen, Fusionsproteine zwischen scFv und dem N-Terminus von VP2 (zweitgrößtes AAV-Kapsidprotein) in das Kapsid von AAV einzubauen. Da wir vor kurzem zeigen konnten, dass Fusionsproteine aus GFP und VP2 in das Kapsid eingebaut werden, dass das GFP auf der Kapsidoberfläche exponiert wird, und dass GFP-markierte Viren infektiös sind, wurde zunächst ein Fusionsprotein aus anti-CD30 scFv-GFP-VP2 hergestellt. Diverse Optimierungen des Verpackungsprotokolls waren nötig, um anti-CD30 scFv-GFP-VP2 enthaltende Vektorpartikel zu generieren. Diese Mutanten konnten HeLa-Zellen transduzieren und interagierten mit einem anti-idiotypischen Antikörper. Es konnte jedoch keine spezifische Transduktion von CD30-positiven Zellen nachgewiesen werden. Außerdem konnte weder nach einer noch nach vierstündiger Inkubation der Zellen mit Vektorlösung Vektor-DNA in oder an Zellen nachgewiesen werden. Weder die Eliminierung des GFP-Anteils noch das Einbringen von *linker*-Sequenzen führte zu einer Verbesserung der Bindungs- oder Transduktionseffizienz. Der Austausch des anti-CD30 scFv gegen ein anti-CEA scFv und ein anti-CA19 scFv führte zu denselben Ergebnissen, woraus geschlossen werden kann, dass die mit anti-CD30 scFV erhaltenen Ergebnisse nicht spezifisch für den anti-CD30 scFv sind.

Vergleicht man Studien, die vollständige Immunglobuline verwenden, mit dieser Studie, so könnte die geringe Vektorpartikelkonzentration einen limitierten Faktoren darstellen. Zudem finden sich pro AAV-Kapsid nur 5 VP2-Proteine, d.h. es können maximal 5 VP2-Fusionsproteine eingebaut werden. Dies ist deutlich weniger als bei *Targeting*-Vektoren, die einen Ligand z.B. in Position 453 inseriert enthalten.

Hier wird der Ligand in alle 60 Kapsidproteinen eingebaut und steht so deutlich häufiger für eine Rezeptorbindung zur Verfügung.

Trotzdem darf festgehalten werden, dass durch die hier durchgeführte Arbeit, das bisher größte Fusionsprotein (~ 127 kDa) in das AAV-Kapsid eingebaut werden konnte. Diese Tatsache zusammen mit der Beobachtung, dass sich sowohl das GFP als auch der anti-CD30 scFv auf der Kapsidoberfläche befinden, eröffnet viele neue Möglichkeiten der Anwendung. So könnte AAV-2 gleichzeitig als Proteincarrier (Fusion mit dem N-Terminus) und als Gencarrier (Transgen) fungieren.

Summary

Gene therapy can be defined as the introduction of nucleic acids into cells with the purpose of altering the course of a medical condition or disease. In many clinical settings, efficient and successful gene therapy relies on the delivery of genes to specific cells in the human body. Such specific delivery can only be achieved through the design of vehicles/vectors that are able to recognize the target cell – targeting.

Adeno-associated virus type 2, a non-pathogenic human virus, has received an increased amount of attention as a vector for gene therapy since it was first cloned into a bacterial plasmid in 1982. Although the first attempt to construct an AAV-2 targeting vector made use of a single chain antibody fragment, it was the insertion of small peptide ligands into the AAV-2 capsid that marked the beginning of AAV-2 vector targeting. Sequence alignment of AAV-2 with CPV led to the discovery of amino acid position 587. Several reports have shown that small peptide ligands, once inserted in this position, are able to mediate transduction of the respective target cells, and that target specificity is retained *in vivo*.

In this work, the available three dimensional structure of AAV-2 is used for the first time for the rational design and construction of targeting vectors. *In silico* analysis revealed that insertions at position 453 should result in a better exposure of the inserted peptides and, as a consequence, in a more efficient interaction with the target receptor. The RGD4C peptide – a ligand for $\alpha V \beta 5$ and $\alpha V \beta 3$ integrins – was inserted in position 453 and/or 587. Moreover, loss of AAV-2 wild-type (wt) tropism was achieved by R585A and R588A – A2 – mutations that abolish binding to the primary receptor – heparan sulfate proteoglycan, HSPG.

All mutants were able to efficiently package and, with the exception of the double RGD4C mutants, to transduce HeLa cells. Interestingly double insertion mutants – r-RGD4C-453&587 and r-RGD4C-453&587-A2 – were able to efficiently bind to cells. Cell free based assays, involving targeting vectors and one target receptor revealed that all insertion mutants were able to bind the target receptor. Surprisingly, addition of A2 mutations to targeting vectors resulted in an increased amount of bound receptors. A mutant containing RGD4C at 453 and A2 mutations – r-RGD4C-453-A2 – emerged as the most efficient mutant. This mutant was also the most efficient vector for the transduction of an HSPG ko cell line – CHO pgsA-745.

Competition studies with soluble peptides verified specificity of transduction in this and other cell lines, as well as in primary Human Umbilical Vein Endothelial Cells – HUVEC, which often serve as a model for tumor endothelial cells. *In vivo* biodistribution studies revealed that, once HSPG binding is abolished, vector distribution is determined by the inserted peptide, independent of the insertion position and independent of the modification that led to elimination of the wt tropism.

Insertion of the NGRI peptide in position 453 – r-NGRI-453 – resulted in a vector that was more efficient than wt AAV-2 in the transduction of HeLa cells. Furthermore, double insertion mutants remained infectious. Insertion of an N587 display library selected peptide in position 453 was not detrimental but did not result in a vector with improved transduction efficiencies. NCBI's Conserved Domain Database was used to identify 453 homologues in other vector systems.

In summary, 453 emerged as a suitable position for the insertion of targeting peptides in AAV-2 and other vector systems. Double insertion mutants will have to be analyzed for each specific case. The increased targeting efficiency after single point mutations of residues linearly distant from the inserted peptide shows for the first time how such mutations can indeed be relevant for the design of targeting mutants. Moreover, high-throughput selection protocols emerge as master tools and should be put into practice for the identification of similar mutants and for the optimization of targeting vectors.

The rising number of reports on the high efficiency of antibody fragments for the construction of targeting molecules motivated the fusion of single chain antibody (scFv) fragments to the capsid of AAV-2. Being most likely too large for insertions in non-terminal positions like 453 or 587, we decided to genetically fuse a scFv to the N-terminus of a viral protein - VP. Furthermore, vectors containing a GFP-VP2 fusion protein have previously been shown to be useful tools for infectious biology studies. Our analysis of this GFP labeled vectors revealed that at least a part of the GFP molecule is present on the outer surface of the capsid. These observations led to generation of an anti-CD30 scFv fused to the N-terminus of a GFP molecule that was fused to the N-terminus of VP2.

Optimization of the packaging procedure, by increasing the amount of the fusion protein encoding plasmid, resulted in an efficient packaging of scFv-AAV-2 mutants. Mutants were able to effectively transduce HeLa cells and to bind an anti-idiotypic antibody homologue to the recognized antigen epitope. Despite this,

targeting mutants were not able to specifically transduce CD30 positive cells. Furthermore it was not possible to detect vector DNA with target cells neither 1 nor 4 hours post-transduction. Engineering similar constructs without the GFP molecule and with or without linker sequences did not result in an improved binding or transduction efficiencies. Substitution of the anti-CD30 scFv by an anti-CEA scFv or an anti-CA19 scFv revealed that the results observed with the anti-CD30 scFV targeting mutants were not idiotype specific. When compared to studies made with whole immunoglobulins, the low vector particle concentration emerges as one of the limiting steps to the application of such targeting approaches. Moreover, while each capsid possesses sixty repeats of G453, only five VP2 proteins exist per capsid. Despite this, the scFv-GFP-VP2 fusion represents the largest fusion (~127 kDa in total) ever assembled in an AAV capsid. This, together with the fact that both GFP and anti-CD30 scFv molecules could be recognized by respective antibodies reinforces the idea that the N-terminus of VP2 can indeed be displayed on the outer surface of the capsid. Our results open the door to many other therapeutic designs where the vector can be used as a carrier for genes and at the same time for high molecular weight proteins assembled in pentavalent forms.

1. Introduction

1.1. Gene therapy

Genes, which are carried on chromosomes, are the basic physical and functional units of heredity. Genes are specific sequences of bases that encode instructions on how to make proteins. Although genes get a lot of attention, it's the proteins that perform most life functions and even make up the majority of cellular structures. When genes are altered so that the encoded proteins are unable to carry out their normal functions, genetic disorders can result.

The application of recombinant DNA technology and gene cloning (which started in the 1980s) and the resulting increase in genomics data during the 1990s have contributed to define some disease-causing genetic factors and to explore the potential of new therapies based on engineered genes and cells (161, 190)

Gene therapy can be defined as the introduction of nucleic acids into cells for the purpose of altering the course of a medical condition or disease. In general with some exceptions, the nucleic acids are DNA molecules encoding gene products or proteins. The original ideas were directed toward treating monogenic (single-gene) disorders, but it has become clear that the gene can be considered a new pharmaceutical agent for treating many types of diseases (96).

Gene therapy is a complex process, involving multiple steps in the human body (delivery to organs, tissue targeting, cellular tracking, regulation of gene expression level and duration, biological activity of therapeutic protein, safety of the vehicle and gene product, to name just a few) most of which are not completely understood.

1.1.1. Types and methods

Gene therapy approaches can be divided into two types: germ line therapy and somatic therapy. In the first type, a gene is inserted into the DNA of the germline cells (egg or sperm) so that the offspring of the patient will have the inserted gene. This more recent approach, theoretically, should be highly effective in counteracting genetic disorders. Somatic gene therapy involves the manipulation of gene expression

11

in cells that will be corrective to the patient but not inherited by the next generation (somatic cells include all the non-reproductive cells in the human body).

For the correction of faulty genes four different approaches are normally used: a) a normal gene may be inserted into a nonspecific location within the genome to replace a nonfunctional gene; b) an abnormal gene can be swapped for a normal gene through homologous recombination; c) the abnormal gene can be repaired through selective reverse mutation, which returns the gene to its normal function; d) the regulation (the degree to which a gene is turned on or off) of a particular gene could be altered.

Transfer of the genetic material can be achieved either *ex vivo* or *in vivo*. In the first case the patient cells are harvested and cultivated in the laboratory. After incubation with carrier molecules containing a corrective or therapeutic gene the cells with the new genetic information are then harvested and transplanted into the patient. Although normally less feasible for wide-scale application due to its complexity, this method is quite attractive due to the improved safety gained by the possibility to separate target from non-target cells. In most cases though, efficient therapy requires direct *in vivo* administration of the vehicle. Although, *in situ* administration may help avoiding the transfer of genetic material to non-target cells, the carrier molecule needs in this case to discriminate between target and non-target cells. Thus, carrier molecules are one of the masterpieces of most gene therapy designs.

1.1.2. Vectors

A carrier molecule called a vector must be used to deliver the therapeutic gene to the patient's target cells. There are two major classes of vectors: viral vectors and non-viral vectors.

Some researchers believe that viral vectors will be most successful because viruses have evolved for millions of years to become efficient vesicles for transferring genetic material into cells, whereas others believe that some of the side effects of such viral vectors and possible previous exposures to the respective viruses rendering the host resistant to transduction (gene transfer into the cell) will preclude their long-term use in gene therapy.

There is no "perfect vector" that can treat every disorder. Like any type of medical treatment, a gene therapy vector must be customized to address the unique

features of the disorder. Furthermore, interpatient variations can not be forgotten and must be taken into account. For such reasons, a wide variety of vectors have been used in clinical trials worldwide (Figure 1).

Adenovirus (24.80%)
Retrovirus (22.30%)
Naked/Plasmid DNA (17.80%)
Lipofection (7.40%)
Vaccinia virus (6.40%)
Poxvirus (6.40%)
Adeno-associated virus (3.90%)
Herpes simplex virus (3.10%)
RNA transfer (1.40%)
Other categories (3.20%)
Unknown (3.00%)
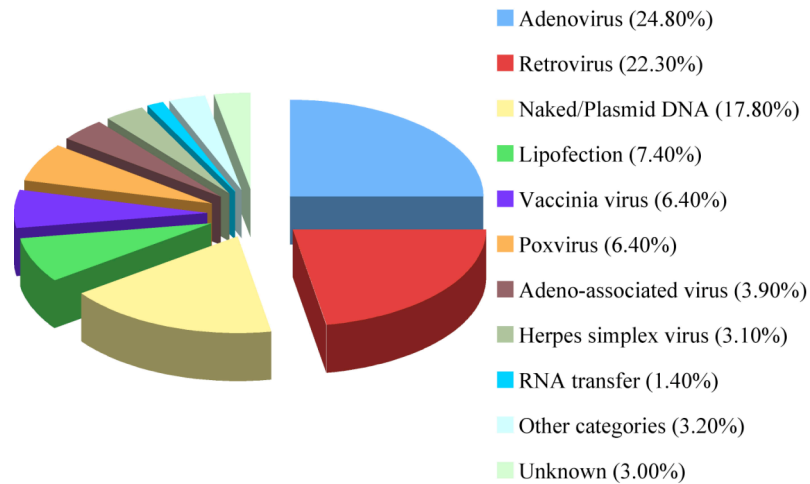
Figure 1. Vectors used in gene therapy clinical trials worldwide. Includes data relative to 1,347 of approved, ongoing or completed clinical trials worldwide. As of March 2008. (1)

1.1.3. State-of-the-art and present goals

Gene therapy is not a new idea. In 1963, Joshua Lederberg (1925-2008) wrote: "We might anticipate the… interchange of chromosomes and segments. The ultimate application of molecular biology would be the direct control of nucleotide sequences in human chromosomes, coupled with recognition, selection and integration of the desired genes…It will only be a matter of time… before polynucleotide sequences can be grafted by chemical procedures onto a virus DNA." Less than 30 years later, the first clinical study using gene transfer was reported (31).

The disease states that have been approached with gene therapy are now widely diverse, including autossomal dominant disorders, many forms of cancer, HIV, and other infectious diseases, inflammatory conditions, and intractable pain (Figure 2). In most instances, the nature of the disease may dictate the vector to be used, since it may involve a specific cell type, expression level, and duration of expression that will be required for therapeutic effect. In general, genetic diseases will require long-lasting gene expression, and so may indicate the use of a gammaretrovirus, lentivirus, or AAV vector; while a tumor vaccine or cytotoxic gene approach to cancer may

require a short burst of gene expression, such as might be produced by an adeno or non viral vector.

Cancer diseases (66.5%)

Cardiovascular diseases (9.0%)

Monogenic diseases (8.2%)

Infectious diseases (6.6%)

Neurological diseases (1.3%)

Ocular diseases (0.9%)

Other diseases (1.9%)

Gene marking (3.8%)

Healthy volunteers (1.9%)
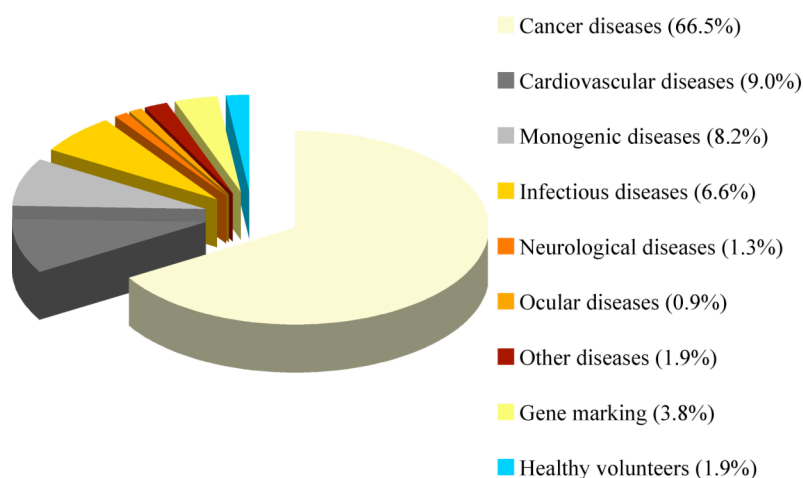
Figure 2. Diseases addressed by gene therapy clinical trials. Includes data relative to 1,347 of approved, ongoing or completed clinical trials worldwide. As of March 2008. (1)

For a disease to be a good candidate for gene therapy, the role of the therapeutic gene in disease pathophysiology must be clearly understood. It seems likely that in future, more gene therapy targets will be identified, primarily as a result of the rapid ability to identify specific gene associations with human diseases, particularly after the completion of the Human Genome Project. This includes both single gene diseases, and, multifactorial diseases in which complex networks of gene and environmental effects are elucidated, and key genetic determinants of disease are identified within those pathways. The future remains uncertain regarding the ultimate clinical impact that gene therapy will have in each of those very distinct fields.

Indeed, clinical progress has been slow. After the first clinical trial in 1990 using a gammaretroviral vector a major setback occurred in September 1999 when a widely publicized death resulting from a gene therapy trial was reported (19, 155). The resulting investigation concluded that the patient died from a massive immune reaction against the used Adenovirus type 5 vector. Fortunately, less than 1 year after a successful trail was published. Two children suffering from a severe combined immunodeficiency disorder (SCID-XI), which had restricted them to life in an isolated environment, were able to leave the hospital and resume normal lives after ex-vivo transduction of their lymphocytes with a gammaretrovirus vector (26). Out of the approximately 18 patients that were treated with the same type of vector 5

developed leukemia (50, 52). While in 4 of these patients the complications resulted from vector integration in a nonrandom manner near the LM02 gene, in the 5th patient unphysiologic expression of the IL2RG transgene is suspected to contribute to the development of the complications (50). Although chemotherapy already led to sustained remission in 3 of the patients with T cell leukemia, it failed in one (70). A clinical trial to correct a clotting disorder, Factor IX deficiency, by hepatic gene transfer using an AAV vector recently showed that transient correction was possible but quite limited in time because of subsequent immune reaction (116). In the end of 2007, 3 patients having an inherited blind disease with onset during childhood underwent subretinal delivery of an AAV vector. Each patient had a modest improvement in measures of retinal function on subjective tests of visual acuity (114). Recently, a clinical setting for the treatment of ADA-SCID using a gammaretrovirus – GIADA1MLV retroviral vector – showed that *ADA* gene transfer is an efficacious treatment for ADA-SCID (25).

The development of versatile vectors with defined and controlled functions is without any doubt one of the present major goals in the field. Indeed, while the natural target cell of one vector might make it the best candidate for the designed therapy, the lack (or not) of integration capacity might make it inadequate. The low amount of vector preparations utilized in most trials linked to the small number of subjects involved in average in each gene therapy clinical trial reveals how important basic aspects like production are still to be optimized (121). Development of massive production and high purification methods that result in stock solutions with high titers and purity is indeed part of the present goals. A lot has been made in the vector field during the last 18 years. Transferring the knowledge obtained with one vector system to another as shown efficient results but many lessons are still to be learned. Furthermore, the lack of more multifunctional groups working each one with a wider variety of systems and the need for more work to be done *in vivo* and *ex vivo* using adequate animal models has created a dependency on other areas of research that made the field develop in short steps.

Despite the early high expectations and the subsequent set-backs, one has to recognize that this new therapeutic modality is still in its infancy. It will neither deliver medical "miracles" (as its early prophets predicted) nor will it "disappear" because of a few disappointing cases (as some of its recent antagonists predict). As with all new technologies, gene therapy has to run its course in its present

"development phase" before it reaches "maturation", when its full potential will be exploited. This in turn will offer significant opportunities to effectively target the causative factors for several disabling diseases afflicting mankind.

1.2. Adeno-associated virus

Adeno-associated virus (AAV) was discovered in 1965 when different groups described small, uniformly formed, virus like particles which were noticed during electron microscopical examination of simian adenovirus type 15 (SV15) (7). These particles were 18-20 nm in diameter and showed an icosahedral symmetry (119). Staining with acridin orange demonstrated that these particles contained DNA, which contributed to the suggestion that those particles were viruses. The particles replicated only in cells that were coinfected with adenovirus. The authors named the particles adeno-associated virus (7).

Today, AAV has been classified as a member of the *Parvoviridae*. With a diameter of only 18 to 30 nm the *Parvoviridae* are among the smallest known viruses (latin: *parvum* = small). Viruses of this family contain a single-stranded DNA genome of approximately 5 kb and a non-enveloped icosahedral capsid. The family of *Parvoviridae* contains two subfamilies: the *Densovirinae* which infects invertebrates and the *Parvovirinae* which is specific for vertebrates. The subfamily *Parvovirinae* includes the genera Parvovirus, Erythrovirus and Dependovirus. Adeno-associated viruses belong to the Dependovirus genus. Parvovirus B19 is the only human pathogen within the *Parvoviridae* (Erythrovirus genus) and causes Erythema infectiosum, hydrops fetalis and abortion (23, 185). All other representatives of this family, including AAV, are not pathogenic for humans (17). On the contrary, AAV seems to be protective against bovine papillomavirus and adenovirus mediated cellular transformation (34, 82, 98, 118) and to have cytotoxic effects in malignant cells (154).

In contrast to the Parvovirus and Erythrovirus genus, which are autonomous *Parvoviridae*, AAV replication, and thus a productive infectious life cycle, depends on co-infection with unrelated helper viruses e.g. adenovirus (Ad), herpesvirus (HSV), human cytomegalovirus (HCMV), or papillomavirus (16, 129). In the absence

of a helper virus AAV establishes a latent form of infection by stably integrating its genome into the host cell genome. Helper viruses can be partially replaced by chemical or physical carcinogens (80, 204-206). This leads to the conclusion that helper viruses induce specific changes in the host cell and thereby providing competence for AAV replication.

Until now, 12 serotypes which share different levels of sequence homology, have been identified (56, 58, 126). AAV-1 to -4 and -6 have been detected as contaminants of adenoviral preparations. AAV-5 was isolated from penile condylomata lata (human wart) (11), AAV-6 seems to be a recombination between AAV-1 and -2 (199). AAV-9 was isolated from human tissues (56). AAV-7 and AAV-8 have been detected in Rhesus monkey, AAV-10 and AAV-11 in Cynomolgus monkey (58, 126). Sera epidemical studies suggest that AAV-2, AAV-3 and AAV-5 are epidemic in humans, whereas AAV-4, -7-11 are endemic in nonhuman primates (58). The natural occurrence of AAV-1, -6 and -12 is not known.

Although the other serotypes have attracted increasing attention during recent years, AAV-2 is still the best characterized serotype, being the first isolated and cloned.

1.2.1. Genomic organization of AAV

Wild type AAV-2 contains a single stranded DNA genome of 4679 nucleotides (178). The genome can be divided into three functional subunits. These are the two open reading frames (ORF) *rep* and *cap* flanked by the inverted terminal repeats (ITR) (24). It contains three promoters (p5, p19 and p40) and a common polyadenylation signal (Figure 3). The 5'-ORF *rep* encodes four Rep proteins, a family of multifunctional, nonstructural proteins. The different Rep proteins are named upon their molecular weight: Rep78, Rep68, Rep52 and Rep40. The larger Rep proteins are controlled from the p5, the smaller Rep proteins from the p19 promoter (112). Splicing of a common intron leads to Rep68, a splice variant from Rep78, and Rep40 from Rep52. The larger Rep proteins are important for site specific integration, control of replication and transcription (27, 142-144). The smaller Rep proteins seem to be involved in accumulation and packaging of single-stranded DNA into the preformed capsid (45, 100). The Rep proteins can act as transactivators of

transcription in the presence of helper virus functions and as repressors of the three viral promoters in absence of a helper virus (106, 142).
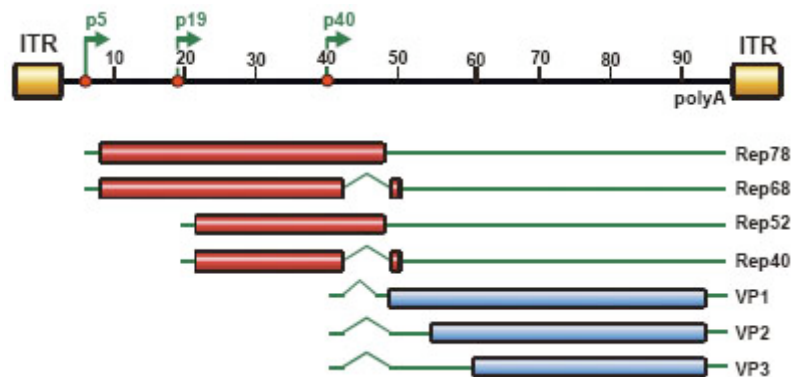
Figure 3. Organization of the AAV genome. The AAV genome encompasses 4680 nucleotides, divided into 100 map units. Indicated are the two inverted terminal repeats (ITRs), the three viral promoters at map position 5, 19, and 40 (p5, p19, and p40) and the polyadenylation signal at map position 96 (poly A). The open reading frames are represented by rectangles, untranslated regions by solid lines and the introns by nicks intercepting the solid lines. Large Rep proteins (Rep78 and Rep68) controlled by the p5 promoter and small Rep proteins (Rep52 and Rep40) driven by the p19 promoter exist in spliced and unspliced variants (Rep68 as a splice variant of Rep78; Rep40 as a splice variant of Rep52). The *cap* genes encoding the three different capsid proteins VP1, VP2, and VP3 are controlled by the p40 promoter. Figure kindly provided by Dr. N. Huttner.

The 3'-ORF *cap* encodes the three capsid proteins VP1, VP2 and VP3, which form the 60 subunits of the viral capsid in a 1:1:10 ratio (105). All three capsid proteins are controlled by the p40 promoter and use the same stop codon. VP2 and VP3 are N-terminal truncated variants of VP1. Synthesis of VP1 is regulated by alternative splicing whereas VP2 is initiated from an unusual translation initiation codon (ACG) (14, 15). The molecular weight of VP1, VP2 and VP3 is 90 kDa, 72 kDa and 60 kDa, respectively. VP3 alone is sufficient for capsid formation, but VP1 is required for viral infection (189). At least *ex vivo* VP2 seems not essential for capsids formation and infectivity (113, 189). Capsid assembly takes place inside the nucleus (193, 194).

The 145 bp long ITRs form hairpins of a T-shaped structure which contains Rep binding sites (RBS) and a terminal resolution site (TRS) which is a specific cleavage site for Rep proteins (90, 120, 176). They serve as origin of replication, are important for site-specific integration and rescue of the provirus from the human chromosome 19 (107, 122, 164).

1.2.2. Infectious biology of AAV

1.2.2.1. Virus cell contact

Of all the serotypes, AAV-2's infectious biology is the best characterized. However, a detailed understanding of intracellular trafficking, endosomal release and viral uncoating is still missing. Moreover, most experiments were performed within the same cell line, the human cervix carcinoma cell line HeLa. The current model of the infection process is depicted in Figure 4.
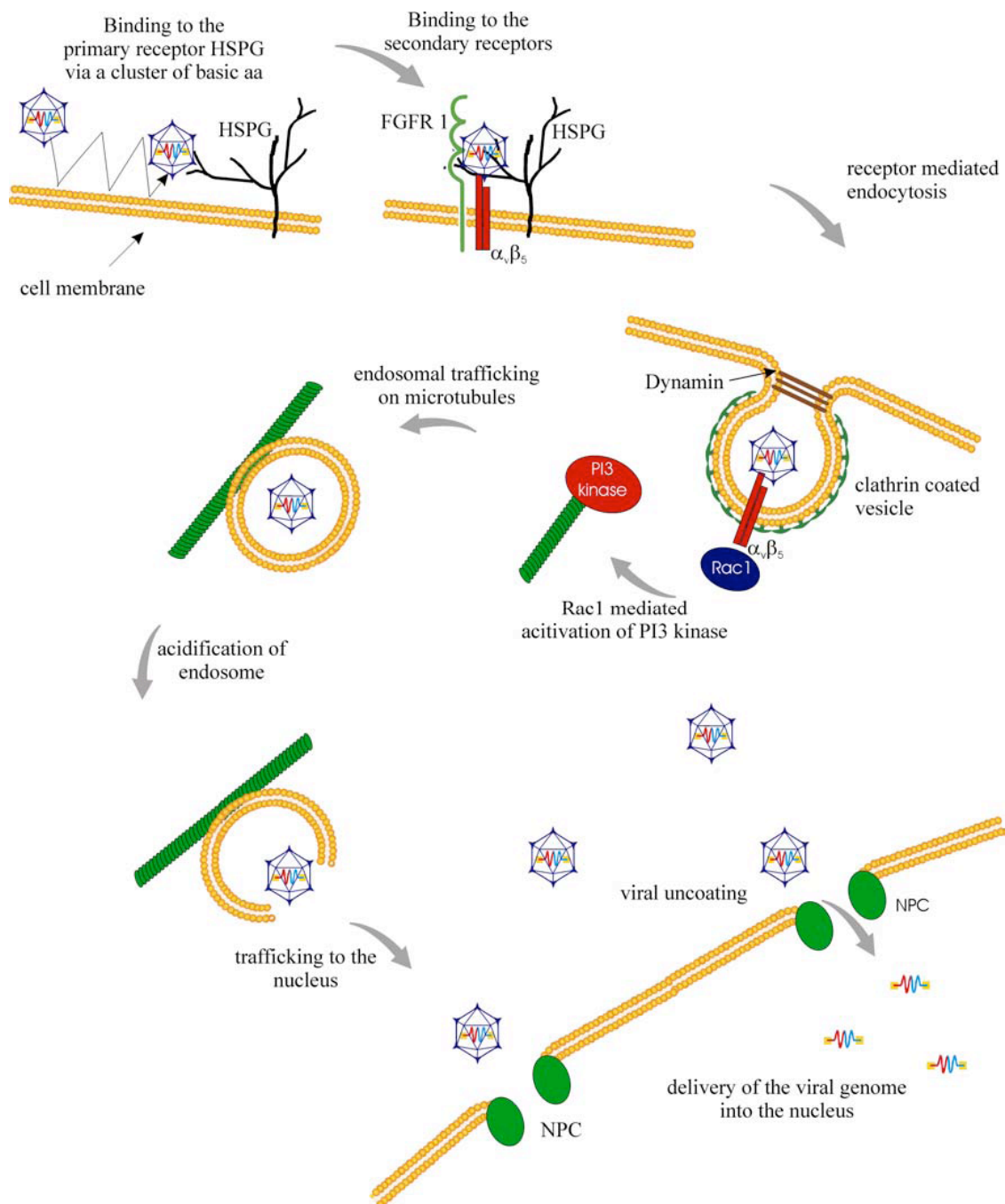
Figure 4. The AAV infection pathway. AAV touches the membrane several times before entering the cell. Attachment to its primary receptor HSPG and co-receptors such as FGFR and αvβ5 integrin is triggering a receptor-mediated endocytosis in a dynamin dependent manner into clathrin coated pits. This internalization is facilitated by the activity of Rac1. Activation of Rac1 subsequently stimulates PI3K pathways which regulate endosome trafficking along the cytoskeleton. The exact mechanism of endosomal release is not clear yet. Viral uncoating takes place before or during nuclear entry. Viral DNA enters the nucleus by an unknown mechanism. (Figure modified from Büning et al. 2003.)

Single Virus Tracing (SVT) studies characterized the motion of AAV-2 outside the cell as normal diffusion with a diffusion coefficient of $D = 7.5 \; \mu m^2/s$. In this studies AAV-2s' diffusion decelerated as it approached the cell membrane, and finally stopped when AAV got in contact with the cell membrane with a mean touching time of 62 ms. Most virions showed multiple contacts to the cell before entering or being finally released from the cell membrane. In average 4.4 repetitive touching events are observed. It is not clear whether these multiple touching events represent a binding and release process to viral receptors or adsorption to cellular structures (170).

Heparan sulfate proteoglycan (HSPG) has been identified as the primary receptor of AAV-2 (182). HSPG binding residues are located within the VP3 region (which is common to all capsid proteins). 5 amino acids have been identified to be involved in HSPG binding: R484, R487, K532, R585 and R588. Mutational analysis showed that especially R585 and R588 are essential for the interaction with HSPG (97, 135, 198). Even though HSPG has been described as AAV-2's attachment receptor, it was shown that AAV-2 is able to enter some cells in the absence of HSPG (21). It was proposed that HSPG is also the primary receptor for AAV-3 whereas a 2,3-O- and 2,3-N-linked sialic acid was identified as the attachment receptor for AAV-4 and -5, respectively (76, 92, 153). For AAV-6 the situation is quite complex. Seiler and colleagues observed that the use of sialic acid as attachment receptor for AAV-6 is dependent on cell type and cell differentiation status (169). Moreover, although AAV-6 can bind to heparin, it does not interfere with viral infection when applied together with virus onto the cell (74). The 37/67-kDa lamin receptor (LamR) was recently described as receptor or AAV-8. AAV-1 does not appear to utilize heparan sulfate, sialic acid or LamR and its receptor remains unknown (152). The same holds true for AAV-7. However, since it closely resembles AAV-1, they may share a common receptor (152). Even less is known about potential (attachment) receptors for AAV-9 to -12 (56, 57, 126, 167).

In addition to the attachment receptor, secondary receptors are required for viral infection. Five coreceptors have been described for AAV-2 so far, human fibroblast growth factor receptor I (hFGFR I), αVβ5-integrin, α5β1-integrin, hepatocyte growth factor receptor (HGFR) and LamR (6, 95, 149, 152, 181). Human FGFR I was also shown to interact with AAV-3 (18). For hFGFR I a function in enhancing the interaction of virion and HSPG was proposed (149). The function of HGFR is not known yet. Since blocking of αVβ5-integrin with antibodies can prevent internalization of rAAV-2 into HeLa cells it was suggested that binding to αVβ5-integrin mediates endocytosis (165). α5β1-integrin is thought to be an alternative coreceptor to αVβ5 (6). For AAV-5 platelet derived growth factor receptor (PDGFR) was identified as coreceptor (38). PDGFR was also discussed to act alone as a receptor for AAV-5 because it is in itself a sialo-glycoprotein (33).

1.2.2.2. Receptor mediated endocytosis of AAV

The endocytotic process was studied for AAV-2 and 5. Following receptor binding AAV-2 enters the cell by a receptor mediated endocytosis through clathrin coated pits in a dynamin dependent manner (13, 43). Single Virus Tracing measurements showed an individual viral uptake within milliseconds. AAV-5 was also predominantly localized in clathrin coated vesicles. However, in rare situations, AAV-5 was found to be endocytosed in noncoated vesicles, representing probably caveolae (10). Similar to ligand-receptor interaction, it was shown that receptor binding of AAV-2 causes intracellular signal transduction. Binding to αVβ5 activates (in addition to mediate endocytosis) Rac1, a small GTP binding protein, stimulating thereby phosphoinositol-3 kinase (PI3K) which facilitates the rearrangement of microfilaments and microtubuli (165). Treatment of infected cells with nocodazole, which leads to depolymerization of microtubules, or with cytochalasin B, which disrupts microfilaments, reduces perinuclear accumulation of AAV-2 (165).

1.2.2.3. Endosomal processing of AAV

Intracellular trafficking and endosomal processing of the virion are further complex steps which are known to be important for efficient cell transduction. These processes seem to be the rate limiting step in many cell types. For example, AAV-2 is

endocytosed in polarized airway epithelial cells from the apical and the basolateral surface. Although the apical in contrast to the basolateral surface does not contain HSPG and $\alpha V\beta 5$ integrin, only a 3- to 5-fold reduction in endocytosis was detected. However, transduction of cells from the apical surface is reduced >200-fold, indicating that in addition "postendocytotic" barriers exist for AAV mediated gene transfer (44). It has been shown that several viruses can penetrate barrier cells (epithelia and endothelia) by transcytosis (20, 136, 195). This process is cell type and serotype specific. For AAV-5 it was shown that this transport pathway is distinct from transduction, cell type and serotype specific (37).

Studies evaluating subcellular distribution of AAV-2 following infection remain ambiguous and sometimes controversial. It was proposed that AAV-2 is released from the early endosome (200) or might traffic through late endosome compartments (42, 77). It was also shown that AAV-2 colocalizes with transferrin (43). Transferrin is known to be recycled through the perinuclear recycling endosome (PNRE) (158, 177). Therefore, it was suggested that this compartment might be involved in the processing of AAV. Recently a dose dependent trafficking was described, observing a predominant trafficking of AAV-2 to the late endosome at low multiplicities of infection (MOI, 100 genomes/cell) and trafficking of AAV-2 to the PNRE at high MOI (10^4 genomes/cell). In addition, dose-response curves showed that viral movement through the PNRE is more competent for transgene expression than movement through the late endosome (41). Furthermore, it was proposed that AAV-2 and -5 localize inside the golgi compartment (10, 137).

1.2.2.4. Endossomal escape of AAV

In addition, to the unsolved question when and where AAV escapes from the endosome, the mechanism of endosomal release is not known. Acidification inside the endosomes seems to be essential in priming AAV for nuclear entry. This assumption is based on the observation that microinjection of AAV-2 particles directly into the cytoplasm (instead of natural infection) did not result in gene expression (40). The same effect can be reached by the addition of inhibitors of acidification like bafilomycin A1 or ammonium chloride (13). It might be that this acidification leads to a conformational change inside the viral capsid. Interestingly, it has been shown that the N-terminal region of VP1 contains a domain that resembles a secretory

phospholipase A2 (sPLA2); a domain that was not known to exist in virus capsids (209). A mutation in the catalytic center of the PLA2 motif of AAV-2 causes a dramatic drop in infectivity (64). PLA2s catalyze the hydrolysis of phospholipid substrates at the 2-acyl ester (sn-2) position to release lysophospholipids and free fatty acids (9, 36, 104). This VP1 domain is located inside the AAV-2 capsid and was shown to be exposed after heat shock (105). This domain might be involved in endosomal escape or nuclear uptake.

1.2.2.5. Nuclear translocation of AAV

Viral translocation into the nucleus is, in contrast to endocytosis and trafficking to the perinuclear region, a slow and inefficient process. Perinuclear accumulation can be observed from 30 min p.i. on (13) and persist also many hours after gene expression has already started (200). Only very few information is available about the mechanism of nuclear import. Having a diameter of 25 nm AAV can potentially pass the nuclear pore complex (NPC). However, it is not clearly demonstrated whether AAV uses the NPC to enter the nucleus. It was shown that AAV interacts with nucleolin, a nuclear shuttle protein (150). Others have suggested a nuclear entry independent of the NPC (78). Inside the unique VP1 and VP2 regions nuclear localization sequence (NLS) are located which are important for capsid assembly (88) but it is not known whether this NLS has a function for an incoming virus. There are also controversial data about the compartment in which uncoating (release of the viral genome out of the capsid) takes place and whether an intact capsid or only the DNA is shuffled into the nucleus. Some groups detected viral capsids inside the nucleus (13, 165). Xiao and colleagues observed a significant difference in the efficiency of nuclear translocation of the viral capsid dependent on presence or absence of a helper virus (200). In the absence of adenovirus, only the viral genome seems to be transported into the nucleus, while in presence of adenovirus, a shuffling of intact viral capsids into the nucleus was observed. By Single Virus Tracing directed motion (reminding of microtubule dependent movements) of viral capsids inside the nuclear area was also observed. The authors suggested that those particles move along nuclear invaginations that are continous with the cytoplasm. Studies with nocodazole which inhibited such directed motions strengthened this hypothesis (170). Recent studies showed no efficient transport of

intact viral capsids, but of viral genomes into the nucleus independent of the presence of a helper virus. Data were generated by taking advantage of a new confocal microscopic software which allowed a more precise localization of signals within the z axis (113). With this method the authors also detected capsids within nuclear invaginations confirming the hypothesis made by SVT studies.

Another interesting aspect of AAV infection is the enhancement of transduction by proteasome inhibitors. This was shown for several serotypes in different cells (AAV-2 (44, 207), AAV-1-4 (72), AAV-5 (207)). An effect of proteasome inhibitors was also observed for AAV-2 *in vivo* in some organs from AAV treated mice: proteasome inhibitors augmented the transduction efficiency in lung from 0 to 10% and liver from 0.5 to 5% whereas inhibitors had no effect on transduction efficiency in muscle and heart muscle (44). Furthermore, it was shown that denaturated capsids of AAV-2 and AAV-5 are ubiquitinated in contrast to intact capsids which were no substrate for ubiquitination (44, 207). This suggests that only AAV capsids that passed the endosomal processing, and thereby underwent a conformational change, are accessible for ubiquitination (207).

1.2.2.6. Latent or lytic cycle

Upon nuclear entry, the presence or absence of a helper virus determines whether AAV enters a lytic or latent life cycle. In the absence of helper functions AAV enters a latent cycle which leads to integration of the viral genome into chromosome 19q13.4 (46). This locus is called AAVS1 (46, 103). Before viral integration, second strand synthesis and a basal expression of the Rep proteins are activated (22, 157). A complex of Rep78 and Rep68 was shown to bind to both, the Rep binding site (RBS) in the viral ITRs and to a homologous sequence in the AAVS1 locus, mediating thereby integration (109, 191).

After super infection with a helper virus, the integrated AAV enters the lytic cycle, leading to viral gene expression, rescue and replication of the AAV genome with subsequent production of viral progeny (17). In the presence of a helper virus during AAV infection, induction of gene expression and replication takes place directly.

1.2.3. Tissue distribution of AAV isolates

The isolation of new serotypes as well as the study of Gao and colleagues led to some important findings on molecular epidemiology of AAV in primate populations (57). This study included 479 non-human primate (NHP) tissues from 258 animals of 7 different species and 259 human tissues from 250 individuals. For NHP, an average of 19% of tissue samples screened were positive for AAV, among which lymph nodes, liver, spleen and heart were the tissues where AAV sequences were most frequently found. Gao and colleagues assumed that the high frequency of AAV detection in lymphoid tissue may implicate the importance of co-infection with helper viruses such as adenovirus which often reside in these tissues. Serological analysis of NHP (Rhesus macaques, Cynomolgus macaques, Japanese and Pig-tailed macaques, Chimpanzees and Baboons) revealed a clear prevalence for AAV-7 and AAV-8.

In the case of human tissue nearly the same frequency (18%) of integrated AAV sequences was detected among the analysed tissue. In contrast to the NHP study, AAV was not detected in lymph nodes and heart. However, this may be due to the limited amount of lymph node and heart samples. Tissues with a high frequency of integrated AAV sequences were bone marrow (39%), liver (33%), spleen (30%), small bowl (22%) and colon (15%). From their results, Gao and colleagues assumed that oral transmission is one of the common routes for AAV infection in humans.

1.2.4. Immune responses to AAV

AAV vectors have been shown to stably transduce many therapeutic targets *in vivo* in the absence of immunological sequelae (186). Yet, in a clinical trial of liver directed gene transfer this rule did not hold true (116). Parameters that determine these and similar occurrences have been proposed to be pre-existing immunity to AAV, the route of administration, the kinetics of expression, the dose, the vector serotype and its ability to transduce antigen-presenting cells (APCs) as well as host species and nature of the specific transgene product (186).

Gene transfer vectors in general and AAV in particular are theoretically capable of activating all arms of the host immune system. For AAV most of the focus has been on its interaction with the adaptive immune system on both human and cellular level. Previous studies on AAV mediated activation of innate immunity

provide an insight into one of its most important strengths as a gene therapy vector: its apparent minimal pro-inflammatory potential (210). AAV does not appear to engage pattern recognition receptors such as toll-like receptors (TLRs) known to initiate such responses (81). The pro-inflamatory context or 'signal zero' is known to determine the many parameters of the immunological outcome. If AAV indeed is ale to evade detection by innate immunity's sensors, the responses of the host should be quite blunted. However, further research is necessary to determine if this holds true.

In regard to a humoral immune response, it is of notice that approximately 80% of the human population has antibodies against the AAV-2 capsid. Furthermore, 18%-35% of the population has AAV-2 neutralizing antibodies. This is indeed, one of the hurdles for AAV-2 based gene transfer (131).

1.2.5. Production of recombinant AAV vectors

The structural properties of the AAV capsid allow the production of recombinant viral particles that carry an up to approximately 4.5 kb long DNA molecule flanked by ITR sequences (183). The production protocol takes advantage of the ability of the two viral genes (*rep* and *cap*) and of the ITR sequences to accomplish their role in the replication of the viral DNA and in the packaging of mature virions even when provided to the host cell in *trans* on exogenous plasmids (108, 163). Therefore, transduction in a permissive cell of two plasmid species, one encoding the two viral ORFs (rep/cap plasmid), and the other coding for an exogenous DNA sequence flanked by ITR sequences (vector plasmid), leads to the production of viral particles containing a DNA molecule coding for the exogenous sequence flanked by the ITRs (Figure 5). Given the absence of the packaging sequences on the rep-cap coding plasmid, no contamination of wt virus will be present in the final viral preparation. Another requirement of this procedure is the concomitant action of a helper factor for the replication of the viral genome. This can be provided by co-infecting the cells with adenovirus. In this case however, the resulting viral preparation will contain adenovirus progeny. Adenovirus free AAV preparations can be obtained by providing the helper function as a third plasmid that contains the essential Ad helper genes (E4, VA and E2a) but lacks the Ad structural and replication genes (29, 67, 201). AAV viral progeny can be harvested 48 h p.i. by

lysing the transfected cells and purified to high titers by one of several described protocols (2, 3, 8, 29, 55, 59, 68, 91, 94, 110, 124, 125, 160, 184, 188, 201, 211).
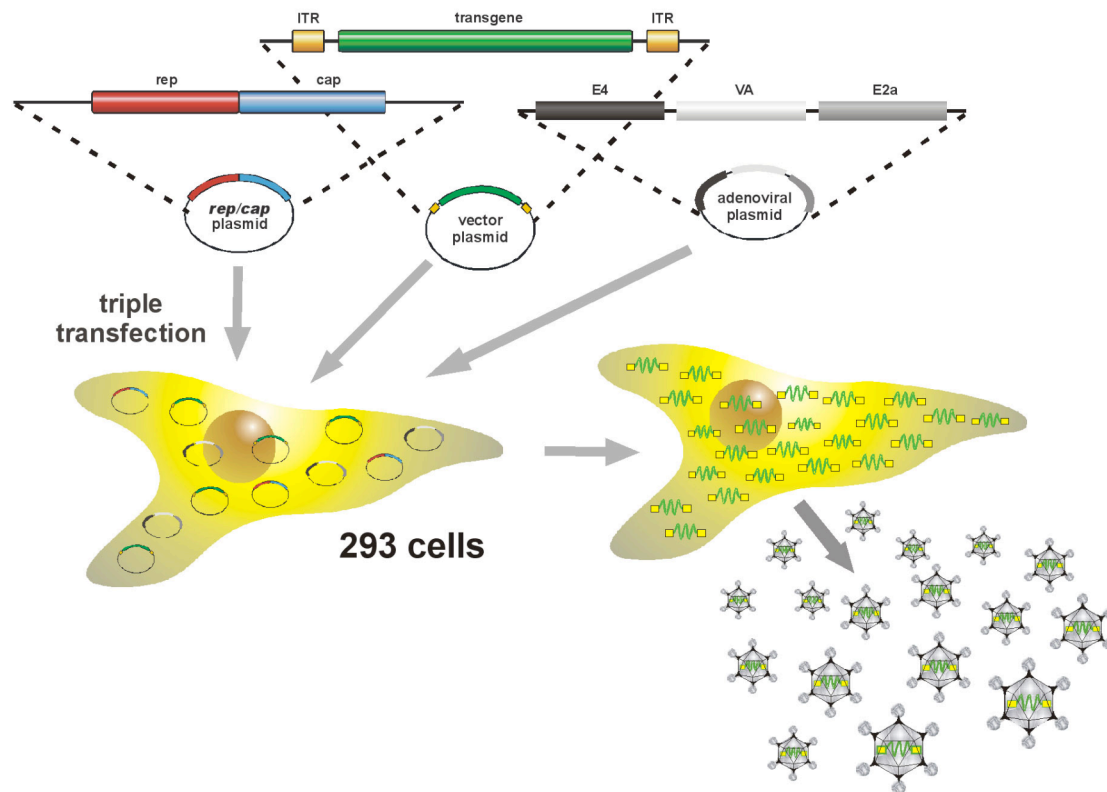
Figure 5. Schematic representation of the rAAV production protocol. Progeny capids carry the DNA sequence comprised between the ITR sequences of the vector plasmid. The resulting vector preparation is devoid of wt AAV and of adenovirus particles. Kindly provided by Dr. Luca Perabo.

The traditional method used to purify AAV from infected or transfected cells has been density equilibrium gradients (cesium chloride, CsCl) (162). Because cesium atoms are heavy, concentrated solutions of CsCl can form density gradients after only a few hours of ultracentrifugation. This method allows the physical separation of full particles (AAV packaging a genome) from empty particles based on their differences in density but it has several disadvantages. Two or three rounds of CsCl centrifugation must be carried out to get purified AAV. Dialysis of CsCl fractions containing AAV against a physiological buffer is necessary prior to *in vivo* use because CsCl can exert toxic effects on animals in the study. Furthermore, it has also been shown that, even after CsCl purification, 1% of the input infectious Ad and/or Ad proteins can still be found as contaminates.

These limitations led to the development of an immunoaffinity column to purify AAV-2 particles (67, 193). This approach makes use of the monoclonal

antibody A20 which recognizes assembled AAV-2 capsids but not unassembled capsid proteins. Despite the low recovery (70%) and purity (80%) of the eluted particles, this method allows a fast and easy preparation of AAV-2 stocks from a cell homogenate.

Zolotukhin and colleagues developed a novel way of purifying rAAV from crude lysates that involved the use of iodixanol gradients and heparin column purification (211). To purify rAAV utilizing iodixanol, step gradients of 15%, 25%, 40%, and 60% were generated and the crude lysate was placed on top of the 15% step. After an hour of centrifugation, the majority of the rAAV bands were within the 40% density step. Approximately 75–80% of the rAAV in the crude lysate is recovered in the iodixanol fraction. For further purification after isolation of rAAV from iodixanol gradients, heparinized columns were used. HPLC chromatography utilizing UNO-S1 heparin columns was capable of yielding a rAAV product that is greater than 99% pure based on polyacrylamide gel electrophoresis and silver staining. A five-fold higher recovery of rAAV particles and a greater than 100-fold increase in infectivity was obtained using this method of purification when compared to the traditional CsCl gradient purification. The main disadvantage to using this system of purification is that AAV must have the ability to bind heparin/HSPG.

Recently, methods have been developed that have the ability to purify all AAV serotypes by utilizing ion exchange chromatography (55, 93, 151). Of notice is the work of Qu and colleagues (151). They separated empty capsids from genome containing capsids by making use of the less anionic character of empty particles. AAV-2 vector purification and particle separation using a cation exchange resin followed by an anion exchange resin allowed a yield of 74% with 86-fold reduction in empty capsids.

In summary, numerous methods have been developed for the production and purification of AAV that are focused on acquiring high vector yields free from contaminating cellular and helper virus proteins and are amenable to scaling up for human clinical trials. Needless to say, as better methods are developed for generating high yields of rAAV, better methods of purification must be generated to acquire them in pure form. In addition, the biotechnology industry is building upon these numerous methods to produce rAAV by scaling up production utilizing large bioreactors containing liters of media and suspension cells, resulting in log increases of vector yield over the conventional small-scale methods described above.

1.3. Targeting vectors

AAV-2's broad host range theoretically allows application of AAV-2 vectors for a variety of diseases but is at the same time a drawback in terms of safety since tissues or organs different from the target may be transduced when, after local application viral vectors are transported away from the target tissue into the body. Although tissue specific regulation can be achieved by using cell type specific promoters, systemic applied AAV-2 based vectors will accumulate in the liver. Thus, they will not be able to transduce other organs.

One possibility to overcome this limitation is the generation of receptor/tissue specific vectors. To do this, viral particles containing a selective receptor binding domain have to be engineered. This enables a stringent interaction with a receptor specific of the targeted cell (vector re-targeting). Besides this selective infectivity, a second advantageous aspect of targeting is the possibility to generate vectors that are able to transduce cell types which are refractory to infection with natural occurring AAVs.

1.3.1. Genetic capsid modifications

In a genetic or direct targeting approach, cell-specific targeting of the vector is mediated by a ligand that is genetically/directly inserted into the viral capsid. When the first attempts were made to target AAV, the three dimensional structure of the capsid was still unknown. Thus, it was hard to predict where to insert a peptide ligand without interfering with capsid assembly and stability while displaying the ligand on the capsid surface in order to mediate binding to the desired receptor.

Antibodies have proven to be an excellent paradigm for the design of high-affinity, protein-based binding reagents. Although the general structure of all antibodies is very similar, a small region at the tip of the protein is extremely variable, allowing millions of antibodies with slightly different tip structures to exist. This region is known as the hypervariable region (Figure 6A). Each of these variants can bind to a different target, known as an antigen. Recently, recombinant monoclonal antibodies (mAbs) have been dissected into minimal binding fragments, rebuilt into multivalent high-avidity reagents and fused with a range of molecules limited only by imagination (Figure 6B)(85).
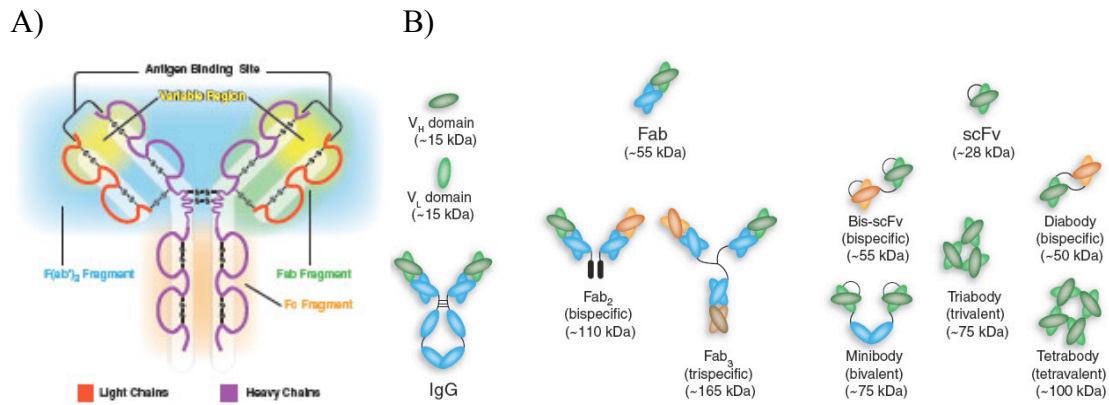
Figure 6. Antibody and antibody fragments. A) Schematic representation of an intact 'classic' IgG molecule. B) A variety of antibody fragments are depicted, including Fab, scFv, single domain VH and multimeric formats, such as minibodies, bis-scFv, diabodies, triabodies, tetrabodies, and chemically conjugated Fab' multimers (sizes given in kilodaltons are approximate). (85)

Thus, it is not surprising that the first re-targeting ligand genetically fused to an AAV capsid was an antibody fragment (208). Yang and colleagues started by using three independent plasmids for expression of VP1, VP2 and VP3 respectively. Independent transfections with the respective plasmids resulted in a VP1:VP2:VP3 ratio of 1:1:1 – expression of a wt AAV encoding plasmid results in a 1:1:10 ratio. They then inserted a single-chain antibody against human CD34 (a cell surface molecule expressed on haematopoietic progenitor cells) at the N-termini of VP1, VP2 and VP3, and showed that all three fusion proteins were expressed. Furthermore, while transfections with VP1 and VP2 only plasmids still resulted in the expression of wt VP3, transfections with scFv-VP1 and scFv-VP2 did not. Recent studies have shown that VP3 is essential for capsid assembly (189). Thus, co-transfection with VP1, VP2 and VP3 only plasmids - with wt VP3 being expressed from the three used plasmids - resulted in detectable AAV-2 particles. When substituting one VP by a scFv-VP - which did not show expression of wt VP3 – no particles were detected. The authors solved this problem by co-transfecting cells with the three wt VP encoding plasmids and one scFv-VP encoding plasmid in addition. Although this approach provided the first demonstration that targeting of AAV-2 by direct modification of the capsid is possible, vector titers were extremely low. Furthermore, mutants were more efficient in transduction of non-target cells than in transduction of target cells. In contrast to this first attempt, several recent reports have shown that fusions to the N-terminus of VP1 or VP2 can be incorporated into the AAV capsid without the need to provide wildtype VP1 (aa 34 (198)) or VP2 (113, 189)). In two examples, fusion of GFP to the N-terminus of VP2 yielded GFP-tagged viruses that

have been used to visualize AAV infectious pathway (113, 189). Furthermore, it was recently shown that the VP1 and probably VP2 N-terminal domains can translocate from the inside to the outside of the capsid (model is depicted in Figure 7) (105).

Recently, in two different approaches, two different scFvs were inserted in the capsid of adenovirus type 5. In one, the wt Ad5 fiber-knob was substituted by an optimized fiber-fibritin chimera that was genetically fused to a scFv (79). Although transduction of target cells was superior to the one achieved with the wt Ad5, when it came to non-target cells, scFv targeting mutant and wt Ad5 were equally efficient. Thus, although targeting was achieved, de-targeting was not. Furthermore, the potential of this vector was not demonstrated *in vivo*. In the second approach using Ad5, a scFv was fused to the minor capsid protein IX via a 75-Ångström spacer sequence (187). Binding to the antigen was demonstrated but transduction of target cells was not shown due to the nature of the receptor (β-galactosidase).

In addition, one or two residues downstream from the N-terminal methionine of the AAV-2 VP2 start codon have been used for insertions (aa 138 (111, 189, 198) and 139 (171)). Since VP1 is an N-terminal extension of VP2, insertions at positions 138 and 139 are displayed within VP1 and VP2 (Fig. 7). The most abundant capsid protein, VP3, remains unmodified. Insertions as large as 32 amino acids were tolerated with only marginally lower packaging efficiencies (111). Larger insertions like the rat fractalkine chemokine domain (76 aa) or the human hormone leptin (146 aa) inserted at aa position 138 decreased VP3 expression, which prevented capsid assembly (189). Providing additional VP3 *in trans* (by a VP3- encoding plasmid) restored capsid assembly with a remaining 5-log decrease in infectivity (189).
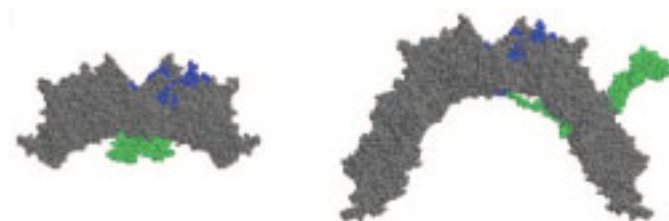
Figure 7. Model of the VP1 N-terminus translocation. A part of an equatorial slice of an AAV-2 capsid where the N-terminal stretch of the VP1 protein (green) was modeled and linked to one of the two VP3 subunits (blue) at the twofold symmetry axis is illustrated. On the right side, partial defolding of the VP1 N-terminus which allows its exposure on the capsid surface through a channel at the fivefold symmetry axis (105).

The first successful demonstration that a genetic capsid modification (direct targeting) by insertion of peptides into a common region of all three AAV capsid proteins can be used to re-target AAV-2 was described by Girod and colleagues in 1999 (62). By sequence alignment of AAV-2 and CPV, from which the three dimensional structure was known at the time, six sites (amino acid positions 261, 381, 447, 534, 573, 587) were expected to be exposed on the surface of the viral capsid and be able to accept the insertion of a ligand without disrupting functions essential for the viral life cycle. This was indeed true for one of the positions, 587. In the meantime 587 and the neighboring position 588, described by Bartlett and colleagues in 2003 (172), have evolved as the most often used sites for insertion of small peptides (up to 34 aa) (66, 128, 130, 139, 172, 192, 196, 197). In all these cases, the inserted ligand, exposed on the capsid surface was able to mediate the transduction of the respective targeting cells. Already five examples of a successful targeting after *in vivo* application of targeting vectors have been described, revealing the potential of this technology (local application (172) and systemic (128, 192, 196)). Besides 587/588 other sites (e.g. amino acid position 34, 161, 261, 328, 381, 447, 448, 459, 522, 534, 553, 573, 584, 591, 664) have been exploited as peptide insertion sites within the AAV *cap* ORF, but have not been proven to mediate infection of the target cell (61, 62, 66, 171, 198). Recently, a double mutant containing the RGD4C motif in 520 and 584 has been created (174). Genomic titers obtained for virions displaying the double insertions were ~ $2x10^7$ per ml. Although this titer was only 3- to 4-fold lower than titers obtained by the authors for their wild-type preparation, the titers are very low in comparison to others (62, 64, 135, 189). The double mutant was unable to bind to heparin and transduced the wild-type AAV-2 refractory cell lines SKOV3ip and C2C12. However, the comparison between double and single insertion mutants with regard to transduction efficiencies is not provided, which renders it impossible to judge if a double insertion shows a superior targeting efficiency. In all these studies target cells were refractory or hard to transduce by AAV-2 with wild-type capsid and targeting resulted in an improved efficiency. But to achieve a real targeting (= redirected tropism) the natural receptor binding has to be eliminated. Of interest in this regard is the fact that insertions at 587/588 are likely to interfere with the binding of two (R585 and R588) of the five positive charged amino acids of the described AAV-2 HSPG binding motif (97, 135), explaining the ablation of HSPG binding of some targeting vectors. However, in some cases binding is only partially affected or

even restored by the inserted peptide. Using our AAV peptide library (see next section) separated by heparin affinity chromatography into a pool of AAV capsid mutants able to (binder pool) or unable to bind heparin (non-binder pool) we were able to propose the following model (141): insertion of bulky or negative charged peptides resulted in AAV capsid mutants unable to bind to heparin/HSPG due to sterical or charge interference. If the peptide consists of small residues like G and A, the insertion is less invasive and the structure of the natural HSPG binding motif maintained functional. Insertion of positively charged peptides could lead to an HSPG binding phenotype by reconstituting a binding motif with one of the original arginines or independently from them.

The ability of a targeting mutant to infect cells independently of HSPG also influences its *in vivo* distribution. We could show that the inability to bind to HSPG correlated with liver and spleen de-targeting after systemic application in mice (141). Thus, the *in vivo* targeting ability of a vector is increased if HSPG-dependent retention of vectors in liver and spleen is avoided either by the use of non-HSPG-binding peptides or the use of a non-binder AAV peptide library for selection of cell/tissue specific targeting vectors.

Stachler and colleagues expanded the targeting field to other AAV serotypes (179). In this approach, amino acid position 590 of AAV serotype 1 was used for the insertion of the RGD-4C peptide. The respective targeting vector reached remarkable higher transduction levels than unmodified AAV-1 on HUVEC, HSaVEC and HeLa C12 and transduction could be competed by the addition of soluble RGD containing peptides. They have then combined this RGD-4C insertion at amino acid position 590 of AAV-1 with VPs of AAV-1 containing the sequence of a biotin acceptor peptide. These hybrid virions utilized the targeting peptide for endothelial cell entry, while the biotin acceptor peptide was used for purification on monomeric avidin affinity columns.

1.3.1.1. Peptide libraries

Depending on their amino acid composition certain peptide insertions may interfere with the stability of the capsid or with the infectious process. Furthermore, the inserted peptides might be expressed in a non-functional structure when inserted in the capsid context. In addition, insertion of a particular sequence for targeting a

desired cell type requires receptor-specific binding peptides, which are unknown for a large number of clinically interesting tissues. An elegant solution to these problems is the use of combinatorial engineering of the capsid and high-throughput selection protocols to screen mutants with desired phenotype (see Figure 8). Using an AAV library of capsids carrying a random insertion at amino acid position 587 (139) or 588 (128), an efficient re-targeting to various cell types *in vitro* and *in vivo* has been achieved.
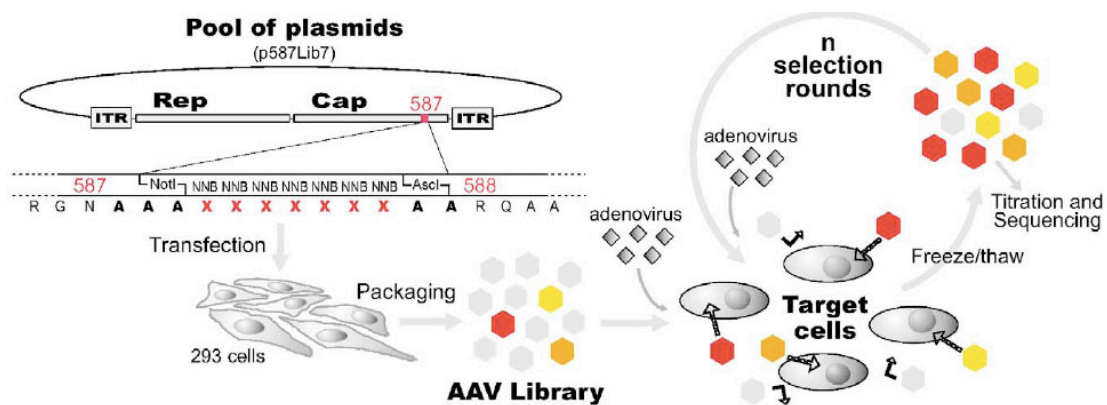
Figure 8. AAV display libraries. Schematic representation of the construction of the library of AAV-2 capsid modified particles and selection protocol for the isolation of retargeted mutants. A pool of randomly generated oligonucleotides was cloned into an AAV-2 genome encoding plasmid at the site corresponding to amino acidic site 587 of capsid protein VP1. Following a standard AAV production protocol, a library of approximately 4×10^6 diferent capsid modified AAV-2 clones can be generated. For the selection of retargeted mutants, target cells were co-infected with the pool of AAV-2 mutants and with adenovirus. The viral progeny collected 48 hrs p.i. was used for the next infection round.

Briefly, Perabo and colleagues performed five rounds of selection with an AAV peptide library on MO7e, a megakaryocytic cell line, and Mec1, which are derived from B-cell chronic lymphocytic leukemia (BCLL) cells in prolymphoid transformation (139). Both cell lines are non-permissive for wild type AAV-2. In two separate selections they isolated RGD containing peptides (RGDAVGV and RGDTPTS) from the MO7e selections able to convey cell transduction, whereas two totally different peptides were selected on Mec1 (GENQARS and RSNAVVP). In transduction experiments performed with rAAV vectors displaying the selected peptides on the capsid surface they observed an up to 100-fold increased efficiency. Competition studies proofed receptor-specificity. Furthermore, one of the mutants selected on Mec1 was able to transduce primary B-CLL cells (up to 54%) which are refractory to AAV-2 infection. Muller and colleagues applied a similar approach for the selection of peptides able to mediate the transduction of human coronary artery

endothelial cells (128). Most of the selected peptides fitted into the consensus sequence NSVRDL$_{G/S}$ and NSVSSX$_{S/A}$ and showed remarkably higher transduction levels than AAV-2 with unmodified capsid on the target cells. Furthermore, one of the peptides (NSSRDLG) enabled heart transduction after systemic application whereas only a weak transduction was observed with unmodified AAV-2 (128).

1.3.1.2. Combinatorial approaches to improve AAV vectors

Combinatorial approaches utilizing AAV libraries consisting of AAV variants with point mutations scattered through wide parts of the capsid have been recently applied in the AAV field to improve *in vivo* application of AAV vectors (115, 140). Masheshri and colleagues used a combination of DNA shuffling and error prone PCR, whereas Perabo and colleagues used simply error prone PCR to introduce these mutations into the *cap* ORF. From these plasmids AAV capsid variants are generated by packaging. To prove the potential of combinatorial libraries and *in vitro* evolution, both groups focused their selections on the identification of AAV variants that escape neutralization by anti-AAV-2 antibodies. When recombinant AAV vectors carrying the selected mutations in the capsid were analyzed for the immune escaping ability up to 5.5-fold higher N50 (amount of serum needed to halve the number of transduced cells) values than the corresponding N50 value obtained for AAV-2 with wild-type capsid was determined. As mentioned, also the selection performed by Masheshri and colleagues aimed to isolate AAV variants able to evade AAV-2 neutralizing antibodies (115). They used a serum generated in rabbits by injection of recombinant AAV-2 into hind limb muscle. Sequence analysis of these and other mutants identified N587I in addition to T716A as key mutations for immune escaping. In *in vivo* experiments, in which selected AAV variants were incubated with neutralizing serum prior to muscle injection 1 to 3 log higher expression levels were determined in comparison to AAV-2 with wild-type capsid. That the position 587 is involved in recognition by neutralizing antibodies is in agreement with observations made by Huttner and colleagues (89). They could show that peptide insertions at this position resulted in AAV targeting mutants able to transduce their target cells even in the presence of human neutralizing anti-AAV-2 antibodies. The position 716 has not been described before although it lies within an already described immunogenic region (127). Interestingly, AAV-4, which is able to escape anti-AAV-2 antibodies, displays

an alanine at this position. In all the mentioned reports, engineered mutants achieved higher transductions values in the presence of neutralizing Ab when compared to wt AAV-2. Still, this does not mean that the achieved transductions were the result of a lower affinity of the neutralizing Ab. Indeed, such capsid modifications may have improved other steps in the transduction process (receptor binding, internalization, trafficking, etc…) that lead to a higher transduction efficiency in the presence of antibodies.

1.3.2. Non-genetic capsid modifications

The non-genetic targeting approach utilizes an associated molecule which mediates the interaction between the viral surface and a specific cell surface molecule. Until now, two different non-genetic approaches have been described for AAV (12, 146). A bispecific antibody displaying affinities for $\alpha IIb\beta 3$ integrin (AP-2 antibody part) and the intact AAV-2 capsid (A20 antibody part) was used by Bartlett and colleagues to bind rAAV-2 to fibrinogen on MO7e and DAMI cells, which are not permissive for wild-type AAV-2 infection (12). The binding is likely to induce a receptor-mediated endocytosis and resulted in transduction efficiencies 70-fold above background (12). Ponnazhagan and colleagues described another way of indirect targeting which is based on the strongest interaction known in nature, avidin/biotin (146). They generated a prokaryotic expression vector that expressed a fusion protein consisting of the core sequence of streptavidin linked via an eight amino acid linker to epidermal growth factor (EGF). The fusion was produced in and purified from *E. coli*. AAV-2 preparations were biotinylated *in vitro* and incubated with the fusion protein, whereby the streptavidin moiety mediated binding to the AAV-2 capsid and the EGF ligand targeted the EGF receptor. An identical strategy was used to target FGFR1. Transduction of AAV-2 via EGFR in an ovarian cancer cell line (SKOV3ip1) was enhanced by 100-fold in comparison to non-modified AAV-2. On the EGFR negative cell line MB-453, no difference between modified and non-modified AAV-2 was observed indicating that the targeted AAV-2 vector still retained its native tropism.

1.3.3. Combining genetic and non-genetic capsid modifications

Inspired by an earlier attempt with Sindbis virus (133, 134), Ried and colleagues tried to develop a general targeting vector using a truncated 34 amino-acid peptide, Z34C (180), from protein A of Staphylococcus aureus (159). Protein A recognizes and binds the Fc part of immunoglobulins (Ig), but not the variable Ig domain, which therefore remains free to bind the antigen. Coupling this vector, rAAV-587Z34C, with antibodies against CD29 (β1-integrin), CD117 (c-kit-receptor) or CXCR4 resulted in a specific, antibody-mediated transduction of haematopoietic cell lines. However, transduction levels were low revealing that a universal AAV targeting vector can be generated and loaded with different targeting molecules to transduce the desired cells via specific receptors, but that further refinements are necessary to make this technique attractive for clinical applications. Arnold and colleagues evolved another possibility of a universal targeting vector. They introduced a biotin acceptor peptide into the AAV capsid protein of AAV-1 at position 520, which becomes biotinylated during packaging. Introduction of the same sequence within the capsid of AAV-2 to AAV-5 was less efficient. The modified vector was able bind to a rat glioma cell line, BT4C, transfected to express an artificial biotin receptor. The inserted biotin acceptor peptide can in principle be used to couple peptide ligands to the AAV capsid, however, this has not been shown.

2. Objectives

Adeno-associated virus (AAV), discovered in 1965 is a member of the *Parvoviridae* family and belongs to the Dependovirus genus. This virus has received a large interest as a vector for gene therapy since it was first cloned into a bacterial plasmid in 1982. After more than 25 years and a large number of publications, AAV and gene therapy have finally entered the long development phase that is necessary for their maturation.

For the design of safe and efficient gene therapy most approaches require the delivery of the genetic material to specific cells after *in vivo* administration. Thus, development of specific targeting vectors is one of the first keys for successful gene therapy. Most AAV-2 targeting approaches are based on the insertion of peptide ligands on the AAV-2 capsid after amino acid position 587. Such insertions have resulted in vectors with modified *in vivo* tropism.

Discovery of position 587 was made by sequence alignment of AAV-2 with CPV (from which the three dimensional structure was known) (62). Other reported positions have not made use of the available three dimensional structure of AAV-2. Thus, today, with the three dimensional structure of AAV-2 in hand, we intend to use *in silico* analysis to identify a more prominent position and to explore its potential for the development of AAV-2 based targeting vectors. Ablation of wild type tropism will be made by previously shown amino acid substitutions (97, 135). Position 587 will be used as a reference and mutants with insertions at both positions will be tested. Known small peptide ligands will be inserted and respective mutants analyzed. After assessing that insertions at 453 do not interfere with any essential viral function the mutants will be assayed for their capacity to bind the target receptor in cell free based assays, to specifically transduce cells *in vitro* and for their *in vivo* tropism.

To the present, only a few number of reports have shown *in vivo* specific gene transfer using AAV-2 targeting vectors based on small peptide insertions. Although efficient in the modification of viral tropism such small peptides are usually still able to bind a wide variety of receptors. Moreover, in several cases, the acceptor molecules are found on various cell types. Thus, the first report – 1998 – on the development of an AAV-2 targeting vector made use of an antibody fragment (208). Antibodies are amongst the most specific, well studied and easy to use molecules. Despite the huge

potential of antibody molecules and of the large number of publications involving AAV targeting vectors only 3 reports combined AAV and antibody molecules for vector targeting. All the mentioned reports failed to present *in vivo* results. Recently in our group, a GFP-VP2 fusion protein was incorporated into the AAV-2 capsid without the need to supply wt VP2. Thus, this, together with the possibility to use well studied single chain antibody fragments as well as the tools required for their characterization from our institute colleagues makes us embrace the design of scFv directed AAVs. Constructs with different spacer sequences between the scFv and the VP2 as well as different scFvs will be used. Also here, known amino acid mutations will be used to ablate wild type tropism. Particles will be assessed for their capacity to incorporate the fusion protein without affecting any essential viral function. Anti-idiotypic antibodies against the paratope will be used to identify functional scFvs. Receptor positive cell lines will be used and once specific *in vitro* transduction is determined the vectors will be administrated *in vivo* using appropriate mouse models.

In summary, this work main objective is the establishment and assessment of new rationally designed basic tools for the development of AAV-2 targeting vectors. Such tools can be transferred to the development of other vector systems.

3. Materials

3.1. Chemicals, solutions and enzymes

Table 1 Substances and suppliers

Substance	Supplier
Agarose	Sigma, Deisenhofen, Germany
Ampicillin	Sigma, Deisenhofen, Germany
Aqua bidest.	Millipore, Billerica, Germany
Biotin Conjugate Streptavidin	Dianova, Hamburg, Germany
Bovine Serum Albumine	AppliChem, Darmstadt, Germany
D-MEM Medium	Invitrogen Corporation, Germany
DNA restriction enzymes	MBI Fermentas GmbH, St. Leon-Rot, Germany
Etidium bromide	Roth, Karlsruhe, Germany
Fetal Calf Serum	Invitrogen Corporation, Karlsruhe, Germany
Heparin	B. Braun Melsungen AG, Germany
HEPES	Roth, Karlsruhe, Germany
Iodixanol	Sigma, Deisenhofen, Germany
MassRuler DNA Ladder Mix	MBI Fermentas GmbH, St. Leon-Rot, Germany
McCoy's 5A Medium	Invitrogen Corporation, Germany
Methanol	Roth, Karlsruhe , Germany
Sodium Chloride	Riedel-de Haën, Seelze, Germany
Sodium Dodecyl Sulfate (SDS)	Merck, Darmstadt, Germany
PAA Medium	PAA Laboratories GmbH, Pasching, Austria
PBS	Invitrogen Corporation, Karlsruhe, Germany
Penicillin/Streptomycin	Invitrogen Corporation, Karlsruhe, Germany

Peptides: GRGDS, GNGRS, GRGES	Bachem, Bubendorf, Swiss
Precision Plus Protein Gel Color Standards	Bio-Rad Laboratories GmbH, München, Germany
Proteinase K	Merck, Darmstadt, Germany
RNase A (100 mg)	Roche Diagnostics GmbH, Mannheim, Germany
RPMI 1640 Medium	Invitrogen Corporation, Germany
Tris	Merck, Darmstadt, Germany
TritonX-100	Sigma, Deisenhofen, Germany
Trypsin-EDTA	Invitrogen Corporation, Karlsruhe, Germany
*Tween*20	Merck, Darmstadt, Germany

If not mentioned the chemicals were bought to Sigma-Aldrich, Taufkirchen, Germany; Merck, Darmstadt, Germany or Carl Roth GmbH & Co., Karlsruhe, Germany.

3.2. Plasmids

pRC: AAV based helper plasmid containing the AAV-2 Rep and Cap coding regions under the control of the wt promoters but lacking the viral ITRs (62).

pXX6-80: encodes for the Adenoviral genes VA, E2A and E4. Kindly provided by RJ Samulski (201).

ssGFP: GFP gene controlled by the human cytomegalovirus (CMV) promoter and hygromycin resistance gene controlled by the thimidine kinase promoter flanked by the AAV ITRs (71).

scGFP: GFP gene controlled by the CMV promoter; a deletion in the terminal resolution sites interferes with strand displacement resulting in a self complementary genome, which is packaged into the viral capsid (72).

pRC A2: contains the AAV-2 Rep and Cap encoding regions just like pRC; R585 and R588 (VP1 numbering) are mutated to alanines for elimination of the HSPG binding ability.

pRC VP2 ko: contains the AAV-2 Rep and Cap encoding regions just like pRC; the start codon of VP2 – ACG - was mutated to ACC.

pRC VP2 ko A2: contains the AAV-2 Rep and Cap encoding regions just like pRC; the start codon of VP2 – ACG - was mutated to ACC; R585 and R588 (VP1 numbering) are mutated to alanines for elimination of the HSPG binding ability.

pRGD4C-587: contains the AAV-2 Rep and Cap encoding regions just like pRC; the RGD4C peptide – ACDCRGDCFCA – is inserted between N587 and R588.

pRGD4C-453: contains the AAV-2 Rep and Cap encoding regions just like pRC; the RGD4C peptide – ACDCRGDCFCA – is inserted between G453 and T454.

pRGD4C-453&587: contains the AAV-2 Rep and Cap encoding regions just like pRC; the RGD4C peptide – ACDCRGDCFCA – is inserted between N587 and R588 and between G453 and T454.

pRGD4C-587 A2: contains the AAV-2 Rep and Cap encoding regions just like pRC; the RGD4C peptide – ACDCRGDCFCA – is inserted between N587 and R588; R585 and R588 (VP1 numbering) are mutated to alanines for elimination of the HSPG binding ability.

pRGD4C-453 A2: contains the AAV-2 Rep and Cap encoding regions just like pRC; the RGD4C peptide – ACDCRGDCFCA – is inserted between G453 and T454; R585 and R588 (VP1 numbering) are mutated to alanines for elimination of the HSPG binding ability.

pRGD4C-453&587-A2: contains the AAV-2 Rep and Cap encoding regions just like pRC; the RGD4C peptide – ACDCRGDCFCA – is inserted between N587 and R588 and between G453 and T454; R585 and R588 (VP1 numbering) are mutated to alanines for elimination of the HSPG binding ability.

pNGRI-587: contains the AAV-2 Rep and Cap encoding regions just like pRC; the RGD4C peptide – ACVLNGRMECA – is inserted between N587 and R588.

pNGRI-453: contains the AAV-2 Rep and Cap encoding regions just like pRC; the RGD4C peptide – ACVLNGRMECA – is inserted between G453 and T454.

pNGRI-453&587: contains the AAV-2 Rep and Cap encoding regions just like pRC; the RGD4C peptide – ACVLNGRMECA – is inserted between N587 and R588 and between G453 and T454.

pNGRI-453-A2: contains the AAV-2 Rep and Cap encoding regions just like pRC; the RGD4C peptide – ACVLNGRMECA – is inserted between G453 and T454; R585 and R588 (VP1 numbering) are mutated to alanines for elimination of the HSPG binding ability.

pGEN-587: contains the AAV-2 Rep and Cap encoding regions just like pRC; the RGD4C peptide – AGENQARSA – is inserted between N587 and R588.

pGEN-453: contains the AAV-2 Rep and Cap encoding regions just like pRC; the RGD4C peptide – AGENQARSA – is inserted between G453 and T454.

pGEN-453-A2: contains the AAV-2 Rep and Cap encoding regions; the RGD4C peptide – AGENQARSA – is inserted between G453 and T454; R585 and R588 (VP1 numbering) are mutated to alanines for elimination of the HSPG binding ability.

pGFP-VP2: encodes the C-terminal fusion of eGFP with the N-terminus of VP2 from AAV-2 under the control of the CMV promoter.

pRSV-HRS3: encodes the anti-CD30 scFv HRS3 (49).

paCD30-GFP-VP2: encodes the C-terminal fusion of RSV-HRS3 to the N-terminus of the GFP-VP2 fusion under the control of the CMV promoter.

paCD30-GFP-VP2-A2: encodes the C-terminal fusion of RSV-HRS3 to the N-terminus of the GFP-VP2 fusion under the control of the CMV promoter; R585 and R588 (VP1 numbering) are mutated to alanines for elimination of the HSPG binding ability.

paCD30-VP2-A2: encodes the C-terminal fusion of RSV-HRS3 to the N-terminus of the VP2 from AAV-2 under the control of the CMV promoter; R585 and R588 (VP1 numbering) are mutated to alanines for elimination of the HSPG binding ability.

paCD30CLVP2-A2: encodes the C-terminal fusion of RSV-HRS3 to the N-terminus of the VP2 from AAV-2 under the control of the CMV promoter; a glycine/serine linker - SSGGGGSGGGGSGGGGS - is inserted between RSV-HRS3 and VP2; R585 and R588 (VP1 numbering) are mutated to alanines for elimination of the HSPG binding ability.

paCD30CL2VP2-A2: encodes the C-terminal fusion of RSV-HRS3 to the N-terminus of the VP2 from AAV-2 under the control of the CMV promoter; a double glycine/serine linker - SSGGGGSGGGGSGGGGSDPSSGGGGSGGGGSGGGGS - is inserted between RSV-HRS3 and VP2; R585 and R588 (VP1 numbering) are mutated to alanines for elimination of the HSPG binding ability.

paCD30GLVP2-A2: encodes the C-terminal fusion of RSV-HRS3 to the N-terminus of the VP2 from AAV-2 under the control of the CMV promoter; the non-globular C-terminal part of eGFP that is fused to VP2 in the GFP-VP2 - ITLGMDEL - is inserted between RSV-HRS3 and VP2; R585 and R588 (VP1 numbering) are mutated to alanines for elimination of the HSPG binding ability.

paCD30LGLVP2-A2: encodes the C-terminal fusion of RSV-HRS3 to the N-terminus of the VP2 from AAV-2 under the control of the CMV promoter; the non-globular C-terminal part of eGFP that is fused to VP2 in the GFP-VP2 - ITLGMDEL - is inserted between RSV-HRS3 and VP2; a glycine/serine linker - SSGGGGSGGGGSGGGGS - is inserted between RSV-HRS3 and GLVP2 fusion; R585 and R588 (VP1 numbering) are mutated to alanines for elimination of the HSPG binding ability.

pKaCD30-VP2: encodes the C-terminal fusion of RSV-HRS3 to the N-terminus of the VP2 from AAV-2 enhanced by the Kozak consensus – GCCACCATGG – under the control of a CMV promoter; R585 and R588 (VP1 numbering) are mutated to alanines for elimination of the HSPG binding ability.

pCA19.9scFv: encodes an anti-CA19.9 scFv (83).

pCA19-GFP-VP2-A2: encodes the C-terminal fusion of CA19.9scFv to the N-terminus of the GFP-VP2 fusion under the control of the CMV promoter; R585 and R588 (VP1 numbering) are mutated to alanines for elimination of the HSPG binding ability.

pBW431-26-scFv: encodes the anti-CEA scFv BW431-26 (86, 87).

paCEA-GFP-VP2-A2: encodes the C-terminal fusion of BW431-26-scFv to the N-terminus of the GFP-VP2 fusion under the control of the CMV promoter; R585 and R588 (VP1 numbering) are mutated to alanines for elimination of the HSPG binding ability.

3.3. Primers

All sequences are listed in 5'-3' orientation. All oligonucleotides were manufactured by MWG-Bioteck AG, Ebersberg, Germany.

Table 2 Primers.

Primer	Sequence (5' - 3')
OP1 RC	TACCAGCACGGTTCAGGTGTT
OP2 RC	ACACGCCATTAGTGTCCACAG
OP1 GL	TTTGCTTACTGGGGCCAAGG
OP1 OS	CCTACTTGGCAGTACATCTACG
OP1 19	CCGTCTAGAGCCCAGGTCAAGCT
OP2 GL	GTCTTTGCCAGTCACGTGGT
OP2 OS	TCCGAACGTGAGAGGATAGG
OP2 19	CCTAGATCTCCCGTCCGAGGAAACTCA
IP1 A2	TACCAACCTCCAGCAGGCAACGCACAAGC
IP1 A2	TACCAACCTCCAGCAGGCAACGCACAAGC
IP1 RGD4C 587 A2	TGCCGCGGAGACTGCTTCTGTGCGGCACAAGCAGCTACCGCAG
IP1 RGD4C 453&587	CACCTCAATGGCAGAGACTCTCTGGTGAAT
IP1 GEN(A)	GAGAACCAGGCGCGTTCCGCAGCGACCACCACGCAGTCAA
IP1 GL	ATCACTCTCGGCATGGACGAGCTGTACAAGTACTCAGATCCTCCGGG
IP1 CL	GAGGCGGTGGGTCATACAAGTACTCAGATCCTCCGGG
IP1 OS	AGCGCTACCGGTCGCCACCATGTCTAGAATGGC
IP1 K1	TCATAATGGTGTCTAGAATGGCCCAGG
IP1 K	GCCACCATGGCCCAGGTGCAAC
IP2 A2	TGTGCGTTGCCTGCCTGGAGGTTGGTAGAT
IP2 RGD4C 587 A2	GAAGCAGTCTCCGCGGCAGTCACACGCGTTGCCTGCCTGGAGG
IP2 RGD4C 453&587	TTCACCAGAGAGTCTCTGCCATTGAGGTGGTA
IP2 GEN(A)	CGCCTGGTTCTCGCCTGCGGCAGCTCCACTTGGAGTGTTTGTTCT
IP2 GL	GTACAGCTCGTCCATGCCGAGAGTGATATCCGCCCGTTTGATTTC

IP2 LGL	GTACAGCTCGTCCATGCCGAGAGTGATTGACCCACCGCCTCCG
IP2 CL	AGGATCTGAGTACTTGTATGACCCACCGCCTCCG
IP2 CL2	ATCTGAGTACTTGTATGACCCACCGCCTCCG
IP2 OS	TGGGCCATTCTAGACATGGTGGCGACCGGTAGCG
IP2 K1	GGCCATTCTAGACACCATGGTGGCGACCGG
IP2 K	CTGGGCCATGGTGGCGACCG
4066-back	ATGTCCGTCCGTGTGTGG
3201-forward	GGTACGACGACGATTGCC
EGFP-1 forward	GCTACCCCGACCACATGAAG
EGFP-1 reverse	GTCCATGCCGAGAGTGATCC
GFPm_f	CTCGATGTTGTGGCGGAT
GFPm_r	GCGCCGAGGTGAAGTT
GAPDHm_f	GAGTCCACTGGCGTCTTCA
GAPDHm_r	TTCAGCTCAGGATGACCTT
BW F	Pho-CAGTCATAATGTCTAGAGGTGTC
BW R	Pho-GGATCCACTTTGATCTCCAC
OL LF	Pho-GATCCGAGTTCCGGTGGCGGAGGGTCTGGCGGTGGAGGCTCCGGAGG CGGTGGGTCA
OL LR	Pho-GATCTGACCCACCGCCTCCGGAGCCTCCACCGCCAGACCCTCCGCCA CCGGAACTCG

3.4. Antibodies and proteins

Primary antibodies

Listed as: antigen; generated in; clonality; manufacturer

A20:   AAV-2 intact capsid; Mouse; Monoclonal; Progen

B1:   VP1, VP2, VP3; Mouse; Monoclonal; Progen

Anti-integrin αV:	anti-integrin αV C-terminal intracellular; Rabbit; Polyclonal; Chemicon
Anti-integrin αVβ5:	anti-human integrin αVβ5; Mouse; Monoclonal; Chemicon
Anti-integrin αVβ3:	anti-human integrin αVβ3; Mouse; Monoclonal; Abcam
Anti-GFP:	anti-GFP; Rabbit; Polyclonal; Molecular Probes
9G10:	anti-HRSV3 anti-idiotypic antibody; Mouse; kindly provided by Hinrich Abken, University Hospital of Cologne, Germany (145)
IgG control:	anti-TNP; Mouse; Monoclonal; BD Biosciences
Anti-CD30:	anti-CD30 PE labeled; Mouse; Monoclonal; BD Biosciences
aCD30-hum.Fc:	anti-CD30 HRSV3 antibody with human Fc; kindly provided by Hinrich Abken, University Hospital of Cologne, Germany

Secondary antibodies

Donkey anti-mouse biotin-conjugated: Jackson ImmunoResearch
     Laboratoires, Inc

Goat anti-rabbit peroxidase-conjugated: Jackson ImmunoResearch
     Laboratoires, Inc

Goat anti-mouse phycoerythrin-conjugated: Abcam

Mouse anti-human IgG (H+L) biotin-conjugated: Jackson ImmunoResearch
     Laboratoires, Inc

Proteins

Integrin αV β5: Chemicon

3.5. Bacteria strain

E.*coli*DH5α: F-, *lac*1-, *rec*A1, *end*A1, *hsd*R17, Δ(*lac*ZYA-*arg*F), U169,
       F80d*lac*ZΔM15, *sup*E44, *thi*-1, *gyr*A96, *rel*A1; (75)

3.6. Eukaryotic cells

Listed as: organism; organ; disease; characteristics; medium and serum; source; references

HEK293: humam; kidney; epithelial; transformed with adenovirus 5 DNA, contains E1A and E2; D-MEM with 10% FCS and 100units/ml of Penicillin/Streptomycin; ATCC CRL-1573; American Type Culture Collection, Rockville, USA; (65, 147).

HeLa: humam; cervix; adenocarcinoma; epithelial; D-MEM with 10% FCS and 100 units/ml of Penicillin/Streptomycin; ATCC CCL-2; American Type Culture Collection, Rockville, USA; (147, 166).

CHO KI: chinese hamster; ovarian; epithelial; DMEM/Ham's F-12 medium with 10% FCS and 100 units/ml of Penicillin/Streptomycin; ATCC CCL-61; kindly provided by Stefan Weiss, Gene Center of the LMU Munich, Germany; (148).

CHO pgsA-745: chinese hamster; ovarian; epithelial; xylosyltransferase I deficient; DMEM/Ham's F-12 medium with 10% FCS and 100 units/ml of Penicillin/Streptomycin; ATCC CRL-2242; kindly provided by Stefan Weiss, Gene Center of the LMU Munich, Germany; (51).

Primary HUVEC: pooled; primary; human; umbilical vein; endothelial; maintained in agreement with supplier instructions; PromoCell.

HepG2: humam; liver; hepatocellular carcinoma; epithelial; D-MEM with 10% FCS, 1 mM sodium pyruvate, 1x non-essential amino-acids and 100 units/ml of Penicillin/Streptomycin; ATCC HB-8065; kindly provided by Ulrike Protzer, University of Cologne, Germany; (101).

L540: human; lymph node; Hodgkin's lymphoma; lymphoblast; RPMI-1640 with 10% FCS and 100 units/ml of Penicillin/Streptomycin; kindly provided by Elke Pogge, University of Cologne, Germany; (39).

LS174T: human; colon; colorectal carcinoma; epithelial; RPMI-1640 with 10% FCS and 100 units/ml of Penicillin/Streptomycin; ATCC CL-188; kindly provided by Hinrich Abken, University of Cologne, Germany; (28).

C15A3: murine; colon; colorectal carcinoma; epithelial; RPMI-1640 with 10% FCS, and 100 units/ml of Penicillin/Streptomycin; kindly provided by Hinrich Abken, University of Cologne, Germany; (84).

3.7. Data treating software

Microsoft Office Excel 2004; WinMDI 2.8; Roche Molecular Biochemicals Lightcycler Software v3.5; Elisa Reader SofMax Pro v1.2.0; PyMol (35); Clone Manager 6; Primer Design 4; CDTree 3.0; Cn3D 4.2.

3.8. GI and Accession numbers

Table 3. GI and Accession numbers

GI	Accession	Descritpion
22219269	1lp3 (PDB)	Adeno-associated virus type 2 coat protein VP2
494746	2CAS (PDB)	Canine parvovirus empty capsid (Strain D) viral protein 2
75569401	Q88273 (SwissProt)	Simian parvovirus coat protein VP2
116774	1s58 (PDB), VP2	Human parvovirus B19 probable coat protein VP1
81924813	P87584 (SwissProt)	Chipmunk parvovirus coat protein VP1
81921778	2g8g (PDB), VP2	Adeno-associated virus type 4 coat protein VP1
81937258	Q67667 (SwissProt)	Goose parvovirus coat protein VP2
116764	1mvm (PDB), VP2	Minute virus of mice coat protein VP1
81925419	P90329 (SwissProt)	Kilham rat virus coat protein VP2

3.9. Laboratory equipment, disposables and kits

- *Eppendorf AG, Hamburg, Germany:* Centrifuge 5810 R; Centrifuge 5415 D; Thermomixer Comfort; Reaction viles 1.5ml, 2ml
- *DuPont GmbH, Bad Homburg:* Sorval Ultracentrifuge Combi
- Beckman Instruments GmbH, München: 5-6B Centrifuge
- Mettler-Toledo GmbH, Schwerzenbach, Switzerland: pH meter SevenEasy
- Ohaus Corporation, NJ, USA: Balance Adventure Pro
- Heidolph Instruments GmbH & Co. KG, Schwabach, Germany: Heater/Magnetic Shaker Heidolph MR 3001
- Molecular Devices GmbH, München, USA: Emax Precision Microplate Reader

- Heraeus, Sepatech GmbH, Osterode, Germany: Hera -80° freeze; Mamalian Incubator Hera Cell 150; Oven
- New Brunswick Scientific, Inc, NJ, USA: Incubator Shaker Innova 4430
- Roche Diagnostics GmbH, Mannheim, Germany: Light Cycler; Roche LightCycler FastStart DNA Master SYBR Green I
- Carl Zeiss Jena GmbH, Göttingen, Germany: Light Microscope Axiovert 25 CFL
- Scientific Industries, Inc, NY, USA: Vortex Genie2
- Bio-Rad laboratories GmbH, München, Germany: Power Pac Basic; Spectophotometer BioRad SmartSpec 3000; Mini-PROTEAN 3 Cell; Mini Trans-Blot Electrophoretic Transfer Cell; Mini Sub-Cell GT Gel Electrophoresis Unit (nucleic acids); Sub-Cell GT Gel Electrophoresis Unit (nucleic acids); Quick Start Bradford Protein Assay
- Becton Dickinson, Heidelberg, Germany: FACSCalibur
- *Qiagen GmbH, Hilden, Germany:* Qiagen EndoFree Plasmid Mega Kit; Qiagen EndoFree Plasmid Maxi Kit; Qiagen DNeasy Tissue Kit
- Amersham Pharmacia Biotech, Freiburg, Germany: Hybond-P PVDF Transfer membrane; Pump P-1; RAP Heparin column (1 ml); ECL plus Western Blotting Detection System
- *Kodak, Cedex, France:* Bio Max Light Film, Scientific Imaging Film
- Beckton-Dickinson GmbH, Heidelberg: Polyesterol tubes 50ml
- VWR International GmbH, Darmstadt, Germany: general laboratory ware
- Beyer GmbH, Düsseldorf, Germany: cell culture plastic ware
- Schleicher & Schuell MicroScience GmbH, Dassel, Germany: Steril filters 0.22μm, 0.45μm; 3MM-Paper
- Nunc, Wiesbaden, Germany: Nunc-Immunoplates
- Eppendorf, Hamburg, Germany: FastPlasmid Mini
- Owl Separation Systems, Portsmouth, USA: electrophoresis chamber

4. Methods

4.1. Visualization of structures and molecular modeling

The molecular graphics system program PyMol (35) was used for visualization and the VIPERdb (156) service for construction of the complete viral particles. The available X-ray structure of AAV-2 (203) and the SWISS Model environment for comparative protein modeling were used for the generation of spatial models (69, 138, 168).

4.2. Bacteria culture

4.2.1. Cultivation of bacteria

Bacteria were grown at 37 °C with LB medium. For growing the bacteria on plates, agar was added to LB medium for solidification. When growing the bacteria in liquid medium, erlenmeyers were filled until 25% with LB medium and bacteria were grown at 37 °C with vigorous shaking.

LB medium (1 l):   10 g tryptone

                            5 g yeast

                            5 g NaCl

                            15 g agar

                            ad 1 l H_2O

4.2.2. Preparation of competent bacteria

Bacteria strand DH5α was grown at 37 °C and vigorous shaking (200 RPM) overnight in 5 ml of LB medium. 10 hours later 2.5 ml was transferred into 250 ml of LB medium and the bacteria were grown until an optical density (OD) of 0.7 to 0.8 measured at 600 nm. Incubation on an ice cold water bath was performed for 10 min followed by a centrifugation at 3000 RPM during 10 min at 4 °C. Pellet was carefully re-suspended at 4°C in 7 ml of cold TFBI buffer. Incubation on ice was done and

followed by a centrifugation step as before. The pellet was carefully re-suspended at 4ºC in 10 ml of cold TFBII. Aliquots were frozen in liquid nitrogen.

TFBI buffer:	30 mM KAc
	100 mM $CaCl_2$
	15% Glycerin
	50 mM $MnCl_2$
	in H_2O
TFBII buffer:	10 mM MOPS
	75 mM $CaCl_2$
	10 mM KCl
	25% Glycerin
	in H_2O

4.2.3. Transformation of bacteria

Competent bacteria were slowly thawn on ice. After adding 50 µl of competent bacteria to the transforming DNA (100 ng – 500 ng) the suspension was mixed and incubated on ice for 30 min. Suspension was then incubated for 60 sec at 42 ºC followed by an incubation on ice for 2 min. 1 ml of LB medium was added and the mixture shaken at 200 RPM and 37 ºC for 60 min.

Bacteria were plated onto plates that already contained LB medium, agar and ampicillin (50 µg/ml) or kanamycin (30 µg/ml). Plates were then incubated overnight at 37 ºC.

Next day a single colony was picked from the plate, grown as before and then analysed.

4.3. DNA techniques

4.3.1. Plasmid amplification and extraction

For plasmid extraction the "Qiagen EndoFree Plasmid Mega Kit" was used and the protocol for "Plasmid or Cosmid DNA Purification Using EndoFree Plasmid Mega Kit" followed.

Transformed bacteria was taken from a 50% glycerol stock kept at -80 ºC and grown in 10 ml of LB medium for approximately 8 h at 37 ºC and vigorous shaking (200 RPM).   This starter culture was diluted 1/1500 into four 2 l erlenmeyers having 600 ml of LB medium each. Culture was grown overnight at 37ºC and vigorous shaking.

The bacterial cells were harvested by centrifugation at 5200 RPM (6000 x g) for 15 min and bacterial pellet was re-suspended in 50 ml of Buffer P1. Then, 50 ml of Buffer P2 was added and mixed gently by inverting 6 times. Incubation was performed at room temperature for 5 min. 50 ml of Buffer P3 was added to the suspension and mixed immediately and thoroughly by inverting 6 times. After screwing the QIAfilter Mega-Giga Cartridge onto a 45 mm-neck glass bottle (500 ml flask was used) the suspension was poured into the QIAfilter Mega-Giga Cartridge and incubation was performed at room temperature for 10 min. The vacuum source was turned on until all liquid had been pulled through, after which 50 ml of Buffer FWB2 was added to the QIAfilter Mega-Giga Cartridge and the vacuum source was turned on once again until all the liquid had been pulled through completely. 12.5 ml of Buffer ER was added to the filtered lysate and mixed by inverting the bottle approximately 10 times. Incubation was then performed on ice for 30 min. Qiagen-tip 2500 was equilibrated by applying 35 ml of Buffer QBT and the column allowed emptying by gravity flow. After this and after finishing the 30 min of incubation on ice, the lysate was applied to the Qiagen-tip and allowed to enter the resin by gravity flow. The Qiagen-tip was then washed with a total of 200 ml of Buffer QC and the DNA was eluted with 35 ml of Buffer QN. DNA was precipitated by adding 24.5 ml of isopropanol (0.7 volumes, room-temperature) to the eluted DNA. After mixing a centrifugation was performed at 4000 RPM for 30 min at 4 ºC. Supernatant was carefully decanted and the DNA pellet was washed with 7 ml of 70% ethanol (prepared with enendotoxin-free water and kept at room temperature). Then centrifugation was performed at 4000 RPM and 4 ºC for 10 min. The pellet was air-

dried for approximately 10-20 min and the DNA was re-dissolved in approximately 500 μl of endotoxin-free Buffer TE.

Alternatively the "Qiagen EndoFree Plasmid Maxi Kit" was used for extractions of fewer amounts of DNA or the Eppendorf FastPlasmid Mini and respective protocols followed.

Buffer P1 (resuspension buffer):	50 mM Tris-Cl
	pH 8.0; 10 mM EDTA
	100 μg/ml RNase A
Buffer P2 (lysis buffer):	200 mM NaOH
	1% SDS (w/v)
Buffer P3 (neutralization buffer):	3.0 M potassium acetate, pH 5.5
Buffer FWB2 (QIAfilter wash buffer):	1 M potassium acetate, pH 5.0
Buffer QBT (equilibration buffer):	750 mM NaCl
	50 mM MOPS, pH 7.0
	15% isopropanol (v/v)
	0.15% Triton X-100 (v/v)
Buffer QC (wash buffer):	1.0 M NaCl
	50 mM MOPS, pH 7.0
	15% isopropanol (v/v)
Buffer QN (elution buffer):	1.6 M NaCl
	50 mM MOPS, pH 7.0
	15% isopropanol (v/v)
TE:	10 mM Tris-Cl, pH 8.0
	1 mM EDTA

4.3.2. DNA quantification

DNA concentration was measured using a BioRad SmartSpec 3000 spectrophotometer. Quantification is made by measuring absorbance at 260 nm. 1 A260 unit of double stranded DNA equals 50 µg/ml H_2O and 1 A260 unit of single stranded DNA equals 33 µg/ml H_2O. Purity is given by the ratio Abs260 nm/Abs280 nm which should be equal or above 1.8. Values below 1.8 indicate that the preparation is contaminated with proteins and aromatic substances while values above 2 indicate a possible contamination with RNA.

4.3.3. Restriction enzyme digest

Digestion with restriction enzymes was performed according to the manufacture instructions in a 20 µl solution containing 1 µg of DNA, 1-10 U of restriction enzyme per 1 µg of DNA and 1x buffer. Alternatively, for cloning, digest of inserts or backbones were performed using higher amounts of DNA and higher or lower amounts of enzyme.

4.3.4. Agarose gel electrophoresis

Stock solution for agarose gels was prepared by adding the desired percentage of agarose to the TBE Buffer, boiling in the microwaves and keeping the solution in the oven at 60 ºC to avoid solidification. When a gel was needed, solution was taken out of the oven, mixed with ethidiumbromide (0.25 µg/ml) and added to the casting chamber. Comp was inserted and, after solidification the gel was taken into the electrophoresis chamber. TBE (1x) buffer was then added to the chamber.

When analyzing DNA from restriction digests 200 ng of DNA was mixed with 1x loading buffer in a total volume of 10 µl. These 10 µl were pipetted to a well of an agarose gel.

Electrophoresis was performed at 75 V and 200 mA.

TBE Buffer (10x; 5 l):	540 g Tris Base
	275 g Boric Acid
	200 ml of 0.5 M EDTA pH 8.0
	ad 5 l H_2O

4.3.5. Cloning

The following plasmids (Table 4) were obtained by site directed mutagenesis of their respective templates using overlapping PCR fragments (using the respective primers IP1 and OP2; IP2 and OP1) and ligation of fragments by a second PCR using the respective primers OP1 and OP2. After digest of the insert and backbone with the respective DNA restriction enzymes ligation was performed.

Table 4 Plasmids cloned by site directed mutagenesis.

Plasmid	Backbone	Insert Template	OP1 (Fw)	OP2 (Rv)	IP1 (Fw)	IP2 (Rv)	R. Site Back.	R. Site Insert
pRC A2	pRC	pRC	OP1 RC	OP2 RC	IP1 A2	IP2 A2	BsiWI/ XcmI	BsiWI/ XcmI
pRGD4C-453-A2	pRGD4C-453	pRGD4C 453	OP1 RC	OP2 RC	IP1 A2	IP2 A2	BsiWI/ XcmI	BsiWI/ XcmI
pRGD4C-587-A2	pRC	pRC A2	OP1 RC	OP2 RC	IP1 RGD4 C 587 A2	IP2 RGD4 C 587 A2	BsiWI/ XcmI	BsiWI/ XcmI
pRGD4C 453&587	pRGD4C-453	pRGD4C-453 / pRGD4C-587	OP1 RC	OP2 RC	IP1 RGD4 C 453&5 87	IP2 RGD4 C 453&5 87	BsiWI/ XcmI	BsiWI/ XcmI
pNGRI-453	pRC	pNGRI-453&587 / pRC	OP1 RC	OP2 RC	IP1 RGD4 C 453&5 87	IP2 RGD4 C 453&5 87	BsiWI/ XcmI	BsiWI/ XcmI
pNGRI-453-A2	pRC	pNGRI-453&587 / pRC A2	OP1 RC	OP2 RC	IP1 RGD4 C 453&5 87	IP2 RGD4 C 453&5 87	BsiWI/ XcmI	BsiWI/ XcmI
pGEN(A)-453	pRC	pRC	OP1 RC	OP2 RC	IP1 GEN(A)	IP2 GEN(A)	BsiWI/ XcmI	BsiWI/ XcmI
pGEN(A)-453-A2	pRC A2	pRC A2	OP1 RC	OP2 RC	IP1 GEN(A	IP2 GEN(A	BsiWI/ XcmI	BsiWI/ XcmI

					)	)		
paCEA-VP2	pGFP-VP2	pBW431-26-scFv	BWF	BWR			Bsp1407 I/BshTI	
pRC VP2 ko A2	pRC VP2 ko	pRC	OP1 RC	OP2 RC	IP1 A2	IP2 A2	BsiWI/ XcmI	BsiWI/ XcmI
paCEA-VP2-A2	paCEA-VP2	pRC	OP1 RC	OP2 RC	IP1 A2	IP2 A2	BsiWI/ XcmI	BsiWI/ XcmI
paCD30-VP2	paCEa-VP2	pRSV-HRS3					BamHI/ XbaI	BamHI /XbaI
paCD30-VP2-A2	paCD30-VP2	paCEA-VP2-A2					HindIII/ BsiWI	HindIII /BsiWI
paCD30LVP2-A2	paCD30-VP2-A2		OL LF	OL LR			BamHI	
paCD30L2VP2-A2	pCD30LVP2-A2		OL LF	OL LR			BamHI	
paCD30GLVP2-A2	paCD30-VP2-A2	paCD30-VP2-A2	OP1 GL	OP2 GL	IP1 GL	IP2 GL	Eco72I/ Eco91I	Eco72I/ Eco91I
paCD30LGLVP2-A2	paCD30LVP2-A2	paCD30LVP2-A2	OP1 GL	OP2 GL	IP1 GL	IP2 LGL	Eco72I/ Eco91I	Eco72I/ Eco91I
paCD30CLVP2-A2	paCD30LVP2-A2	paCD30LVP2-A2	OP1 GL	OP2 GL	IP1 CL	IP2 CL	Eco72I/ Eco91I	Eco72I/ Eco91I
paCD30CL2VP2-A2	paCD30L2VP2-A2	paCD30L2VP2-A2	OP1 GL	OP2 GL	IP1 CL	IP2 CL2	Eco72I/ Eco91I	Eco72I/ Eco91I
pOSaCD30-VP2-A2	paCD30-VP2-A2	paCD30-VP2-A2	OP1 OS	OP2 OS	IP1 OS	IP2 OS	Eco105I/ Eco91I	Eco105 I/Eco91 I
paCEALGLVP2-A2	paCEA-VP2-A2	paCD30LGLVP2-A2					BamHI	BamHI
pK1aCD30-VP2-A2	pOSaCD30-VP2-A2	pOSaCD30-VP2-A2	OP1 OS	OP2 OS	IP1 k1	IP2 K1	Eco105I/ Eco91I	Eco105 I/Eco91 I
paCD30-GFP-VP2	pGFP-VP2	pk1aCD30-VP2-A2					NheI	NheI/B amHI
pKaCD30-VP2-A2	pK1aCD30-VP2-A2	pK1aCD30-VP2-A2	OP1 OS	OP2 OS	IP1 K	IP2 K	Eco105I/ Eco91I	Eco105 I/Eco91 I
paCEA-GFP-VP2	paCD30-GFP-VP2	paCEA-VP2-A2					XbaI/ BamHI	XbaI/ BamHI

paCA19-GFP-VP2	paCD30-GFP-VP2	pCA19.9sc Fv	OP1 19	OP2 19			XbaI/ BamHI	XbaI/ BamHI
paCD30-GFP-VP2-A2	paCD30-GFP-VP2	paCEA-VP2-A2					EheI/ EcoRI	EheI/ EcoRI
paCEA-GFP-VP2-A2	paCEA-GFP-VP2	paCEA-VP2-A2					EheI/ EcoRI	EheI/ EcoRI
pCA19-GFP-VP2-A2	pCA19-GFP-VP2	paCEA-VP2-A2					EheI/ EcoRI	EheI/ EcoRI

4.4. Eukaryotic cell culture

4.4.1. Cultivation of cells

Cells were cultivated at 37 ºC and 5% CO_2 in humid atmosphere. For medium information see page 49. Cells were grown with antibiotics - Penicilin/Streptomycin (P/S).

4.4.2. Trypsinisation

Cells were washed with PBS, trypsin (0.5 g/L) was added in an amount that covered the bottom of the plates, followed by an incubation at 37 ºC (duration depending on the cell line). When the cells detached from the plate, reaction was stopped with medium containing at least 10% FCS.

4.4.3. Seeding / Passaging

Cells were transferred into a new plate or flask containing fresh medium, that was warmed up to 37 ºC. Agitation of the plate with movements in cross were made in order to spread the cells homogeneous and cultivation was performed.

4.4.4. Freezing and thawing cells

Cells were trypsinized, suspension collected in a falcon tube and pelleted at 1200 RPM. Supernatant was removed and cell pellet was re-suspended with freezing solution. 1 ml of cell suspension was added to each freezing vial and taken immediately into a slowly freezing chamber at -80 ºC.

For thawing the cells, the freezing vials were taken out of liquid nitrogen storage and the suspension let to thaw, after which it was taken to a flask or plate and medium that was warmed up to 37 ºC was added to the flask or plate.

Freezing solution: 90% FCS

10% DMSO

4.4.5. Counting

After trypsinizing and diluting the cells, 10 µl were transfered into a hematocytometer. The number of cells in each of the four squares was counted and an average was made for more precise determination. The amount of cells (n) determined equals n x 10^4 per ml.

4.5. Production of AAV-2 vectors

4.5.1. Production of HBS-buffer

Weighted:

5.955 g HEPES

8.18 g NaCl

1.5 ml 0.5 M NaP (pH 7.29)

HEPES and NaCl were dissolved in endotoxin free water (Sigma) to a final volume of 400 ml and 5 aliquots of 20 ml were used to adjust the pH to 6.6; 6.7; 6.8; 6.9 and 7.0, respectively, using a "Mettler Toledo seveneasy" pH meter. The aliquots were sterile filtrated and used to test which of the different pH values is more efficient in the formation of CaP crystals for transfection of DNA into cells. The pH of the original solution was then adjusted and endotoxin free water was added until 375 ml. The solution was then sterile filtrated.

4.5.2. AAV vector packaging

15 cm petris dishes were used for seeding 7.5 x10^6 293 cells/plate in 25 ml DMEM with Glutamax plus 10% FCS and 1% P/S.

24 hours later (cells showed approximately 80% confluence) medium was exchanged to 10% FCS and 1% P/S (approximately ~ 25ml/plate).

The transfection was performed 2 hours later:

1 ml 250 mM CaCl$_2$

7.5 µg pRC (or mutated pRC plasmid; codes for the viral proteins necessary for viral replication and for the capsid proteins)

7.5 µg pTransgene (codes for the transgene that is flanked by the viral packaging signals to allow the transgene to be packaged into the viral capsid)

22.5 µg pXX6-80 (codes for E2a, E4 and VA of Ad 5)

(when one of the viral capsid proteins -VP2- was supplied *in trans* as a fusion protein 7.5 µg of pscFv-VP2 were added additionally)

Solution was mixed by vortexing and 1 ml HBS-Puffer slowly added. Solution was once more mixed by vortexing and exactly 2 minutes after, the solution was added to the cells.

24 hours later (approximately 100% confluence), medium was exchanged with 20 ml DMEM with Glutamax plus 2% FCS and 1% P/S.

The cells were harvested 24 hours later by scrapping them from of the plate, collecting them in a conic centrifuge tube and centrifuging them at 1500 RPM for 15 min. The supernatant was wasted and the pellet re-suspended in 500 µl of lysis buffer per plate harvested (150 mM NaCl; 50 mM Tris/HCl, pH 8.5). The cells were 3 times submitted to thermal shock by using liquid nitrogen and a water bath at 37 ºC.

To avoid contaminations with cellular DNA or RNA, or plasmid DNA, the suspension was treated with 50 U of Benzonase per ml of suspension at 37 ºC for 30 min.

The falcons were centrifuged for 30 min, at 4 ºC, 4000 RPM; solution was transferred into a new falcon (pellet was discarded) and filled up with PBS to 11 ml, centrifuged again for 30 min at 4 ºC and 4000 RPM.

4.5.3. Iodixanol gradient purification

An iodixanol step gradient centrifugation was performed using four different iodixanol solutions (see below for the composition of each solution). After adding the viral solution to the tube used for centrifugation a needle reaching the bottom of the tube was used to slowly add (using an "Amersham Biosciences Pump P-1") all the solutions starting with the lightest one and ending with the heaviest one.

The centrifugation was performed at 63000 RPM for 2 h at 4ºC and subsequently the 40% iodixanol phase harvested.

15% Iodixanol :		25% Iodixanol :		40% Iodixanol:	
10xPBS	5 ml	10xPBS	5 ml	10xPBS	5 ml
1M MgCl$_2$	50 µl	1M MgCl$_2$	50 µl	1M MgCl$_2$	50 µl
2.5M KCl	50 µl	2.5M KCl	50 µl	2.5M KCl	50 µl
5M NaCl	10 ml	Optiprep	20 ml	Optiprep	33.3 ml
Optiprep	12.5 ml	0.5% Phenolred	75 µl	Sigma water	ad 50 ml
0.5% Phenolred	75 µl	Sigma water	ad 50 ml		
Sigma water	ad 50 ml				

60% Iodixanol:		PBS M/K:	
1M MgCl$_2$	50 µl	10xPBS	50 ml
2.5M KCl	50 µl	1M MgCl$_2$	0.5 ml
Optiprep	50 ml	2.5M KCl	0.5 ml
0.5% Phenolrot	25 µl	Sigma water	ad 0.5 l

4.6. Vector titration

4.6.1. Genomic titer

For extraction of genomic DNA from viral particles the "Qiagen DNeasy Tissue Kit" was used and the protocol for "Isolation of Total DNA from Cultured Animal Cells" was performed.

10 µl of virus were diluted in 200 µl of PBS; 20 µl of Proteinase K (25 mg/ml) and 200 µl of Buffer A was added and the solution was mixed by vortexing. After 10 min incubation at 70 ºC, 200 µl of ethanol (96-100%) was added and the solution was again mixed by vortexing. The mixture was then pipetted into the DNeasy Mini Spin Column placed in a 2 ml collection tube. A centrifugation at 8000 RPM for 1 min was performed, the flow through was discarded and the column placed in a new 2 ml

collection tube. 500 µl of buffer AW1 was added and a centrifugation was performed as before. After adding a new 2 ml collection tube 500 µl of buffer AW2 were added and a centrifugation was done for 3 min at 14000 RPM. The flow through was discarded and a clean 1.5 ml reaction tube was used. 200 µl of 100 mM Tris pH 8.0 was added to the column and incubated for 1 min at room temperature. Elution was performed by centrifuging at 8000 RPM for 1 min.

The genomic titer was then determined by Real Time Polymerase Chain Reaction (RT-PCR) using a "Roche LightCycler FastStart DNA Master SYBR Green I" kit.

Primers: EGFP-1 forward (sense); EGFP-1 reverse (anti-sense)

LightCycler protocol:

#	Cycles	Analysis Mode	Target Temp.	Inc. Time	Temp. Transition Rate (°C/s)	Secondary Target Temp.	Step Size (°C)	Step Delay (Cycles)	Acquisition Mode
1	1	None	95	10 sec	20.00	0	0.0	0	None
2	40	Quantification	95	10 sec	20.00	0	0.0	0	None
			64	5 sec	20.00	0	0.0	0	None
			72	10 sec	20.00	0	0.0	0	Single
3	1	Melting Curves	95	0 sec	20.00	0	0.0	0	None
			67	10 sec	20.00	0	0.0	0	None
			95	0 sec	0.10	0	0.0	0	Cont
4	1	None	40	30 sec	20.00	0	0.0	0	None

4.6.2. Transducing titer

7.0×10^4 HeLa cells were seeded in each well of a 12-well plate. 24 h later eight dilutions of the vector solution were made (dilutions of 1 to: 5.0×10^2; 5.0×10^3; 5.0×10^4; 5.0×10^5; 1.65×10^3; 1.65×10^4; 1.65×10^5; 1.65×10^6). The medium in the wells was substituted by each vector dilution. Three wells were used as negative control. To

verify if vector particles are responsible for cell transduction one well was used to perform a "heparin control". For this the lower dilution of the vector was added together with 425 IU of heparin to a well in replacement of the old medium. After 48 h of incubation at 37 ºC and 5% CO_2 the cells were trypsinized, washed with PBS, the number of cells in the negative control was counted and the probes analyzed by Fluorescent Activated Cell Sorting (FACS).

A gate was established having 1% of the cells in the control as background fluorescence. The same gate was then used for determining the results of the different dilutions. Based on the amount of cells in the control, the amount of GFP expressing cells obtained from each dilution and the respective dilution factor, the transducing titer was determined using 10% of GFP expressing cells (10% equals MOI = 0.1; each GFP expressing cell is the result of a single vector transduction) as reference.

4.6.3. Capsid titer

The determination of the capsid titer was performed using the monoclonal anti-AAV intact particle A20 antibody.

Based on the genomic titer and the fact that the capsid titer is normally 10x higher, eight serial dilutions were made in PBS in order to obtain concentrations in the linear range of the ELISA (between $1.0x10^7$ and $1.0x10^9$ capsids/ml). An AAV preparation which titer was previously determined using the commercially available AAV titration kit (Progen) was used as standard.

Nunc-Immunoplates were coated with 100 µl of each respective vector dilution and incubated overnigh at 4 ºC. Next morning after three washing stepts with Washing Buffer using 200 µl per well, Blocking Buffer was added to the wells (200 µl/well). After an incubation for 2 h at room temperature Blocking Buffer was removed and A20 antibody (supernatant, diluted 1:4 in Blocking Buffer) was added (100 µl/well). Another incubation step at room temperature was performed this time for 1 h followed by another 3 washings like before. Biotin conjugated anti-mouse antibody diluted 1:25,000 in Blocking Buffer, was added to the well (100 µl/well) and incubation performed for 1 h. After another 3 washings like before, Horseradish-Peroxidase conjugated streptavidin diluted 1:500 in Blocking Buffer was added to the wells (100 ml/well) and incubation was performed for 1 h at room temperature. After

performing 3 washings like before and 2 washings with water (200 µl/well) Start Solution was added to the wells (100 µl/well).

Color reaction was stopped by adding 50 µl of Stop Solution into each well and the intensity of the color reaction was measured using a photometer at 450 nm.

Washing Buffer:	0.05% Tween20
	in PBS
Blocking Buffer:	3% BSA
	5% Sucrose
	0.05% Tween20
	in PBS
Start Solution:	1 mg TMB
	100 µl DMSO
	10 ml of 0.1 M NaOAc pH 6.2
	1 µl of 30% H_2O_2
Stop Solution:	1 M H_2SO_4

4.7. Cell transduction

Cells were seeded and 24 h thereafter incubated with the respective vectors. In transduction assays where GFP was used as transgene the cells were harvested 48 h p.t., washed and resuspended in PBS. The percentage of GFP expressing cells was determined by flow cytometry using a BD FACS Calibur system. A minimum of 5000 cells was counted for each sample.

4.7.1. Competition studies

Competition studies were performed by transducing cells with rAAV-2 capsid mutants and respective controls in the presence or absence of 300 µM of GRGDS or GRGES peptides or 5 IU/µl soluble heparin. Values were normalized to non-

competed transductions and the respective inhibition values were calculated as the difference to the respective non-competed transductions.

4.7.2. Binding particles

4 h post-infection cells were washed 4 times with PBS and scraped from the wells. For isolation of DNA the "Qiagen DNeasy Tissue Kit" was used and the protocol for "Isolation of Total DNA from Cultured Animal Cells" was performed. Amount of vector genomes found in the cells was determined by quantitative PCR using the primers: EGFP-1 forward and EGFP-1 reverse. Relative amount of binding particles was calculated as the ratio of amount of detected particles-to-amount of given particles.

4.8. Protein techniques

4.8.1. Protein quantification

Protein quantification was done using a BioRad Quick Start Bradford Protein Assay.

The 1x dye reagent was removed from the 4 ºC storage, warmed up to ambient temperature and inverted a few times before use. Each standard and unknown sample solution was pipeted into separate clean test tubes. The 1x dye reagent was added to each test tube and mixed by vortexing. Incubation was performed for 5 min at room temperature. Protein solutions and standards were assayed in triplicate.

The spectrophotometer was set to 595 nm. The zero was made using the blank samples (0 µg/ml using water and dye reagent).

4.8.2. Western blot

Western blot analysis was performed on protein extracts obtained from vector packaging (see Page 61, AAV vector packaging) or on iodixanol gradient purified vector solutions. Laemmli Buffer was added and the samples were boiled at 98 ºC for 5 min. If not indicated 30 µg of protein or 1.0×10^{10} vector particles were loaded into

the gel. Running buffer was added in agreement with chamber manufacturer specifications and the electrophoresis was performed at 80 V and 25 mA.

After protein separation by SDS-PAGE the proteins were transferred to a nitrocellulose transfer membrane (Hybond-ECL from Amersham Bioscience) using a "BioRad Mini Trans-Blot Electrophoretic Transfer Cell" in agreement with the manufactures' instructions.

After blotting the membrane was blocked using 5% milk powder and 0.1% Tween 20 in PBS during 60 min shaking at RT. The blocking solution was substituted by the primary antibody solution (B1, supernatant, diluted 1:20 in Blocking Buffer) and left for 1h shaking at room temperature. Three washing steps were performed – 3x 0.1% Tween/PBS shaking for 5 min at RT. The solution on the membrane was re-placed by the secondary antibody (anti-Mouse/PO diluted 1:10,000 in Blocking Buffer) and left for 1 h shaking at RT. Three washing steps like before, and 2 ml of the substrate solution for the peroxydase-conjugated secondary antibody was added to the membrane after which the substrate solution was spread throw the membrane by using a plastic foil in which the membrane was inserted. A radiographic film was exposed to the membrane and subsequently the development of the film was done.

Laemmli Buffer:	50 mM Tris pH 6.8
	100 mM DTT
	2% SDS
	50% Glycerol
	0.2 g/ml BPB (stored at -20ºC)
Transfer buffer pH 8.3:	0.30% Tris Base
	1.44% Glycin;
	0.02% SDS
Stacking gel, 5% (2 ml):	1.4 ml distilled water
	0.33 ml acrylamide stock solution, 30% (w/v)
	0.25 ml 1.0 M Tris (pH 6.8)
	0.02 ml 10% sodium dodecyl sulfate (SDS)
	0.02 ml 10% ammonium persulfate (APS)
	2 µl N,N,N,N-Tetramethylethylenediamine

Resolving gel, 8% (5 ml):   2.3 ml distilled water

1.3 ml acrylamide stock solution, 30% (w/v)

1.3 ml 1.5 M Tris (pH 8.8)

0.05 ml 10% SDS

0.05 ml 10% APS

3 µl TEMED

4.8.3. ELISA

4.8.3.1. Integrin binding assay

Outer surface display of the RGD4C peptide and its ability to bind to soluble integrin was determined by ELISA. Two Nunc-Immunoplates were coated with purified anti-AAV-2 capsid antibody A20 (1 µg/ml diluted in PBS) overnight at 4 ºC. Next, plates were washed three times with Washing Buffer (200 µl/well). Unspecific binding was blocked by incubation with Blocking Buffer for 2h at RT (200 µl/well). 1×10^{10} particles per well were added to the plate diluted in blocking buffer. Incubation was performed for 2 h at RT, followed by a washing step as described above. One plate was used to determine soluble receptor binding ability of the different vectors (ELISA A), the other plate was used to determine the amount of intact viral capsids per well (ELISA B).

ELISA A: αVβ3 integrin, 1 µg/ml, was added to the plate diluted in Binding Buffer (100 µl/well). Incubation was performed as before, followed by another washing step and incubation with anti-integrin αV C-terminal intracellular antibody diluted in Binding Buffer (1 µg/ml, 100 µl/well). After incubation at RT for 2 h, followed by a washing step, a peroxidase-conjugated anti-rabbit antibody diluted in Binding Buffer (1:10,000) was applied (1 h at RT, 100 µl/well).

ELISA B: Biotinylated anti-AAV-2 A20 antibody, diluted 1:20 in Blocking Buffer was added to the plate. Incubation and washing steps were performed as before followed by incubation with streptavidin-peroxidase.

After 2 h of incubation with peroxidase-conjugated anti-rabbit antibody (ELISA A) or with streptavidin-peroxidase (ELISA B) at RT, plates were washed once with washing buffer and twice with water before the peroxidase reaction was started as describe above (as described above, 4.6.3. Capsid titer). The reaction was

stopped after 10 min and the reaction product was measured ($Abs_{\lambda=450nm}$). Relative receptor binding was calculated as the ratio of ELISA A ($\alpha V\beta 3$ binding) to ELISA B (intact AAV particles).

4.8.3.2. Anti-GFP and anti-idiotypic ELISA

ELISA plates were coated with the respective capturing antibody and incubation performed for 2 h at room temperature. After one washing step as described above unspecific binding was blocked by incubation with Blocking Buffer overnight at 4 °C.

Next day protein solution was added to the plates diluted in Blocking Buffer and incubated for 2 h at RT. After another washing step detection antibody was diluted in Blocking Buffer and added to the wells. After 2 h of incubation at RT another washing step was performed. A peroxidase conjugated streptavidin or secondary antibody was added and incubation performed for another 2 h at RT. After one washing step and two times "washing" with water the peroxidase reaction was started and stopped as described above.

Alternatively, plates were coated with the analyzed proteins (vectors).

The following antibodies were used in the various ELISAS.

Antibody:	Final concentration:
Anti-GFP	1 µg/ml
9G10	10 µg/ml (as capture Ab)
	2.5 µg/ml (as detection Ab)
IgG control	10 µg/ml (as capture Ab)
	2.5 µg/ml (as detection Ab)
A20	2.5 µg/ml
Washing Buffer:	1% Tween20
	in PBS

Blocking Buffer:	1% Milk Powder
	1% Tween20
	in PBS

Binding Buffer :	20 mM Tris-HCl
	15 mM NaCl
	2 mM CaCl$_2$
	1 mM MgCl$_2$
	1 mM MnCl$_2$,
	1% Milk Powder
	1% Tween20
	in PBS
	pH 7.5

4.9. Immunophenotyping

At the time point of vector transduction, cells in control wells were harvested, washed twice and incubated with a primary antibody in agreement with manufacter instructions. After 30 min of incubation on ice and two washing steps, incubation with a secondary antibody (goat polyclonal anti-mouse IgG Phycoerythrin conjugated) was performed.

Antibody binding was determined by flow cytometry using a BD FACS Calibur system. A minimum of 5000 cells was counted for each sample.

4.10. Biodistribution study in mice

7 week old C57BL6 female mice were purchased from Charles River Laboratories (Charles River Laboratories, Wilmington, USA). 1.0×10^{10} genomic particles were injected into the tail vein. Organs were harvested 42 h p.i. and DNA was isolated (QIAGEN DNeasy Tissue Kit). Using the GAPDH gene as reference relative quantification of transgene was done using quantitative PCR (using the ROCHE, SYBR Green kit) and the following primers: GFPm_f and GFPm_r; GAPDHm_f and GAPDHm.

5. Results

5.1. G453 as a new AAV-2 insertion site

Most published targeting approaches are based on insertion of small peptide ligands within the *cap* open reading frame (ORF). This ORF codes for three structural proteins - VP1 (90 KDa), VP2 (72 kDa), and VP3 (60 kDa) - that share most of their amino acid sequence and that build up the capsid at a 1:1:10 ratio (105). Preferred sites for peptide insertions are amino acid position 587 and 588 (according to VP1 numbering), which are located in a region common to all three capsid proteins.

Other sites within the *cap* gene of AAV-2 also tolerate insertion of small peptides (63, 66, 102, 171, 174, 198). Four of these sites (amino acid position 34, 447, 520 and 584) have been examined for their usefulness in AAV vector targeting (63, 174, 198). Mapping of all targeting insertion sites and analysis of the accessible surface profile of AAV-2 revealed that none is found at the most prominently exposed region of the AAV-2 capsid (Figure 9 A, B). Instead, T454, located in the β-turn - S452, G453, T454, T455 - connecting the anti-parallel β strands GH2 and GH3 emerged as the most accessible and exposed residue on the AAV-2 capsid flanked by two also well exposed residues – G453 and T455 (Figure 9 A, B, C). Just like N587, T454 makes part of one of the 3 GH loops that build up the "threefold-proximal" peaks clustered around each icosahedral threefold rotation axis (Figure 9C, D). β-turns are commonly found to link two strands of anti-parallel β-sheet, forming a β-hairpin, and such secondary structure elements have been postulated as possible nucleation sites for the protein folding pathway (47, 48, 99). Interestingly, insertions at N587 – also located in a β-turn – are well tolerated while insertions in the GH2/GH3 β-strands are not (62). Indeed, it is also known that helices and β-sheets are the major stabilizing structures in proteins. Thus, by comparison with N587, insertion of targeting peptides at a better exposed position like G453 (between G453 and T454) should result in mutants with higher affinity to their target receptor.

A)

B)

C)

VP3 capsid protein

D)
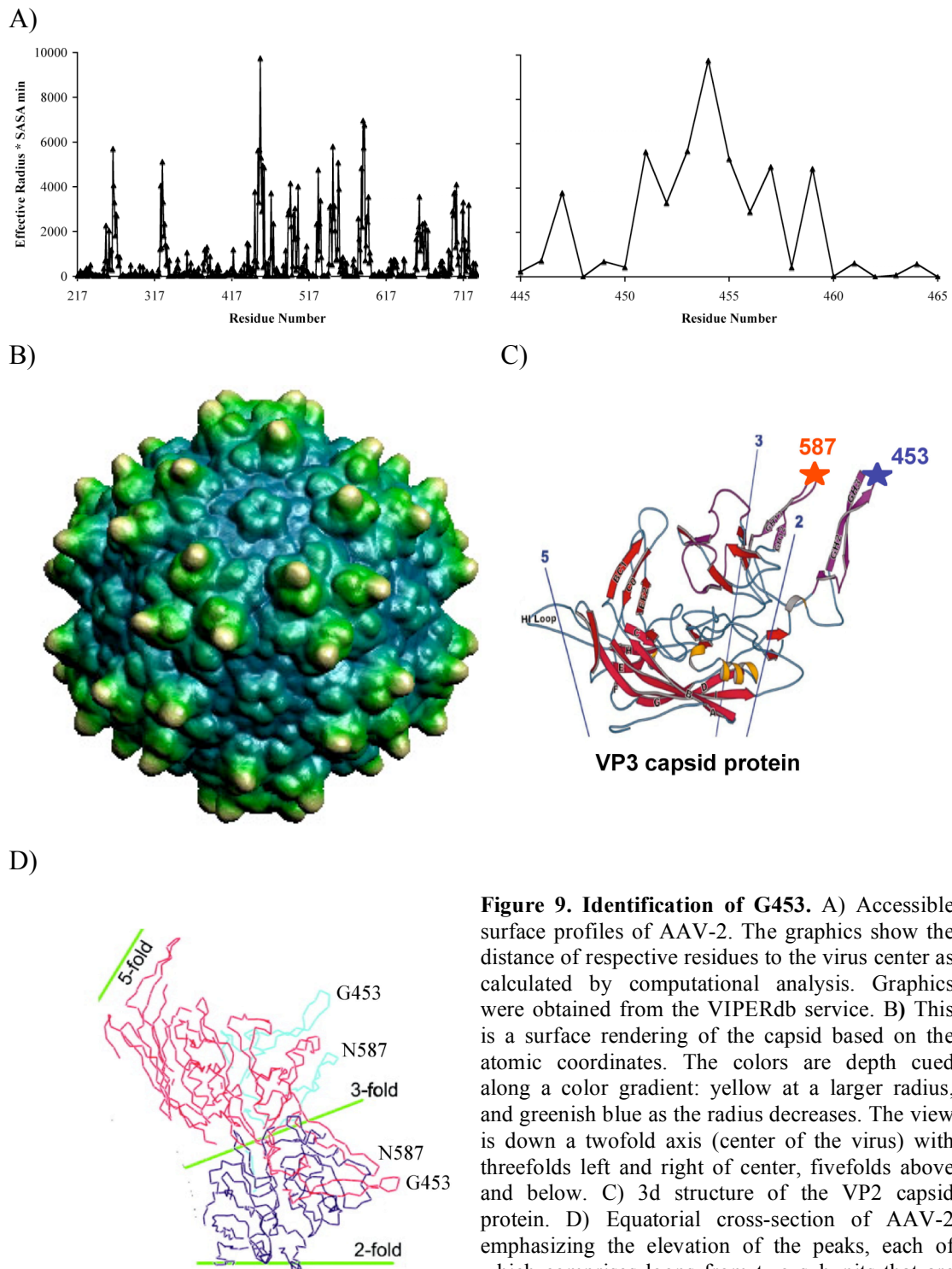
Figure 9. Identification of G453. A) Accessible surface profiles of AAV-2. The graphics show the distance of respective residues to the virus center as calculated by computational analysis. Graphics were obtained from the VIPERdb service. B) This is a surface rendering of the capsid based on the atomic coordinates. The colors are depth cued along a color gradient: yellow at a larger radius, and greenish blue as the radius decreases. The view is down a twofold axis (center of the virus) with threefolds left and right of center, fivefolds above and below. C) 3d structure of the VP2 capsid protein. D) Equatorial cross-section of AAV-2 emphasizing the elevation of the peaks, each of which comprises loops from two subunits that are colored differently. (156, 202)

5.1.1. Insertion of the RGD4C peptide

To explore if position 453 is suitable for the display of targeting peptides and to compare the usefulness of this exposed position with the traditionally preferred

position (587/588), we designed a set of AAV capsid mutants carrying a model ligand at position 453, 587 or both (Figure 10). Mutants carrying an insertion at position 453 are expected to be able to use HSPG as the primary receptor just like wild-type AAV-2 (r-wt). Two arginine-to-alanine substitutions of residues R585 and R588 (A2) have been shown to eliminate AAV-2's HSPG binding (135). We therefore designed a second 453 insertion mutant with R585A and R588A substitutions. For comparison, the same substitutions were combined with peptide insertion at position 587 and with a double peptide insertion (Figure 10). As a model ligand we chose RGD4C – ACDCRGDCFCA – since it is known to target cellular and soluble integrin receptors (eg. $\alpha V\beta 5$ and $\alpha V\beta 3$ integrins), competing peptides are commercially available, and it has already been used for re-targeting of AAV-2 (4, 172, 174). An overview of the different capsid insertion mutants with details on the respective capsid modifications is provided in Figure 10.

Vector	Cap amino acid sequence	
	453	587
r-wt	…PSGTTT……………………………RGNR…	
r-A2	…PSGTTT………………….…..*A*GN*A*…	
r-RGD4C-453	…PSG<u>ACDCRGDCDFCA</u>TTT…….. RGNR…	
r-RGD4C-453-A2	…PSG<u>ACDCRGDCDFCA</u>TTT…….. *A*GN*A*…	
r-RGD4C-587	…PSGTTT…………………….... RGN<u>ACDCRGDCDFCA</u>R….	
r-RGD4C-587-A2	…PSGTTT…………………….... *A*GN<u>ACDCRGDCDFCA</u>*A*….	
r-RGD4C-453&587	…PSG<u>ACDCRGDCDFCA</u>TTT…….. RGN<u>ACDCRGDCDFCA</u>R…	
r-RGD4C-453&587-A2	…PSG<u>ACDCRGDCDFCA</u>TTT…….. *A*GN<u>ACDCRGDCDFCA</u>*A*…	

Figure 10. Amino acid sequence of the different viral vectors. Depicted is the amino acid sequence of r-wt, r-A2 and the different capsid insertion mutants in the region around position 453 and 587. The inserted RGD4C peptide motif (ACDCRGDCFCA) flanked by alanine residues is underlined. R585A and R588A substitutions are shown in *italic*.

From all six capsid insertion mutants spatial models were created *in silico*. Based on these models, the inserted RGD motif should be displayed on the capsid surface pointing away from the opposite spike. Examples are presented in Figure 11.
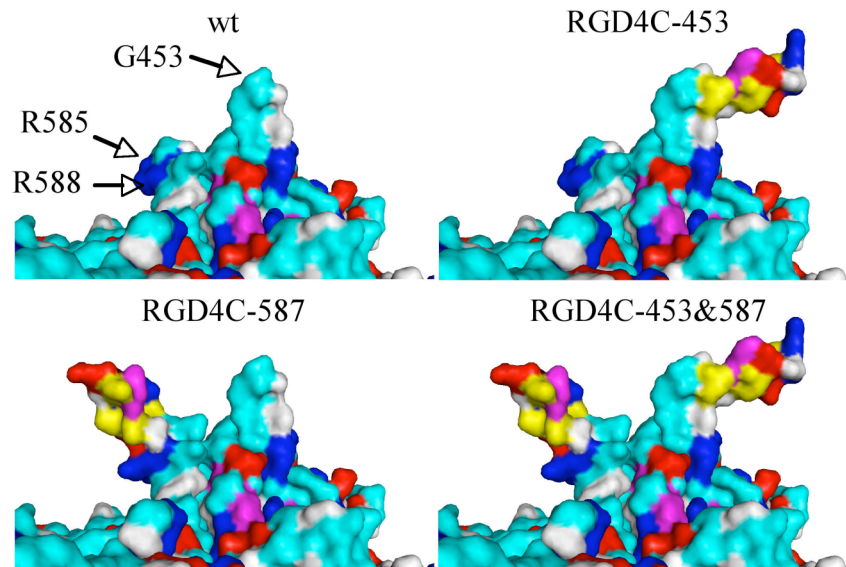
Figure 11. Spatial models of capsid insertion mutants. A) Close-up of the 3-fold symmetry axis in wild-type AAV-2 showing G453 at the top of the spike. Picture B), C) and D) spatial models of mutants carrying the RGD4C peptide motif (ACDCRGDCFCA) at position 453, 587 or both positions. Colors used in A) to D): white = hydrophobic; yellow = semipolar; cyan = polar; blue = positive; red = negative and magenta = aromatic amino acids.

5.1.1.1. RGD4C insertion at 453 does not interfere with vector packaging or cell transduction

We produced the various capsid insertion mutants as recombinant AAV-2 vectors coding for green fluorescent protein. As controls, r-wt and a r-AAV-2 capsid mutant with R585A and R588A substitutions (r-A2) were produced (Figure 10). All vectors showed comparable genomic particle titers ranging from 1.55×10^{11} per ml for r-RGD4C-453&587 to 1.11×10^{12} per ml for r-wt (Table 5).

The capsid titer was determined by ELISA and used to calculate the total-to-full particle ratio to directly compare the different vectors for packaging efficiency. As depicted in Table 5, all vectors showed comparable ratios ranging from 15 for r-wt to 2.2 for r-RGD4C-453&587-A2.

Table 5. Vector titers of r-wt, r-A2 and RGD4C insertion mutants. n.d. = not determined; u.d.l. = under detection limit; wt = phenotype comparable to AAV with wild-type capsid according to Kern and colleagues. (a): Numbers indicate independent packaging; (b): genomic titers determined by quantitative PCR, shown is the mean value of 3 titrations; (c): capsid titer was determined by ELISA using A20 (antibody, which recognizes intact AAV-2 capsids), shown is the mean value of 2 titrations; (d): definition according to Kern and colleagues (97): wt phenotype indicates a packaging ratio of < 50; (e): determined on HeLa cells, shown is the mean value of 2 titrations; (f): provides a simple comparison of how many genome-containing particle of each mutant were required to achieve the same number of transduced HeLa cells as with one AAV-2 with wild-type capsid (definition according to Opie and colleagues (135)).

vector preparation (a)	gen. titer (per ml) (b)	cap. titer (per ml) (c)	packaging efficiency (cap-to-gen ratio)	phenotype based on cap-to-gen ratio (d)	transducing (inf.) titer (per ml) (e)	cap-to-inf ratio	rel. cap-to-inf value (f)
r-wt	7.07E+11	1.09E+13	15.4	wt	6.84E+10	159	1
r-wt (2)	7.29E+11	7.21E+12	9.9	wt	n.d.	-	-
r-A2	1.11E+12	1.00E+13	9.1	wt	2.75E+07	365382	2302
r-RGD4C-453	4.97E+11	1.12E+12	2.3	wt	1.63E+08	6886	43
r-RGD4C-453-A2	6.12E+11	1.54E+12	2.5	wt	2.55E+08	6047	38
r-RGD4C-453-A2 (2)	5.32E+11	7.33E+12	13.8	wt	n.d.	-	-
r-RGD4C-587	4.73E+11	1.17E+12	2.5	wt	1.22E+08	9588	60
r-RGD4C-587-A2	2.42E+11	2.83E+12	11.7	wt	6.45E+08	4385	28
r-RGD4C-453&587	1.55E+11	1.34E+12	8.7	wt	u.d.l.	-	-
r-RGD4C-453&587 A2	2.25E+11	5.02E+11	2.2	wt	u.d.l.	-	-

For detecting if all viral preparations possessed the correct ratio of viral proteins VP1:VP2:VP3 – 1:1:10 respectively (105) – Western blot analysis was performed (Figure 12). As expected, all viral preparations showed the correct VP1:VP2:VP3 ratio and insertion mutants showed a retarded migration pointing towards an increase in protein size. Unexpectedly, proteins with A2 mutations also showed slower migration when compared to their R585 and R588 homologues.
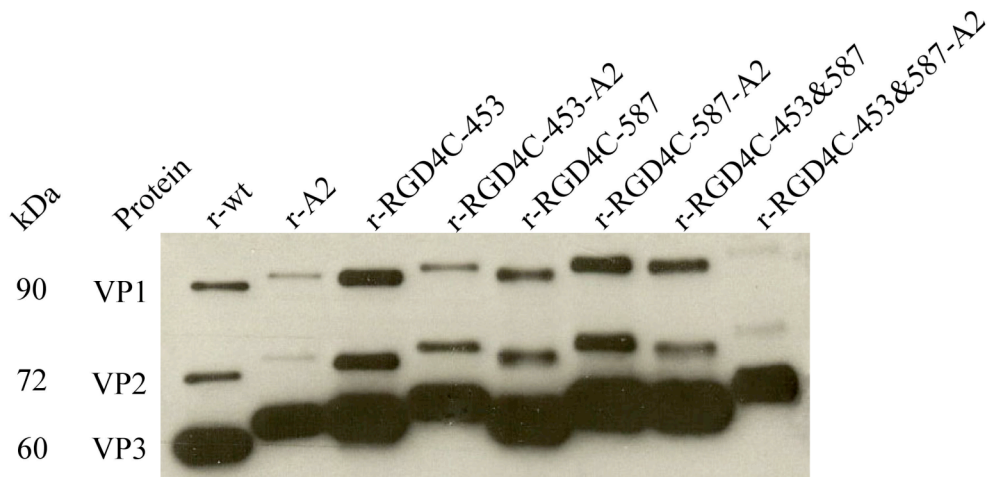
Figure 12. Western blot analysis of iodixanol gradient-purified AAV capsids. After iodixanol gradient purification the same amount of viral capsids (10^{10}) were separated by sodium dodecyl sulfate - 8% polyacrylamide gel electrophoresis and analyzed by Western blotting with the B1 antibody.

We used the cervix carcinoma cell line HeLa, known to express HSPG (73) and $\alpha V\beta 5$ (172), and to be susceptible to AAV transduction/infection (73), to determine the transduction efficiency of the different capsid insertion mutants in

comparison to r-wt and r-A2. The values obtained were used to calculate the capsid-to-infectious particle ratio to compare the different vectors for their transduction ability.

As depicted in Table 5, r-wt showed the best transduction efficiency while r-A2s' ability to transduce HeLa cells was significantly reduced, most likely due to its inability to bind to HSPG. Interestingly, both double insertion mutants showed an even lower transduction ability than r-A2 revealing that such mutants are severely impaired in transduction. With or without the combination with A2 mutations, all single insertion mutants were able to efficiently transduce HeLa cells. Of notice is the fact that the combination of RGD4C insertion with A2 mutations resulted in a slight increase in transduction efficiency (cap-to-inf ratio of: r-RGD4C-453 vs. r-RGD4C-453-A2 and r-RGD4C-587 vs. r-RGD4C-587-A2). With r-wt as a reference, r-RGD4C-587-A2 showed the lowest decrease in transduction efficiency on HeLa cells (rel. cap-to-inf value).

5.1.1.2. Inserted peptide is displayed on the capsid surface and is able to bind its target receptor

Next, we determined whether the inserted peptide is exposed on the surface of the different capsid insertion mutants and is able to bind its receptor, $\alpha V\beta 3$ integrin. Although at varying degrees all insertion mutants were able to bind the target molecule while r-wt and r-A2 did not show any binding (Figure 13).

Unexpectedly, r-RGD4C-453 and r-RGD4C-587 showed the lowest receptor binding ability of all insertion mutants. This was surprising since 453/454 is the most exposed position of the capsid (Figure 9) and should therefore allow a good access to its target receptor, and 588 has already been used successfully to create RGD4C containing AAV-2 based targeting vectors (172). Even more striking was the observation that for both insertion sites, the combination of peptide insertion with R-to-A substitutions significantly enhanced target molecule binding (50-fold for r-RGD4C-453-A2, 33-fold for r-RGD4C-587-A2). Although to a smaller degree, the same was observed with the double insertion mutants (1.1-fold) (Figure 13).
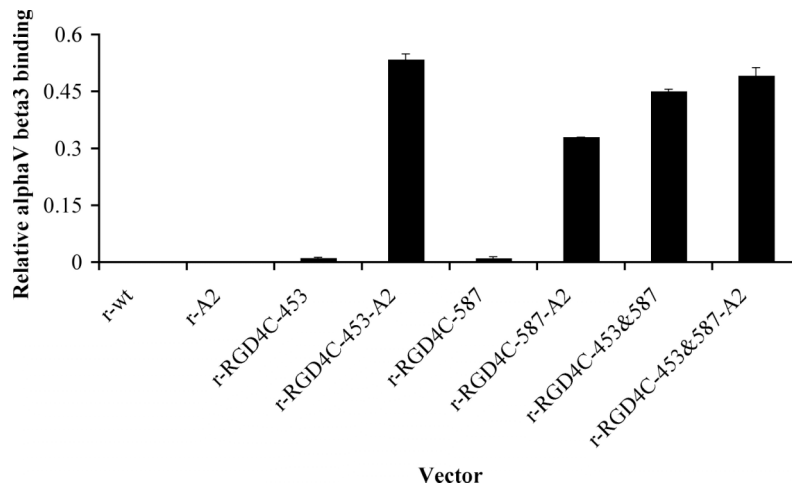
Figure 13. Binding of r-RGD4C mutants to their target receptor. The ability of intact viral capsids to bind a soluble RGD4C receptor - αVβ3 integrin - was determined by ELISA. Two independent experiment were performed. Shown is the mean value of αVβ3 molecules detected per intact capsid from triplicate measurements with error bars representing the standard error of the mean.

Since double insertion mutants should contain two RGD4C motifs per capsid protein, both double insertions mutants were expected to show superior target receptor binding in comparison to single insertion mutants. This was indeed the case when comparing the double insertion mutants with r-RGD4C-453, r-RGD4C-587 and r-RGD4C-587-A2. Interestingly, despite the efficient binding to their target receptor double insertions mutants revealed a deficiency in transduction ability (Table 5). r-RGD4C-453-A2 emerged as the mutant with the highest amount of receptors bound per intact capsid. This confirms our initial hypothesis and highlights the potential of this position for mediating efficient ligand-receptor interactions.

5.1.1.3. Cell transduction is mediated by inserted peptide

To assess the specificity of the capsid insertion mutants HeLa cells were transduced by the different vectors in the presence of a competing GRGDS peptide, a non-competing GRGES control peptide or the HSPG analogue heparin (Figure 14A).

Both controls, r-wt and r-A2, showed the expected results. No competition with GRGDS or GRGES was observed for r-wt and r-A2. Furthermore, addition of heparin completely abolished cell transduction by r-wt but not by r-A2. Although the r-RGD4C-453 capsid contained RGD4C peptides, no interference was observed after addition of GRGDS peptide or GRGES peptide, while addition of heparin abolished cell transduction. In contrast, transduction of HeLa cells by r-RGD4C-453-A2, r-

RGD4C-587, r-RGD4C-587-A2 and the double insertion mutants were competed by the GRGDS peptide, whereas the GRGES peptide or heparin had no effect.
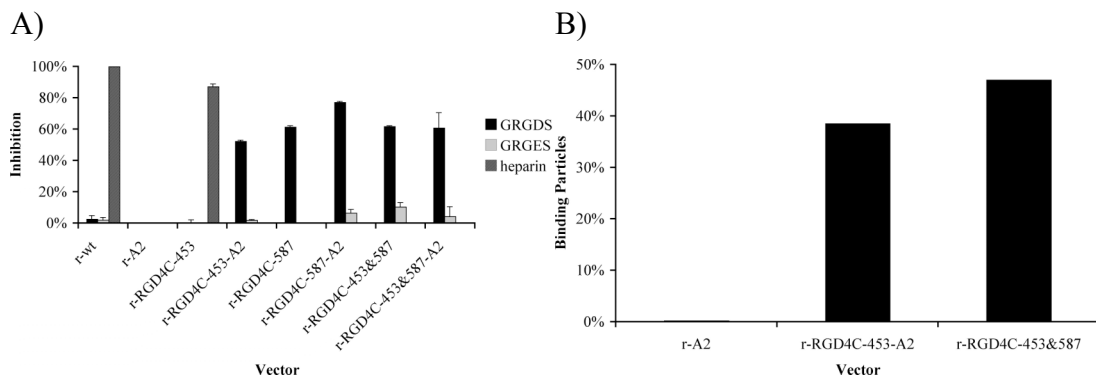
Figure 14. Specificity of r-RGD4C mutants. HeLa cells were transduced by the different vectors. Approximately 50% of transduction efficiency was achieved with each vecto. A) Transduction was performed in the presence of competing GRGDS or control GRGES peptides or soluble heparin. Shown is the mean value of two independent experiments performed in triplicates. Error bars represent the standard error of the mean. B) 4h post-transduction cells were washed 4 times with PBS and scraped out of the wells. Amount of vector genomes found in the cells was determined by quantitative PCR. Show is the ratio between the amount of viral genomes used for transduction and the amount of viral genomes determined 4h post-transduction.

In agreement with these results and with the fact that both double insertion mutants showed an efficient binding to their target receptor (Figure 13) is the observation that 4 hours p.i. the same relative amounts of r-RGD4C-453&587 and r-RGD4C-453-A2 can be found with cells (Figure 14 B) while no r-A2 can be detected. This shows that double insertion mutants' low ability of cell transduction is the result of a non-effcient post-binding step.

These results demonstrate that r-RGD4C-453-A2, r-RGD4C-587, r-RGD4C-587-A2 and the double insertion mutants transduce cells independently from AAV-2s' primary receptor, but through the specific interaction of the inserted RGD4C motif presented on the viral capsid with an integrin receptor expressed on the cell surface.

5.1.1.4. r-RGD4C-453-A2 shows superior transduction on CHO pgsA-745

Next, we assessed the different capsid insertion mutants for their ability to transduce the Chinese Hamster Ovarian (CHO) cell derivative pgsA-745. CHO pgsA-745 cells contain a defect in xylosyltransferase, an enzyme involved in the first sugar transfer in glycosaminoglycan synthesis, and thus do not produce glycosaminoglycans like HSPG. However, CHO pgsA-745 cells display integrins on their surface and

should therefore be an ideal target for capsid mutants displaying an integrin binding motif like RGD4C. CHO KI cells and their cell derivative CHO pgsA-745 were transduced with 1,000 genomic particles per cell for each vector and analyzed by flow cytometry 48h p.i. (Figure 15 A).

On CHO pgsA-745 r-wt reached a transduction efficiency of only 7%. This low transduction efficiency may be due to the lack of HSPG on the cell surface, since a 2-fold higher transduction efficiency was determined for r-wt on CHO KI.
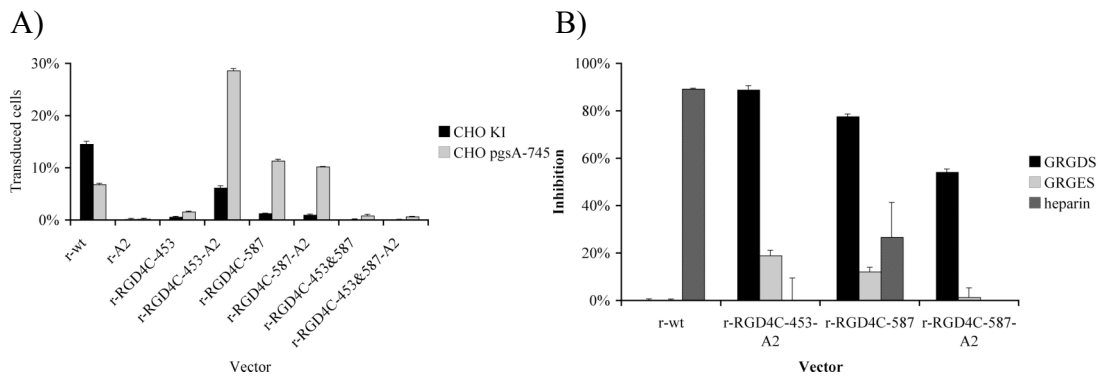
Figure 15. Infection of Chinese Hamster Ovarian Cells (CHO). A) CHO KI cells and their HSPG negative cell derivative pgsA-745 were transduced with 1,000 genomic particles per cell and amount of transgene expressing cells was determined by flow cytometry 48h p.t.. B) Cells were transduced with 1,000 genomic particles per cell in the presence of competing GRGDS or control GRGES peptides or soluble heparin. Shown is the mean value of triplicate measurements with error bars representing the standard error of the mean.

Even lower transduction efficiency was observed on both cell lines for r-A2, r-RGD4C-453 and both double insertion mutants. Although r-RGD4C-587-A2 was superior in receptor binding (Figure 13) and capsid-to-infectious particle ratio (Table 5), r-RGD4C-587 and r-RGD4C-587-A2 were equally efficient in transducing CHO pgsA-745 cells reaching 11% and 10%, respectively (Figure 15). Both mutants were significantly less efficient than r-RGD4C-453-A2 in CHO pgsA-745 cell transduction. While r-wt showed the best transduction efficiency on CHO KI, r-RGD4C-453-A2 emerged as the most efficient vector on the HSPG negative cell line CHO pgsA-745. Competition studies with soluble RGD containing peptides confirmed receptor specificity of CHO pgsA-745 transductions (Figure 15 B).

5.1.1.5. Transduction of αVβ3 and αVβ5 positive primary human cells

Tumor endothelial cells are clinically relevant targets for anti-tumor gene therapy, since tumors >1 mm^3 depend on vascularization for growth and metastasis formation (53). The best available model system for tumor endothelial cells are primary angiogenic human umbilical vein endothelial cells (HUVEC) which express HSPG (54), αVβ5 and αVβ3 integrins (Figure 16 A).

Therefore, we decided to test the most efficient capsid insertion mutant, r-RGD4C-453-A2, for its ability to transduce primary angiogenic HUVEC. r-wt, that was used as a control, and r-RGD4C-453-A2 were both able to transduce primary angiogenic HUVECs (Figure 16 B). Furthermore, while r-wt transduction was dependent on HSPG, r-RGD4C-453-A2 transduced primary angiogenic HUVECs in a HSPG independent manner (Figure 16 C).

A)

B)

C)
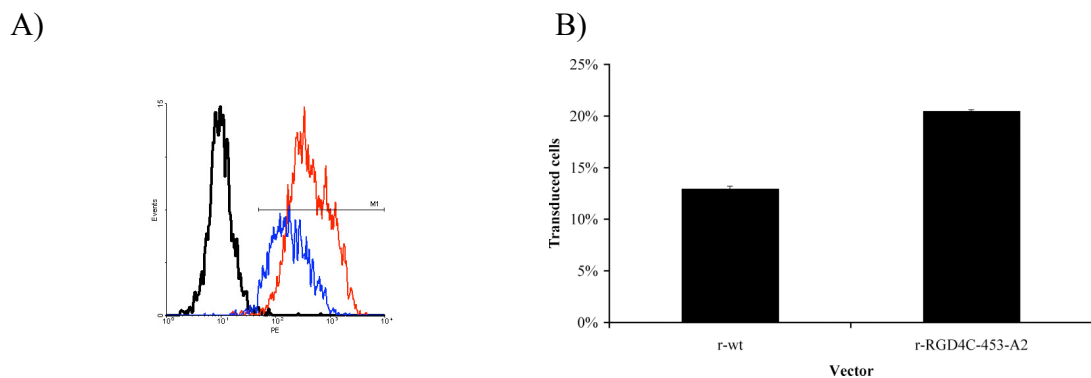
Figure 16. Transduction of primary Human Umbilical Vein Endothelial Cells (HUVEC) by r-RGD4C-453-A2. A) Receptor distribution on primary HUVEC at a passage number below 5 were determined by staining with anti-αVβ3 (blue line) and anti-αVβ5 (red line) antibodies as described in Material and Methods. B) Primary HUVEC cells analyzed for receptor display at day of transduction were transduced with 10,000 genomic particles per cell of r-RGD4C-453-A2 and r-wt and analyzed for the amount of transgene expression 48h p.t. by flow cytometry. C) Cells were transduced with 10,000 genomic particles per cell in the presence of soluble heparin. Shown is the mean value of two experiments performed with triplicate measurements. Error bars represent the standard error of the mean.
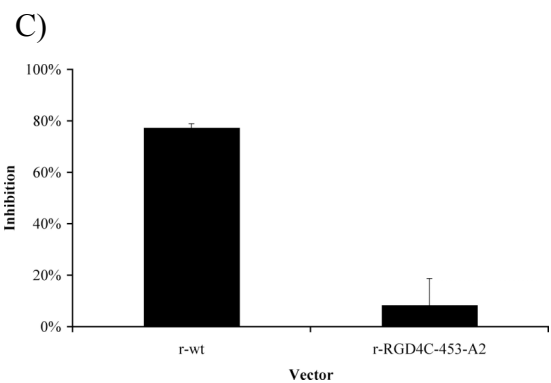
5.1.1.6. *In vivo* biodistribution

r-RGD4C-453-A2 and r-RGD4C-587 transduce cells via the same peptide, RGD4C (Figure 14, Figure 15). Furthermore, transduction in both cases occurs independently of AAVs' primary receptor (Figure 14, Figure 15). However, the two capsid insertion mutants differ in the position used for peptide insertion and in the capsid modification leading to the non-HSPG binding phenotype. *In vitro*, these differences translate into variations in receptor binding (Figure 13) and in transduction efficiency (Figure 15). To investigate whether these differences also lead to alterations in their *in vivo* tropism, $1x10^{10}$ genomic particles of r-RGD4C-453-A2 and r-RGD4C-587 were injected into the tail vein of 7 weeks old C57BL6 female mice. Mice treated in parallel with r-wt served as controls. We decided to analyze vector genomes instead of transgene expression since it allowed us to compare different vector tropisms independently from the ability of the cell to process AAV correctly and to express transgenes from AAV vector genomes. Animals were sacrificed 42 h p.i., liver, spleen, heart, lung, kidney and muscle were harvested and vector genome distribution was assessed by quantitative PCR (Figure 9).
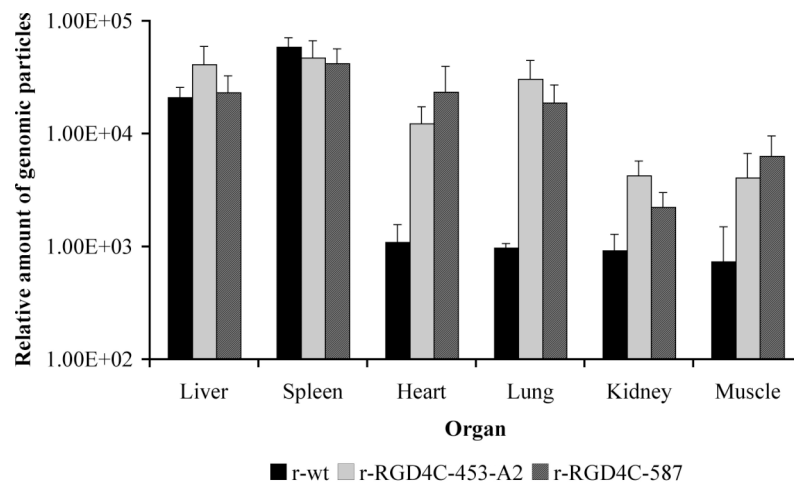
Figure 17. *In vivo* biodistribution of different HSPG ko and RGD4C insertion mutants. $1x10^{10}$ genomic particles of r-wt, r-RGD4C-453-A2 and r-RGD4C-587 were infused into the tail vein of 7 weeks old C57BL6 female mice (n= 3). Organs were harvested 42h p.i. and DNA was isolated. Absolute quantification of vector DNA and GAPDH DNA were performed by quantitative PCR. Values for vector DNA were normalized to GAPDH levels. Values are the mean of three mice in each group analyzed in two independent PCR runs with DNA obtained from two independent isolations. Error bars represent the standard error.

As expected, r-wt was mainly detected in liver and spleen. Significantly fewer vector genomes were found in other organs (~ 40-fold less). Despite the differences observed between r-RGD4C-453-A2 and r-RGD4C-587 *in vitro*, no differences were

detectable *in vivo*. Both mutants showed an identical biodistribution. However, in comparison to r-wt, variations were observed. Vector genomes of r-RGD4C-453-A2 and r-RGD4C-587 accumulated in heart, lung, kidney and muscle, with the most obvious difference to r-wt in the heart and in the lung.

In a recent publication, we correlated liver and spleen retention of rAAV-2 based targeting vectors with the ability to interact with HSPG (141). We thus expected to see a detargeting from liver and spleen for r-RGD4C-453-A2 and r-RGD4C-587 in comparison to r-wt. In contrast to our assumption, the amount of vector genomes detected in these organs was comparable for all three vectors. To further investigate these observations we used the hepatocellular carcinoma cell line HepG2 as a model for hepatocytes and transduced this cell line with all three vectors in the presence and absence of either GRGDS or GRGES peptides, or of heparin.
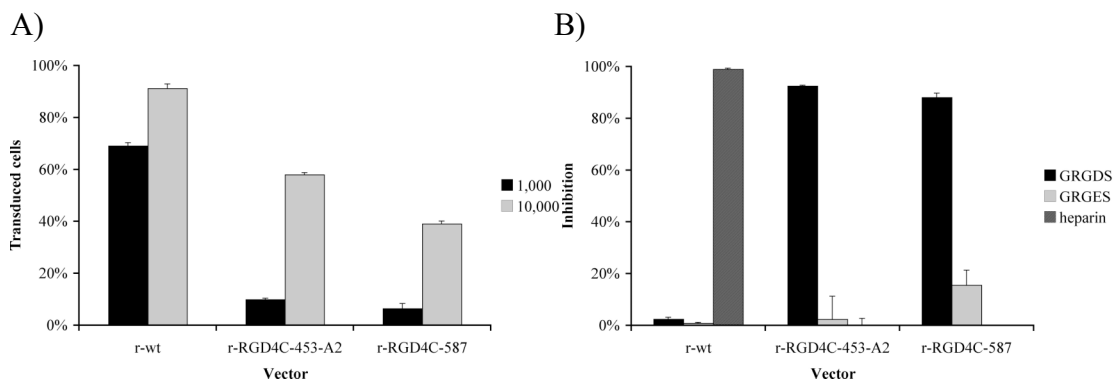
Figure 18. Transduction of HepG2 cells. A) The hepatocellular carcinoma cells HepG2 were transduced with 1,000 and 10,000 genomic particles per cell respectively and amount of transgene expressing cells determined by flow cytometry 48h p.t.. B) Cells were transduced with 10,000 genomic particles per cell in the presence of competing GRGDS or control GRGES peptides or soluble heparin. Triplicate experiments were performed. Shown is the mean value of one representative experiment made with triplicate measurements with error bars representing the standard error of the mean.

As depicted in Figure 18 A, all vectors were able to transduce HepG2 with r-wt emerging as the most efficient vector. r-wt mediated transduction of HepG2 was dependent on r-AAV-2's interaction with HSPG (as seen by heparin competition studies) and could not be blocked by GRGDS or GRGES peptides (Figure 18 B). In contrast, transduction of HepG2 cells by r-RGD4C-453-A2 and r-RGD4C-587 was inhibited by addition of GRGDS peptides but not by heparin or GRGES peptides (Figure 18 B), suggesting that transduction of liver (and possibly also of spleen) by r-RGD4C-453-A2 and r-RGD4C-587 was mediated by integrin binding through the inserted RGD4C peptide and not by HSPG binding as in the case of r-wt. Thus, r-wt

and capsid insertion mutants differ in the ligand-receptor interaction that led to liver (and spleen) transduction.

5.1.1.7. Stability of vector particles

Insertion of peptides in the capsid of AAV-2 is likely to affect its secondary and tertiary structure and by doing so, some of the physical properties of AAV-2. The CHO pgsA-745 cell line was used to analyze the resistance of our vectors to consecutive freezing cycles (Figure 19).
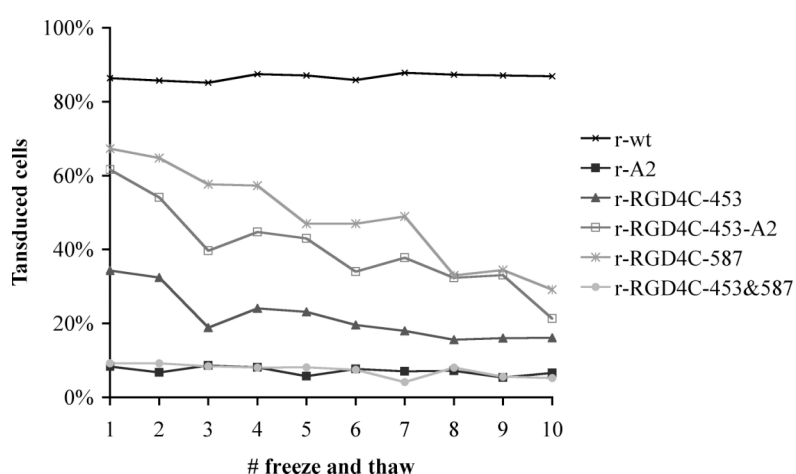
Figure 19. Vector Stability. The Chinese Hamster Ovarian cell derivative pgsA-745 was transduced with the respective vectors after successive freeze and thaw cycles. Amount of genomic particles per cell: r-wt – 8,000; r-A2 – 10,000; r-RGD4C-453 – 10,000; r-RGD4C-453-A2 – 2,500; r-RGD4C-587 – 4,000; r-RGD4C-453&587 – 10,000. Amount of transgene expressing cells was determined by flow cytometry 48h p.t.. Shown is the value of one single measurement.

r-wt transduction efficiency was not affected along the 10 consecutive freezing events. r-RGD4C-453, r-RGD4C-453-A2 and r-RGD4C-587 showed a decay in their transduction efficiency along the 10 consecutive freezing cycles that dropped to half of the initial efficiency. r-A2 and r-RGD4C-453&587 were to low in transduction efficiency to allow the visualization of any alteration. Furthermore, r-RGD4C-587-A2 and r-RGD4C-453&587-A2 were not included in these experiments since they were, at this time, not yet engineered.

5.1.2. Insertion of the NGRI peptide

To investigate if other peptides can also be inserted in position 453, we decided to substitute the RGD4C peptide by the NGRI peptide – ACVLNGRMECA.

This cyclic NGR peptide homes into tumors more effectively than linear peptides containing the NGR motif (4). NGRI targets APN (also known as CD13 (175)). Although there are several subpopulations of APN (132), which are relatively widely distributed in the body, only one isoform is believed to be the receptor for the NGR peptide. This isoform was shown to be expressed exclusively in angiogenic vessels, such as the neovasculature found in tumor tissues (30, 32). By using a different receptor to target the same type of cells that RGD4C does, NGRI directed r-AAV-2 mutants could complement r-RGD4C mutants and vice-versa.

5.1.2.1. NGRI double insertion mutant is not impaired in cell transduction

As with r-RGD4C mutants we started by evaluating the packaging efficiency of our mutants. As depicted in Table 6, based on their capsid-to-genomic ratio, all mutants showed a wt phenotype. r-NGRI-587-A2 and r-NGRI-453&587-A2 were not produced as we decided to focus our analysis on 453 single insertion mutants.

Table 6. Vector titers of r-wt, r-A2 and NGRI insertion mutants. u.d.l. = under detection limit; wt = phenotype comparable to AAV with wild-type capsid according to Kern and colleagues.. (a): genomic titer was determined by quantitative PCR, shown is the mean value of 3 titrations; (b): capsid titer was determined by ELISA using A20 (antibody, which recognizes intact AAV-2 capsids), shown is the mean value of 2 titrations; (d): definition according to Kern and colleagues (97): wt phenotype indicates a packaging ratio of < 50; (d): determined on HeLa cells; (e): provides a simple comparison of how many genome-containing particle of each mutant were required to achieve the same number of transduced HeLa cells as AAV-2 with wild-type capsid (definition according to Opie and colleagues (135)).

vector preparation	gen. titer (per ml) (a)	cap. titer (per ml) (b)	packaging efficiency (cap-to-gen ratio)	phenotype based on cap-to-gen ratio (c)	transducing (inf.) titer (per ml) (d)	cap-to-inf ratio	rel. cap-to-inf. value (e)
r-wt	1.40E+12	7.21E+12	5.2	wt	4.34E+10	166	1
r-A2	1.11E+12	6.47E+12	5.8	wt	u.d.l.	-	-
r-NGRI-453	1.36E+12	5.33E+12	3.9	wt	4.09E+11	13	0.078
r-NGRI-453 A2	8.29E+11	3.37E+12	4.1	wt	6.13E+08	5490	33
r-NGRI-587	8.58E+11	6.57E+12	7.7	wt	9.55E+08	6877	41
r-NGRI-453&587	5.35E+11	4.81E+12	9.0	wt	5.72E+08	8409	51

Furthermore, western blot analysis revealed that all mutants possessed the correct ratio of the capsid structural proteins VP1, VP2, and VP3 – 1:1:10 respectively – with the insertion of peptides in VP1, VP2, and VP3 resulting in proteins with a slower electrophoretic mobility (Figure 20). In agreement with

previous observations, A2 mutants also showed slower electrophoretic mobility (Figure 12, Figure 20).
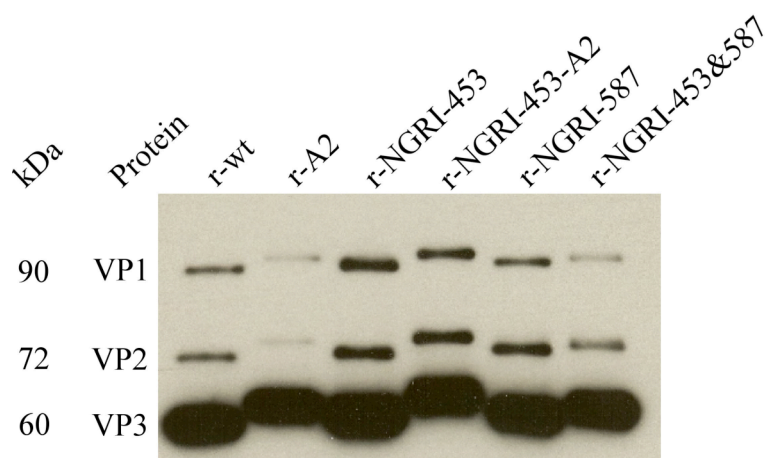
Figure 20. Western blot analysis of iodixanol gradient-purified AAV capsids. After iodixanol gradient purification the same amount of viral capsids (10^{10}), were separated by sodium dodecyl sulfate polyacrylamide gel (8%) electrophoresis and analyzed by Western blotting with the B1 antibody.

All mutants were able to transduce HeLa cells (Table 6) with r-NGRI-453 mutant being even more efficient than r-wt (rel. cap-to-inf value). Interestingly, while r-RGD4C double insertion mutants were severely impaired in transduction (Table 5), the r-NGRI-453&587 double insertion mutant was able to transduce HeLa cells to the same extent as r-NGRI-453-A2 and r-NGRI-587 (Table 6).

5.1.2.2. Efficiency of NGRI mutants in the transduction of primary HUVECs

Primary Human Umbilical Vein Endothelial Cells, a model system for tumor endothelial cells, known to express APN, were treated with all r-NGRI mutants and respective controls – r-wt and r-A2. As depicted in Figure 21 A, while r-NGRI-453 emerged as the most efficient vector its A2 homologue, r-NGRI-453-A2 was not able to transduce HUCECs.

Transduction of HUVECs by r-wt and r-NGRI-453 was inhibited by soluble heparin while transduction by r-NGRI-587 and r-NGRI-453&587 was not (Figure 21 B).
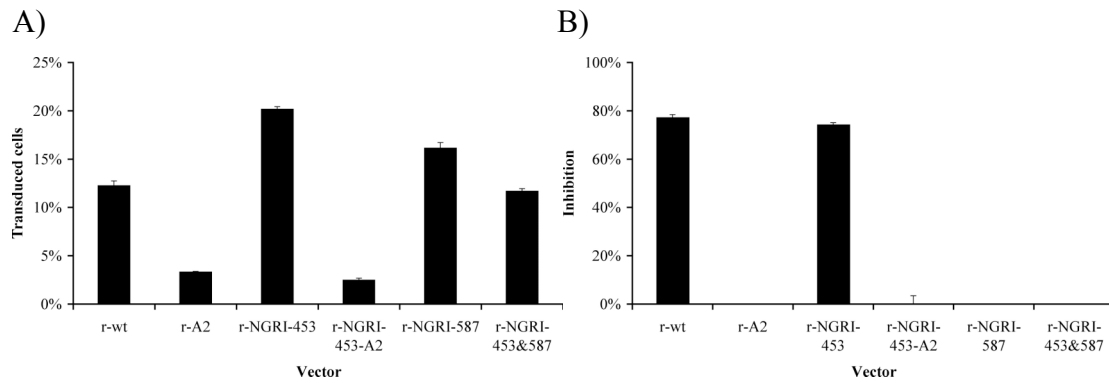
Figure 21. Transduction of primary Human Umbilical Vein Endothelial Cells (HUVEC) by NGRI mutants. A) Primary HUVEC cells were transduced with 10,000 genomic particles per cell and analyzed for the amount of transgene expression 48h p.t. by flow cytometry. B) Cells were transduced with 10,000 genomic particles per cell in the presence of soluble heparin. Shown is the mean value of two experiments performed with triplicate measurements. Error bars represent the standard error of the mean.

5.1.3. Insertion of an N587 display library selected peptide

In the recent years, AAV-2 display library approaches for the transduction of non-permissive cells and enhancement of specificity have proven to be a valuable tool for the generation of targeting AAV-2 mutants and identification of targeting peptides.

Having this in account, we decided to investigate if a peptide selected in position 587 of the AAV-2 capsid could be inserted in position 453 and still mediate transduction of the target cells.

The chosen peptide was GEN – AGENQARSA – which was obtained from selections on Mec1 cells (a B-CLL cell derivative) (139). Insertion of this peptide in position 587 has previously shown to increase the transduction of Mec1 cells in a GEN dependent manner (as proven by competition studies with soluble peptides and heparin).

5.1.3.1. GEN insertion in 453 does not interfere with vector packaging

We first analyzed the packaging efficiency of our mutants. As depicted in Table 7, based on the capsid-to-genomic ratio all r-GEN mutants showed a wt phenotype.

Table 7. Vector titers of r-wt and GEN insertion mutants. wt = phenotype comparable to AAV with wild-type capsid according to Kern and colleagues. (a): genomic titer was determined by quantitative PCR, shown is the mean value of 3 titrations; (b): capsid titer was determined by ELISA using A20 (antibody, which recognizes intact AAV-2 capsids), shown is the mean value of 2 titrations; (c): definition according to Kern and colleagues (97): wt phenotype indicates a packaging ratio of < 50.

vector preparation	gen. titer (per ml) (a)	cap. titer (per ml) (b)	packaging efficiency (cap-to-gen ratio)	phenotype based on cap-to-gen ratio (c)
r-wt	1.68E+11	9.86E+11	5.9	wt
r-GEN-453	1.58E+12	9.27E+12	5.9	wt
r-GEN-453-A2	5.49E+11	5.32E+12	9.7	wt
r-GEN-587	3.69E+11	1.65E+12	4.5	wt

5.1.3.2. GEN insertion in 453 does not result in an improved vector

For testing the transduction efficiency of our mutants, we used their target cells – Mec1. As depicted in Figure 22, r-wt emerged as the most efficient vector for transduction.
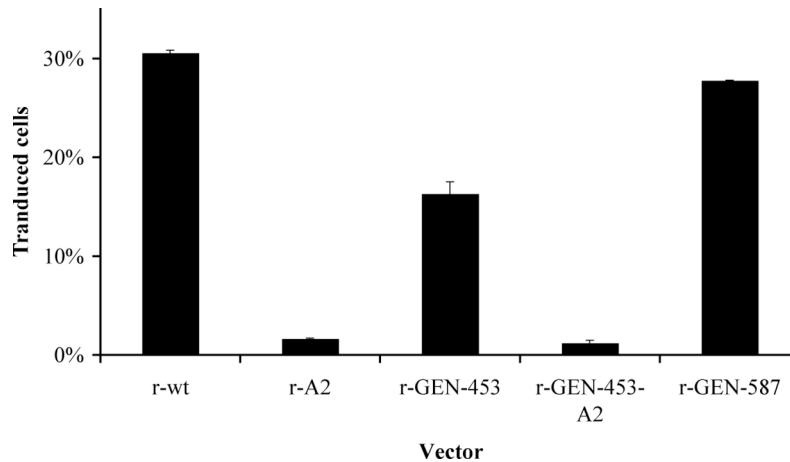
Figure 22. Transduction of Mec1 cells. The B-CLL cell derivative Mec1 cells were transduced with 10,000 genomic particles per cell and analyzed for the amount of transgene expression 48h p.t. by flow cytometry. Shown is the mean value of triplicate measurements. Error bars represent the standard error of the mean.

Although r-GEN-587 was only the second best vector, transductions achieved by this vector were previously shown to be dependent on the inserted peptide and independent of HSPG. r-GEN-453, with an unmodified HSPG binding site was the 3rd best vector. Its A2 homologue, r-GEN-453-A2 was not able to efficiently transduce the target cells.

5.1.4. Translation to other *Parvovirinae*

Proteins are generally composed of one or more functional regions, commonly termed domains. Different combinations of domains give rise to the diverse range of proteins found in nature. The identification of domains that occur within proteins can therefore provide insights into their function. Domains can be thought of as distinct functional and/or structural units of a protein. These two classifications coincide rather often, as a matter of fact, what is found as an independently folding unit of a polypeptide chain also carries specific function.

In molecular evolution such domains may have been utilized as building blocks, and may have been recombined in different arrangements to modulate protein function. Conserved domains can be defined as recurring units in molecular evolution, the extents of which can be determined by sequence and structure analysis. Conserved domains can be described by multiple local sequence alignments. Computational biologists have compiled collections of such alignments representing conserved domains that can be accessed by using services like the NCBI's Conserved Domain Database (CDD) (117). The CDD is a collection of multiple sequence alignments for ancient domains and full-length proteins.

Submission of the AAV-2 capsid protein VP2 to the CDD identified one major domain. This domain, part of the Parvovirus coat protein superfamily (pfam00740, imported from the Pfam database) includes G453 and N587. Within this superfamily, the 8 proteins that more resemble AAV-2 VP2, include: other AAV serotypes, other Dependovirus, Erythrovirus and Parvovirus (Figure 23 A). Of all, AAV-4 seems to have the highest homology to AAV-2 while the Parvovirus Canine parvovirus seems to have the lowest (Figure 23 B).

Analysis of the respective sequence alignments led to the identification of the AAV-2 G453 homologues in the other 8 *Parvovirinae* (Figure 23 C). The N587 homologues were also identified. Analysis of the complete capsid of CPV, B19, AAV-4 and MVM revealed that the G453 homologues were indeed located in the outer surface of the respective viral capsids (Figure 23 C, D, data not shown). Despite this, CPV, B19, AAV-4, and MVM G453/T454 homologues are not the best-exposed residues in each respective capsid (Figure 23 D, data not shown). Furthermore, in the case of B19, the most exposed residue – K396 – matches AAV-2 N587 (Figure 23 C, D).

A)

Viruses
└─ ssDNA viruses
   └─ Parvoviridae
      └─ Parvovirinae
         ├─ Parvovirus
         │ ├─ Feline panleukopenia virus
         │ │ └─ Canine parvovirus (CPV)
         │ ├─ Minute virus of mice (MVM)
         │ └─ Kilham rat virus (KRT)
         ├─ Erythrovirus
         │ ├─ Simian parvovirus (SP)
         │ ├─ Human parvovirus B19 (B19)
         │ └─ unclassified Erythrovirus
         │   └─ Chipmunk parvovirus (ChPV)
         └─ Dependovirus
            ├─ Adeno-associated virus - 4 (AAV-4)
            ├─ Adeno-associated virus - 2 (AAV-2)
            └─ Goose parvovirus (GPV)

B)

C)

D)

E)

Figure 23. Translation to other Parvovirinae. A-C) Retrieved from the NCBI's Conserved Domain Database after submission of the AAV-2 capsid protein VP2. A) Taxonomy tree. Tree like structure that lays out the phylogeny of organisms, as recorded in NCBI's taxonomy database. B) A phylogenetic tree, where the taxa represented at the end nodes are aligned sequences or sequence fragments. The length of each tree segment is indicated. C) Protein alignment. D) One quarter of the B19 complete capsid is shown. The distances of the respective residues to the virus center as calculated

by computational analysis were obtained from the VIPERdb service. E) 3d structure of the B19 VP2 capsid protein.

Comparison of the 3D structure of AAV-2 and B19 shows that the G453 and N587 homologues identified by protein alignment also have a very close homology at the structural level (Figure 9 C –Page 72–,Figure 23 D). In AAV-2 as well as in B19 both residues are located at the top of two structurally close loops. While in AAV-2 the G453 loop has higher exposure than the N587 loop, in B19 this relation is inverted. Indeed, AAV-2 G453 and its *Parvovirinae* homologue residues are suitable for insertion of small peptides.

5.2. Fusing scFvs to AAV-2's VP2 for the generation of new targeting mutants

Antibodies have been proven to be an excellent paradigm for the design of high-affinity, protein-based binding reagents.

The basic functional unit of each antibody is an immunoglobulin (Ig) monomer which is a "Y" shaped molecule that consists of four polypeptide chains; two identical heavy chains and two identical light chains connected by disulfide bonds. The paratope - responsible for the recognition of the epitope on the antigen molecule - is shaped at the amino terminal end of the antibody monomer by the variable domains from the heavy (V_H) and light chains (V_L) at the tip of the "Y". Single chain variable fragments (scFv) can be engineered by fusing the variable regions (V) of the heavy and light chains of immunoglobulins with the help of a short linker (usually serine, glycine) for the prevention of dissociation. These smaller proteins (~ 28 kDa; when comparing for example to IgG ~ 150 kDa) retain the specificity of the original immunoglobulin despite removal of the constant regions. Such scFvs have emerged in the recent years as credible alternatives to whole Ig molecules (85, 123).

In a recent publication our group fused the C-terminus of a GFP molecule (27 kDa) to the N-terminus of the AAV-2 capsid protein VP2. Such fusion proteins (99 kDa) were efficiently incorporated into the AAV-2 capsid without the loss of infectivity.

With the intention of generating a CD30 targeting vector the same approach was followed and the C-terminus of an anti-CD30 scFv fused to the N-terminus of VP2.

5.2.1. GFP is located on the outer surface of the capsid

Previously published models of the AAV-2 capsid structure propose a flexible N-terminus of VP2 as well as of VP1 (105). In agreement with this model these N-terminus would be located on the inner side of the viral capsid and, during infection, pass through the pores on the 5-fold symmetry axis becoming exposed on the outer surface.

In order to proper interact with their target receptor, targeting molecules must be present on the outer surface of the capsid. We therefore analyzed the location of the N-terminus of the GFP-VP2 fusion protein prior to cell transduction.

Analysis of AAV-2 particles containing the GFP-VP2 fusion protein (r-GFP) was first made by immobilization of the particles on an ELISA plate previously coated with an anti-GFP antibody. Detection of intact AAV-2 particles was then done using the anti-AAV-2 intact capsids monoclonal antibody A20 (Figure 24).
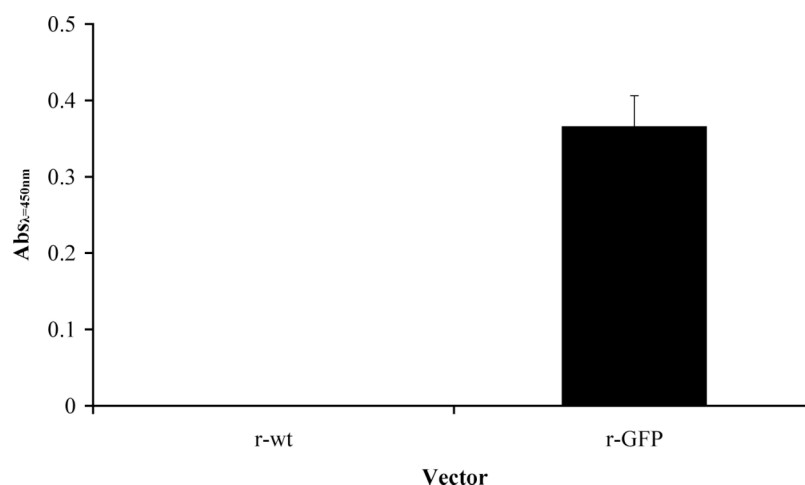
Figure 24. Surface exposure of GFP. 1.0×10^{10} iodixanol gradient purified capsids containing the GFP-VP2 fusion protein (r-GFP) were added to an ELISA plate that had been previously coated with an anti-GFP antibody as described in the Methods section. r-wt with wt VP2 was used as a control. Detection of intact capsids was done using the anti-AAV-2 monoclonal antibody A20. PBS coated wells were used as controls and respective values deduced. Shown is the mean value of duplicate measurements. Error bars represent the standard error of the mean.

The strong signal obtained from the r-GFP vector preparation in comparison to the absence of signal from the AAV-2 preparation possessing wt VP2 (r-wt) reveals that the recognized epitope of the GFP molecule is indeed exposed on the outer surface of the vector. This observation highlights the potential of the N-terminus of VP2 for the insertion/fusion of targeting molecules that once exposed on the outer surface of the vector could interact with their respective receptor.

5.2.2. aCD30-GFP-VP2

Based on the previous observation that GFP is present on the outer surface of the AAV-2 capsid we decided to fuse the C-terminus of an anti-CD30 scFv (~ 28 kDa) to the N-terminus of the GFP-VP2 fusion protein creating the following fusion: aCD30-GFP-VP2 (127 kDa). Such construct, by having the GFP molecule as a

linker/spacer, should create the possibility for the paratope to interact with the antigen. At the same time, GFP tagged capsids can be a useful tool for infectious biology studies.

Analysis of our construct and respective viral preparations was first made by Western blotting of protein purified by high-speed centrifugation of cell lysates (Figure 25).

For the production of viral vectors HEK293 cells must be infected with an helper virus or transfected with a plasmid encoding helper functions as the plasmid pXX6-80. Since the GFP transgene was supplied by the pssGFP plasmid, control was done by transfecting cells with pXX6-80 and pssGFP (Figure 25 A, lane: pXX6-80 + pssGFP).

For the production of vectors a plasmid encoding the viral Rep and Cap proteins must be supplied - pRC. In the case of vectors with VP2 fusion proteins wt VP2 is not expressed from this plasmid – pRC VP2 ko – and the respective fusion is supplied *in trans* (Figure 25 A, lanes: pRC VP2 ko and pGFP-VP2, respectively).

The anti-CD30-GFP-VP2 fusion was also analyzed by Western blotting (Figure 25 A, lane: paCD30-GFP-VP2).

Wild type AAV-2, produced by transfecting the cells with pXX6-80, pssGFP, and pRC was used as reference for the expression and size of the structural proteins (Figure 25 A, lane: r-wt).

Production of vectors containing the GFP-VP2 fusion protein can be achieved by transfection with pXX6-80, pssGFP, pRC VP2 ko, and pGFP-VP2 (Figure 25 A, lane: r-GFP). The same holds true when using paCD30-GFP-VP2 instead of pGFP-VP2 for the production of mutants with an incorporated anti-CD30-GFP-VP2 fusion protein (Figure 25 A, lane: r-GFP-aCD30).

For the separation of vector capsids from other extracted proteins an iodixanol step gradient purification was performed. Vector capsids were recovered from the 40% iodixanol phase and analyzed by Western blotting (Figure 25 B).

As expected, transfection with pXX6-80, pssGFP and pRC resulted in the expression of the different capsid proteins VP1 (90 kDa), VP2 (72 kDa) and VP3 (60 kDa) with a ratio of 1:1:10 respectively (Figure 25 A, r-wt). After iodixanol gradient purification this ratio was still the same (Figure 25 B, r-wt). In contrast, the VP1 : GFP-VP2 : VP3 ratio significantly differed from the expected 1:1:10, respectively (Figure 25 A, pGFP-VP2 vs. pRC VP2 ko, and r-GFP respectively). The non-specific

antibody binding around 60 kDa and 140 kDa can be used as control for the total amount of protein loaded (Figure 25 A).

A)   B)
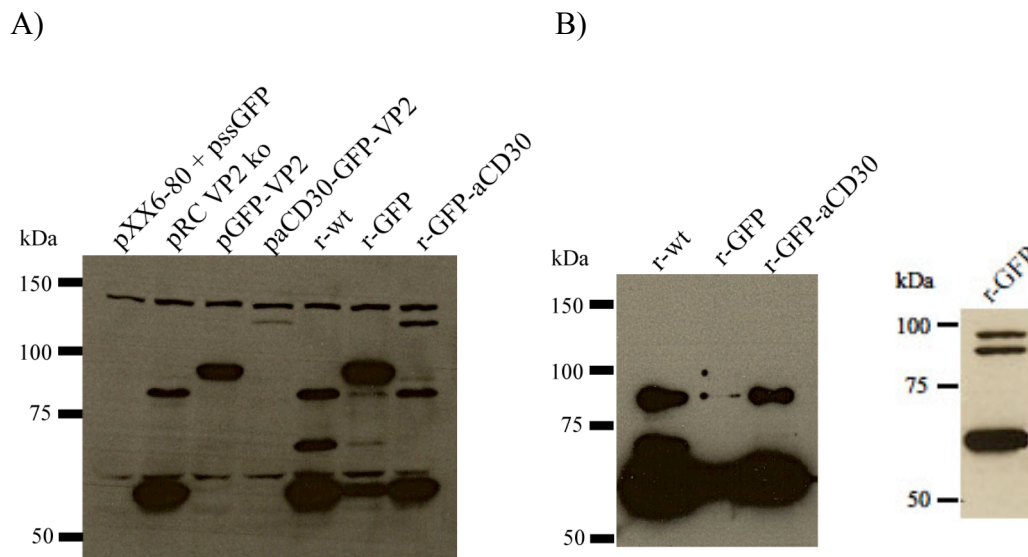
Figure 25. Western blot analysis of r-GFP-aCD30. A) HEK293 cells were transfected with pXX6-80, pssGFP and AAV-2 capsid protein coding plasmids. Protein extraction was performed and 30 µg of protein were separated by SDS-PAGE and analyzed by Western blotting using the B1 antibody. B) After iodixanol gradient purification r-wt, r-GFP and r-GFP-aCD30 were separated and analyzed by the same methods (20 µl, 40 µl and 40 µl respectively).

Co-transfection with pXX6-80, pssGFP, pRC VP2 ko and pGFP-VP2 results in an AAV-2 vector with incorporated GFP-VP2 fusion proteins – r-GFP (Figure 25 B, r-GFP). This co-transfection also resulted in a decreased amount of VP1 and VP3 (Figure 25 A, pRC VP2 ko vs. r-GFP). Since VP3, the most abundant capsid is essential for packaging of vector particles, less particles were recovered (data not shown and Figure 25 B, r-GFP).

Lower amounts of the aCD30-GFP-VP2 protein were found in HEK293 in comparison to GFP-VP2 (Figure 25 A, paCD30-GFP-VP2 vs. pGFP-VP2 respectively). The same was observed when trying to package this constructs by co-transfecting the cells with pRC VP2 ko (Figure 25 A, r-GFP-aCD30 vs. r-GFP respectively). Protein extracts revealed a ratio of VP1 : aCD30-GFP-VP2 : VP3 of 1:1:10 but the fusion protein was not detectable after iodixanol gradient purification (Figure 25 A and B, r-GFP-aCD30). This observation points towards an inefficient incorporation the aCD30-GFP-VP2 fusion protein into the AAV-2 capsid. The amount of genomic particles detected on the 25% and 60% phases of the iodixanol

gradient was, for all vectors, inferior to the amount found on the 40% phase – not allowing analysis by Western blotting (data not shown, see Table 8).

5.2.3. aCD30nVP2

The increasing size of VP2 as a capsid protein (from ~ 72 kDa for VP2 to ~ 127 kDa for aCD30-GFP-VP2) can make the fusion protein intolerable on the AAV-2 capsid.

Taking this in account new fusion proteins containing the anti-CD30 scFv and the VP2 proteins were engineered (Figure 26 A):

- aCD30-VP2: a fusion of the C-terminus of the scFv to the N-terminus of VP2; an exact parallel to the GFP-VP2 fusion protein.
- aCD30CLVP2: a version of the aCD30-VP2 construct with a glycine/serine linker between the scFv and the VP2; as described above glycine/serine linkers are commonly used in the engineering of scFv for prevention of dissociation of the V_H from the V_L; linkers made of such small amino acids should provide good flexibility.
- aCD30CL2VP2: just like aCD30CLVP2 but with a double glycine/serine linker.
- aCD30GLVP2: just like aCD30-VP2 but, the non-globular C-terminal part of GFP that is fused to VP2 in the GFP-VP2 construct - ITLGMDEL - is inserted between the anti-CD30 scFv and VP2 as linker.
- aCD30LGLVP2: just like aCD30GLVP2 but with a glycine/serine linker inserted between the anti-CD30 scFv and the non-globular C-Terminal part of GFP.

Although not indicated all these fusions contained mutations on the VP3 common region leading to R585A and R588A substitutions (see Page 101).

Western blot analysis of HEK293 cells lysates obtained after co-transfection with pXX6-80 and the respective constructs showed once again a lower amount of aCD30nVP2 fusion proteins in comparison to the GFP-VP2 construct (Figure 26 B, ~ 100 kDa).

When using this constructs to generate vector particles, aCD30nVP2 were not detected after density gradient purification (data not shown).
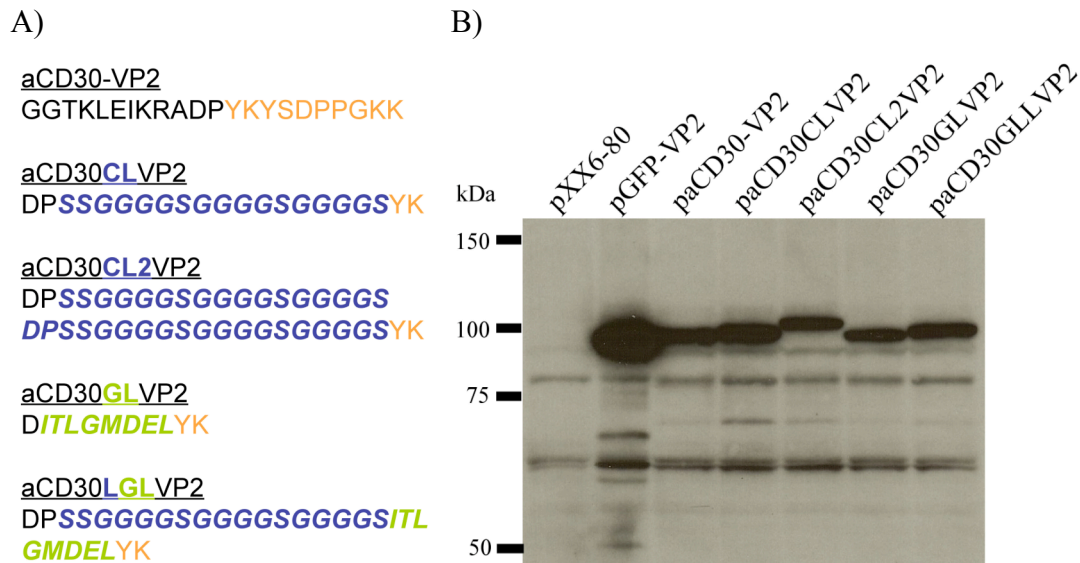
Figure 26. Western blot analysis of different aCD30-VP2 constructs. A) Amino acid sequence of the different aCD30-VP2 constructs. Sequences are shown in a N-terminus to C-terminus orientation. B) HEK293 cells were transfected with pXX6-80 and plasmids coding for different aCD30-VP2 constructs. Protein extraction was performed and 30μg of protein were separated by SDS-PAGE and analyzed by Western blotting using the B1 antibody.

5.2.4. Optimizing expression in *cis*

Production of AAV-2 particles with 100% substitution of VP2 by the GFP-VP2 protein showed that in protein extracts the ratio of VP1 : GFP-VP2 is below 1 (Figure 25 A, r-GFP). Despite this, purification of vectors from such extracts resulted in vector preparations with the correct VP1 : GFP-VP2 ratio - 1 : 1 (Figure 25 B, r-GFP). The same did not hold true when packaging vectors with aCD30nVP2 fusion proteins. The inefficient incorporation of aCD30nVP2 fusion proteins into AAV-2 capsids may be the result of the low amounts of the aCD30nVP2 proteins. Thus, a higher expression of the constructs may be required for their incorporation into complete capsids.

The Kozak consensus translation initiation site, known to improve translation efficiency in eukaryotic cells, is present in the GFP-VP2 construct encoding plasmid. This sequence which occurs on eukaryotic mRNA has the consensus (gcc)gccRccAUGG, where R is a purine three bases upstream of the start codon which is followed by another G. This consensus was eliminated during the cloning of the aCD30nVP2 constructs and is not present in any of the fusion proteins that contain the anti-CD30 scFv.

96

Direct fusion of the anti-CD30 scFv to VP2 results in a protein with approximately the same size of GFP-VP2 (Figure 26 B, paCD30-VP2 and pGFP-VP2 respectively). Having this in account, the aCD30-VP2 construct was chosen as background for the complete recover of the Kozak consensus as well as the complete sequence between the CMV promoter and the start codon. The plasmid pKaCD30-VP2 was engineered and used for co-transfection of HEK293 cells (Figure 27, pKaCD30-VP2) and production of vector particles (Figure 27, r-aCD30-K-A2).
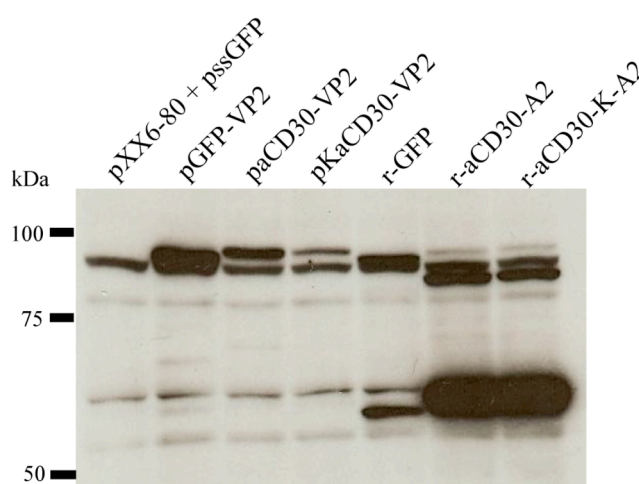
Figure 27. Western blot analysis of an aCD30-VP2 construct containing the Kozak consensus. HEK293 cells were transfected with pXX6-80, pssGFP and AAV-2 capsid protein coding plasmids. Protein extraction was performed and 30 µg of protein were separated by SDS-PAGE and analyzed by Western blotting using the B1 antibody.

Inclusion of the Kozak consensus did not increase the amount of the aCD30-VP2 fusion protein in HEK293 cells after transfection (Figure 27, paCD30-VP2 and pKaCD30-VP2). As a result, the ratio of VP1 : aCD30-VP2 remained higher than 1 (Figure 27, r-aCD30-A2 and r-aCD30-K-A2).

5.2.5. Optimizing expression in *trans*

Unlike with AAV-2 vectors containing wt VP2, vectors with VP2 fusion proteins are packaged by using two independent plasmids – one coding for the VP2 fusion, and one coding for VP1 and VP3. Increasing the amount of aCD30nVP2 plasmid used for transfection should increase the amount of the respective fusion protein in the transfected cells.

HEK293 cells were co-transfected with pXX6-80, pssGFP, pRC VP2 ko, and paCD30-GFP-VP2. The amount of transfected paCD30-GFP-VP2 was raised 2, 3, 4, 5 and 6 times. Protein extracts were analyzed by Western blotting (Figure 28 A).

A)
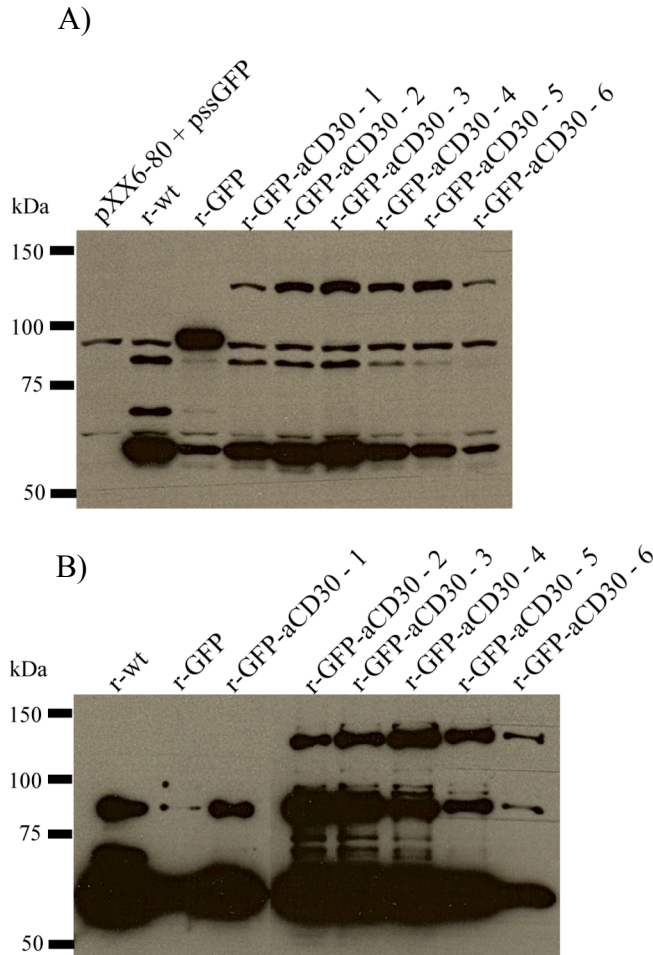
Figure 28. Western blot analysis of r-GFP-aCD30 vectors packaged with increased amounts of paCD30-GFP-VP2. A) HEK293 cells were transfected with pXX6-80, pssGFP and AAV-2 capsid protein coding plasmids. Amount of paCD30-GFP-VP2 supplied in trans during packaging was raised 1 to 6 times (r-GFP-aCD30 - 1 to r-GFP-aCD30 – 6 respectively). Protein extraction was performed and 30 µg of protein were separated by SDS-PAGE and analyzed by Western blotting using the B1 antibody. B) After iodixanol gradient purification r-wt, r-GFP and the several r-GFP-aCD30 vectors were separated and analyzed as in A (20 µl, 40 µl and 40 µl respectively).

Increasing the amount of the aCD30-GFP-VP2 encoding plasmids used for transfection resulted in a decrease of the VP1 : aCD30-GFP-VP2 ratio.

The amounts of VP1, VP2, and VP3 found in HEK293 cells increased with the amount of paCD30-GFP-VP2 plasmid used for transfection until a threshold value of 3x. Beyond this threshold the amount of the different capsid proteins started to decrease.

The vector preparations in the above analyzed protein extracts were then purified by iodixanol gradient purification. The increase of paCD30-GFP-VP2 used, resulted in a decrease of the VP1 : aCD30-GFP-VP2 ratio until this ratio reached a value of 1 with the use of 4x more plasmid (Figure 28). The amount of VP1 and VP3 decreased with the increase of paCD30-GFP-VP2 used. Indeed, the use of 4x more

paCD30-GFP-VP2 resulted in AAV-2 particles with natural amount aCD30-GFP-VP2.

As depicted in Table 8 the amount of particles recovered after iodixanol gradient purification was significantly lower when packaging vectors with VP2 fusion proteins (Table 8, gen. titer, 40% iodixanol phase). This was especially true in the case of r-GFP. Surprisingly, more particles of r-GFP-aCD30-x than r-GFP were recovered. Moreover, genomic titers are in agreement with the amount of VP1 and VP3 detected in these iodixanol purified preparations (Figure 28, for r-wt 20 µl were loaded while for the remaining vectors 40 µl were loaded in the well).

Furthermore, the highest amount of each vector preparation was found within the 40% phase of the iodixanol gradient. r-GFP-aCD30 vectors were 1.3 to 2.2 times less infectious than r-wt on HeLa cells. This can still be considered a wt phenotype.

In summary, by increasing the amount of paCD30-GFP-VP2 plasmid used for transfection of HEK293 cells during vector production, we obtained infectious particles that efficiently incorporated the aCD30-GFP-VP2 fusion proteins.

Table 8. Vector titers of r-wt and aCD30-GFP-VP2 mutants. n.d. = not determined; u.d.l. = under detection limit; wt = phenotype comparable to AAV with wild-type capsid according to Kern and colleagues. (a) Amount of paCD30-GFP-VP2 supplied in trans during packaging was raised 1 to 6 times (r-GFP-aCD30 - 1 to r-GFP-aCD30 – 6 respectively)**.** (b): after iodixanol gradient purification different phases of the gradient were recovered and genomic titers determined by quantitative PCR, shown is the mean value of 3 titrations; (c): transducing titers of the 40% phase were determined on HeLa cells, shown is the mean value of 2 titrations; (d): provides a simple comparison of how many genome-containing particle of each mutant were required to achieve the same number of transduced HeLa cells as AAV-2 with wild-type capsid (definition according to Opie and colleagues (135)).

vector preparation (a)	gen. titer (per ml) (b)			transducing (inf.) titer (per ml) (c)	gen-to-inf ratio	rel. cap-to-inf value (d)
	25%	40%	60%			
r-wt	6.63E+09	2.49E+11	2.48E+09	1.65E+09	150.93	1.0
r-GFP	1.65+09	6.00E+09	1.03E+08	1.52E+07	394.65	2.6
r-GFP-aCD30-1	3.41E+09	6.53E+10	3.09E+09	2.07E+08	315.62	2.1
r-GFP-aCD30-2		9.38E+10		4.67E+08	200.77	1.3
r-GFP-aCD30-3		6.72E+10		3.01E+08	223.28	1.5
r-GFP-aCD30-4	2.19E09	2.40E+10	1.28E+10	8.54E+07	280.49	1.9
r-GFP-aCD30-5		1.72E+10		5.57E+07	308.88	2.0
r-GFP-aCD30-6		5.41E+09		1.65E+07	327.96	2.2

5.2.6. Functional scFv

Interaction between the vector and its receptor is fundamental for transduction. In the case of a scFv driven AAV-2 vector this interaction has to be made between the paratope (on the scFv) and the epitope (on the antigen). Such interaction can be mimicked by the use of an anti-idiotypic antibody that recognizes the paratope. An anti-idiotypic antibody recognizes an unique set of antigenic determinants of the variable portion of another antibody – the idiotope.

Protein extracts from vector producing cells and their respective iodixanol gradient purified preparations were immobilized in an ELISA plate previously coated with an anti-idiotypic antibody - 9G10 - that recognizes the anti-CD30 scFv paratope. Detection was then made using an anti-GFP antibody for detection of the anti-CD30/GFP fusion (Figure 29 A). Detection was also made with an anti-AAV-2 antibody (A20) for detection of functional anti-CD30 scFv in intact AAV-2 particles (Figure 29 B). As negative controls a vector containing different scFv-GFP-VP2 fusion protein was used (see Figure 33) and a mouse IgG fraction used for the coating of the plates. As positive controls, anti-CD30 scFv with human Fc was used (detected with an anti-human Fc antibody) and an anti-AAV-2 antibody was used for the coating of the plates.

Functional - antigen recognition and binding - anti-CD30 scFv fused to the GFP molecule was detected in protein extracts (Figure 29 A, r-GFP-aCD30 (Prot. Ext.)). This is supported by the strong difference between the r-GFP-aCD30/anti-idiotypic signal, the IgG coated control and the r-GFP-XYX (where XYX stands for another scFv that recognizes a different antigen) preparation. The anti-CD30 scFv/GFP fusion was not detectable after iodixanol gradient purification (Figure 29 A, r-GFP-aCD30 (Grad)).

Using the anti-AAV-2 intact capsids A20 antibody it was not possible to detect intact AAV-2 capsids with a functional (Figure 29 B, r-GFP-aCD30). Despite this, functional anti-CD30 molecules were detected in iodixanol gradient purified preparations by coating iodixanol gradient purified r-GFP-aCD30 and detecting the paratope with the anti-idiotypic antibody 9G10 (Figure 29 C).

In summary, functional molecules were detected before and after gradient purification but not in intact AAV-2 capids. None of the production and purification steps seems to damage the anti-CD30 scFV.

A)

B)

C)
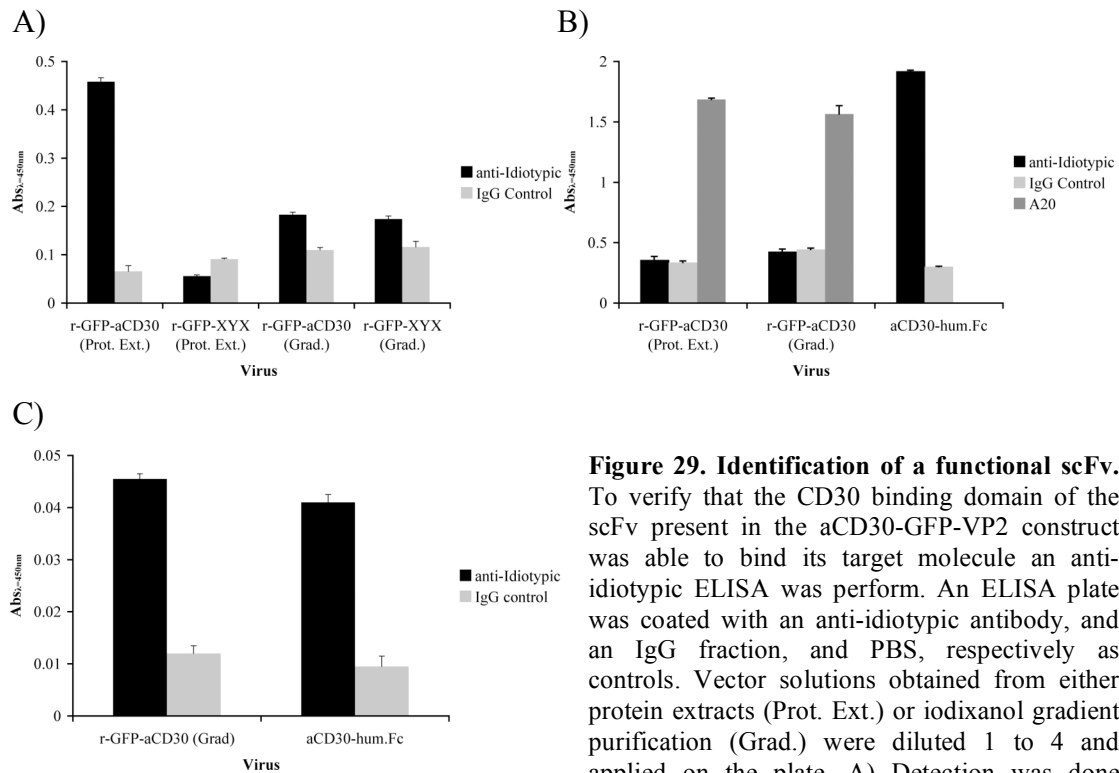
Figure 29. Identification of a functional scFv. To verify that the CD30 binding domain of the scFv present in the aCD30-GFP-VP2 construct was able to bind its target molecule an anti-idiotypic ELISA was perform. An ELISA plate was coated with an anti-idiotypic antibody, and an IgG fraction, and PBS, respectively as controls. Vector solutions obtained from either protein extracts (Prot. Ext.) or iodixanol gradient purification (Grad.) were diluted 1 to 4 and applied on the plate. A) Detection was done using and anti-GFP antibody. B) Alternatively detection was done using biotinylated anti-AAV-2 antibody A20. Also, as controls, coating was done using purified anti-AAV-2 antibody A20 and aCD30-hum.Fc purified protein was detected with an anti-hum.Fc antibody. C) An ELISA plate was coated with iodixanol gradient purified r-GFP-aCD30 (dil 1:4), purified aCD30-hum.Fc as positive control and PBS as negative control. Detection was made with an anti-idiotypic antibody. PBS values were deduced. Shown is the mean value of duplicate measurements. Error bars represent the standard error of the mean.

5.2.7. Transduction of target cells

In gene therapy, transduction of the target cells is in most cases the major goal. Vector preparations obtained either by protein extraction of vector producing cells or iodixanol gradient purification of such extracts were used in transduction assays. To compare the infectivity of vectors in such preparations HeLa cells were transduced with r-wt obtained from protein extraction of vector producing cells and in parallel with r-wt from iodixanol gradient purified preparations of the same extracts. The resulting genomic to infectious ratios values were 92 and 61, respectively. The preparations can be considered as equally infectious.

AAV-2 wt is able to enter a large amount of cell types through the binding to its primary receptor – HSPG. Avoiding this binding is a very important tool when studying targeting mutants that bind to new receptors. For this, two arginines in the VP3 common region of the AAV-2 capsid proteins can be mutated to alanines –

R585A and R588A, according to VP1 numbering. Thus, by eliminating the binding to wild type receptors one straitens the transduction to the interaction of the new inserted ligand with its target receptor.

A GFP coding AAV-2 vector with an incorporated aCD30-GFP-VP2 fusion protein and R585A and R588A (A2) substitutions was packaged and named r-GFP-aCD30-A2. In agreement with the above described results 4x more paCD30-GFP-VP2-A2 was used for the packaging of this mutant. r-GFP-aCD30 was packaged as a control. r-wt, r-GFP and their A2 homologues were also packaged as controls. Following purification r-wt and r-A2 preparations contained approximately 10x more genomic particles than r-GFP-aCD30 and r-GFP-aCD30–A2 preparations and about 100x more genomic particles than r-GFP and r-GFP-A2 preparations (data not shown).

Western blot analysis of gradient purified vectors indicates that A2 mutants possess VP1, VP2, or VP2 fusion proteins, and VP3 with a slightly higher molecular weight than their R585 and R588 counterparts (Figure 30 A, e.g. r-wt vs. r-A2). The low titers of r-GFP and r-GFP-A2 did not allow a clear detection of the VP1 capsid protein. In these r-GFP and r-GFP-A2 vectors the GFP-VP2 : VP1 and the GFP-VP2 : VP3 ratios are much higher than the expected values of 1 and 0.1, respectively. r-GFP-aCD30 and r-GFP-aCD30-A2 showed an aCD30-GFP-VP2 : VP1 ratio slightly higher than 1.

As target cells, the human Hodgkin's lymphoma derived cell line L540 was used. One of the characteristics of this cell line is the high expression of the CD30 antigen in its entire cell population (Figure 30 B).

r-GFP-aCD30-A2 was used for transduction of L540 cells (Figure 30 C). r-wt and r-A2 were used as controls. The low titers of r-GFP and r-GFP-A2 forced the exclusion of these vectors from this experiment. Vectors obtained after protein extraction by high speed centrifugation of cells lysates of vector producing cells (Protein Extracts) and following iodixanol gradient purification of the respective extracts (Gradient) were used. Since all vectors contain a GFP coding gene (as transgene) GFP molecules are expected to be found in preparations that were not submitted to iodixanol gradient purification. This molecule may also be able to interact with cells. Despite this, there was not any detectable fluorescence 1 h post-transduction. Apart from r-wt, no other vector was able to transduce the target cells. Transduction by r-wt obtained from protein extraction of vector producing cells and

following iodixanol gradient purification of the respective extracts resulted in the same number of GFP expressing cells. The amount of GFP molecules per cell (determined by the mean fluorescence intensity - MFI) was also equal (data not shown).
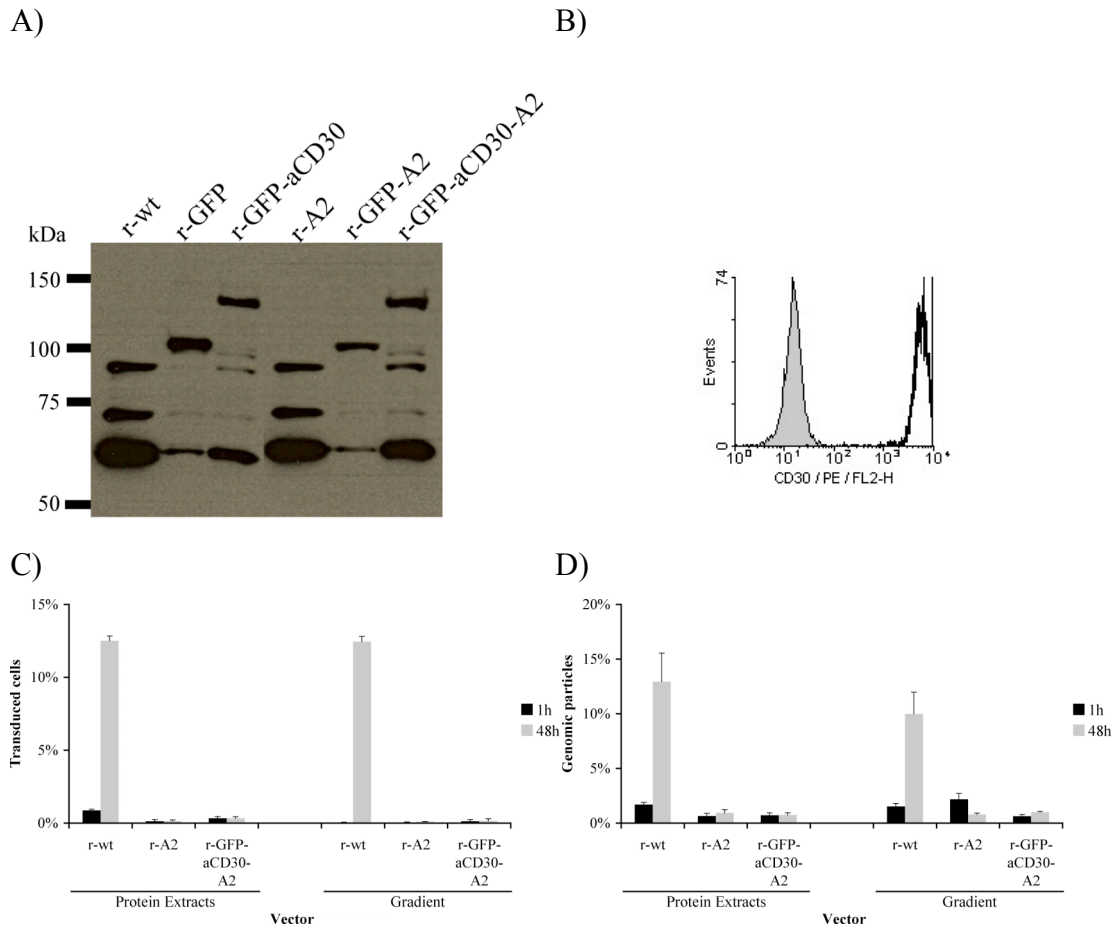
Figure 30. Transduction of CD30+ cells by r-GFP-aCD30-A2. A) After iodixanol gradient purification the different vectors were separated by SDS-PAGE, and analyzed by Western blotting using the B1 antibody (20 µl of r-wt, 20 µl of r-A2 and 40 µl of each of the remaining vectors). B) The presence of the target molecule – CD30 – on L540 cells at the time of infection was determined by staining with an anti-CD30 antibody (thicker black line) and analyzed by flow cytometry. C) The different vector preparations obtained either from protein extraction of vector producing cells or iodixanol gradient purification of the respective protein extracts were used to transduce L540 cells (MOI = 10,000 gen.p./cell). Amount of transgene expressing cells was determined by flow cytometry 1 h and 48 h p.t. D) Alternatively, cells were collected, washed three times in PBS and used to perform DNA isolation. Amount of vector genomes found in the cells was determined by quantitative PCR. Show is the ratio between the amount of viral genomes used for transduction and the amount of viral genomes determined 1 h and 48 h p.t. Shown is the mean value of triplicate measurements. Error bars represent the standard error of the mean.

For transduction, after binding of the vector to the target receptor, the vector transgene must also find a way to reach the nucleus. To determine if, despite the lack of transduction capacity, there was binding of the targeting mutants to the cells

carrying the target receptor, detection of vector DNA was performed 1 h and 48 h p.t. (Figure 30 D). 1 h at 37 ºC should give enough time for the scFv to bind the antigen and at the same time not be enough for the cells to harm the vector (e.g. by proteossomal degradation). r-wt vector DNA was detected 48 h p.t. (Figure 30 D). Apart from this no vector DNA was detected at any other time point or when other vectors were used.

A)
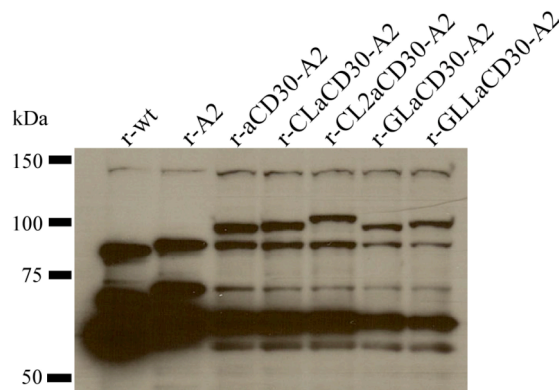
B)
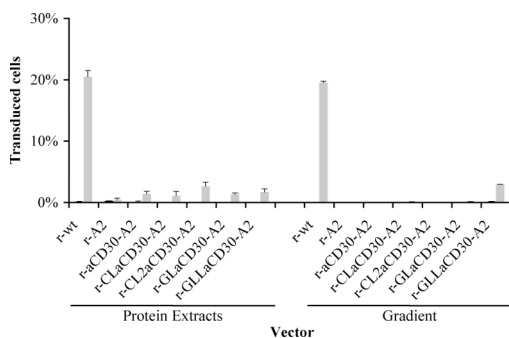
C)
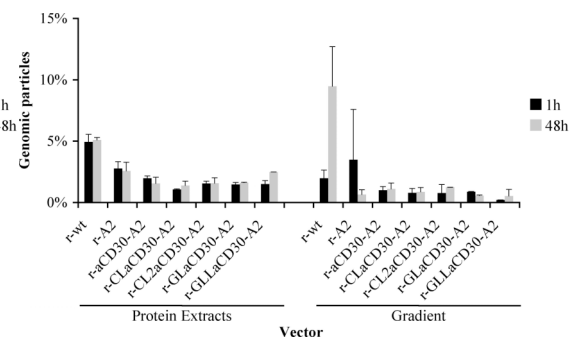
Figure 31. Transduction of CD30+ cells by different r-aCD30-A2 vectors. Vectors were packaged by increasing the amount of the aCD30-VP2 constructs by 4x. A) After iodixanol gradient purification the different vectors were separated by SDS-PAGE, and analyzed by Western blotting using the B1 antibody (20 µl of r-wt, 20 µl of r-A2 and 40 µl of each of the remaining vectors). B) The different vector preparations obtained either from protein extraction of vector producing cells or iodixanol gradient purification of the respective protein extracts were used to transduce L540 cells (MOI = 10,000 gen.p./cell). Amount of transgene expressing cells was determined by flow cytometry 1 h and 48 h p.t. C) Alternatively, cells were collected, washed three times in PBS and used to perform DNA. Amount of vector genomes found in the cells was determined by quantitative PCR. Show is the ratio between the amount of viral genomes used for transduction and the amount of viral genomes determined 1h and 48 h p.t. Shown is the mean value of triplicate measurements. Error bars represent the standard error of the mean.

By increasing 4x the amount of paCD30nVP2-A2 used for vector packaging, vectors containing the anti-CD30 scFv fused to VP2 (without GFP as linker molecule) and with R585A and R588A substitutions were packaged. Western blot analysis

indicated once more that R585A and R588A substitutions result in a VP1, a VP2 and a VP3 of higher molecular weight (Figure 31 A, r-wt vs. r-A2). The aCD30nVP2 : VP1 ratio was in all vectors very close to 1 (Figure 31 A, r-aCD30-A2 to r-GLLaCD30-A2).

Once more, only r-wt was able to transduce L540 cells (Figure 31 B). The amount of vector DNA found with L540 cells 48 h p.t. was the same when using r-wt after protein extraction from vector producing cells and gradient purified particles (Figure 31 C, r-wt, 48 h, Protein Extracts vs. Gradient). Despite this and the equal transduction efficiency, the amount of vector DNA found 1 h p.t was higher when using r-wt obtained only by protein extraction (Figure 31 C, r-wt, 1 h, Protein Extracts vs. Gradient). Furthermore, in this case, the amount of DNA found after 1 h, equals the amount found after 48 h (Figure 31 C, Protein Extracts, 1 h vs. 48 h). No significant amount of vector DNA was found when using any of the other vectors.

5.2.8. anti-CA19.9 scFv

To determine if the lack of transduction and binding efficiency of r-GFP-aCD30 was due to the anti-CD30 scFv, a different scFv was fused to N-terminus of the GFP-VP2 protein and vectors with R585A and R588A substitutions packaged. 5x, 10x and 15x higher amounts of the plasmid coding for the aCA19-GFP-VP2 fusion protein were used during packaging. Western blot analysis revealed that the best aCA19-GFP-VP2 : VP1 ratio – 1 : 1 – could be achieved by using 5x more of the respective plasmid (Figure 32 A). This vector was used in following experiments and named r-GFP-aCA19-A2.

r-wt, r-A2 and r-GFP-aCA19-A2 obtained by protein extraction from vector producing cells (Protein Extracts) or following iodixanol gradient purification of the respective extracts (Gradient) were used to transduce the CA9.9 positive human colon carcinoma derived cell line LS174T (Figure 32 B, C). Transduced cells were only detectable 48 h p.t. when using r-wt (Figure 32 C, r-wt, Protein Extracts and Gradient). The same holds true for the amount of vector DNA, which was only found in relevant amounts 48 h p.t. when using r-wt (Figure 32 D, r-wt, Protein Extracts and Gradient). The low fluorescence detected with r-GFP-aCA19-A2 is an artefact that results of a change in cell granularity and shape (as detected by flow cytometry; data not shown), which were probably due to the high percentage of vector volume.
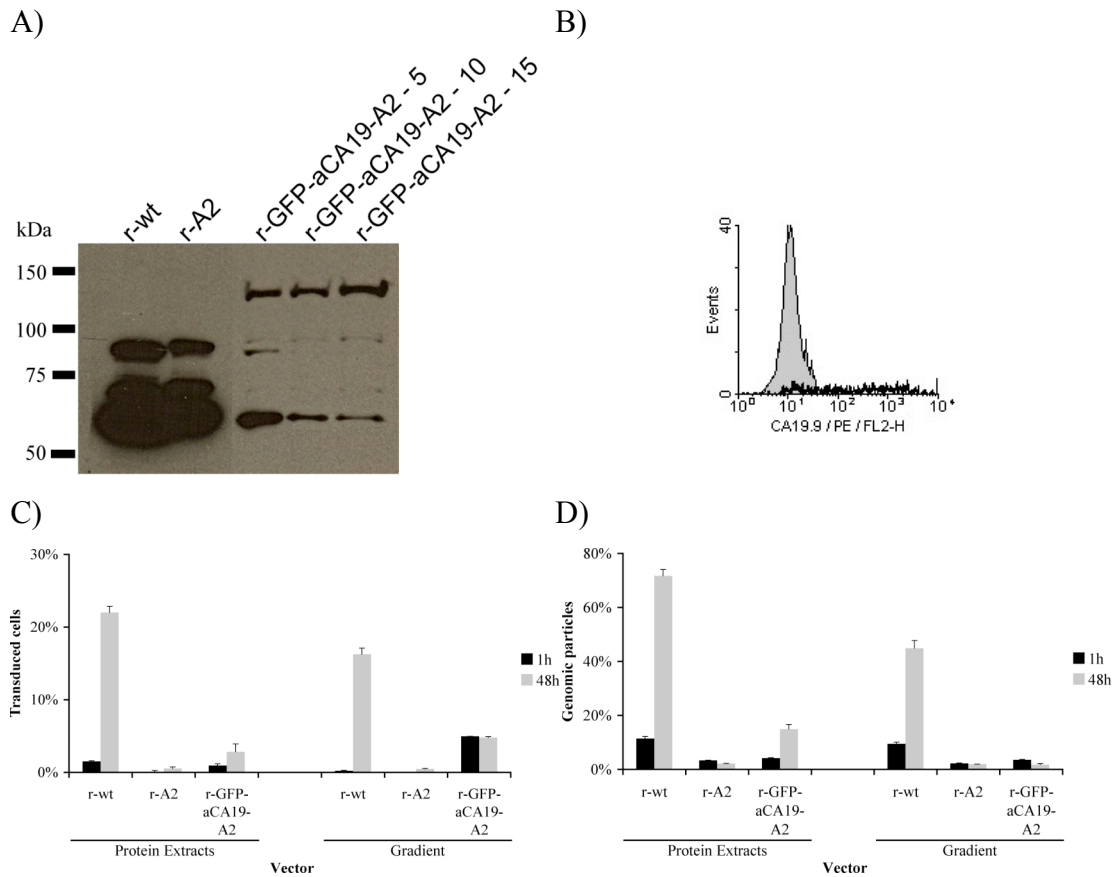
Figure 32. AAV-2-GFP-aCA19.9 A) r-GFP-aCA19 was packaged by increasing the amount of paCA19-GFP-VP2 supplied *in trans* 5 to 15x (r-GFP-aCA19-A2-5 to r-GFP-aCA19-15 respectively). After iodixanol gradient purification the different vectors were separated by SDS-PAGE, and analyzed by Western blotting using the B1 antibody (20 µl of r-wt, 20 µl of r-A2 and 40 µl of each of the remaining vectors). r-GFP-CA19-A2-5 was used in the following experiments. B) The presence of the target molecule – CA19.9 – on LS174T cells at the time of infection was determined by staining with an anti-CA19.9 antibody (thicker black line) and analyzed by flow cytometry. C) The different vector preparations, obtained either from protein extraction of vector producing cells or iodixanol gradient purification of the respective protein extracts, were used to transduce LS174T cells (MOI = 5,000 gen.p./cell). Amount of transgene expressing cells was determined by flow cytometry 1 h and 48 h p.t. D) Alternatively, cells were collected, washed three times in PBS, and used to perform DNA isolation. Amount of vector genomes found in the cells was determined by quantitative PCR. Shown is the ratio between the amount of viral genomes used for transduction and the amount of viral genomes determined 1 h and 48 h p.t. Shown is the mean value of triplicate measurements. Error bars represent the standard error of the mean.

5.2.9. anti-CEA scFv

One other scFv was used for exclusion of idotype specific problems in the construction of AAV-2 vectors with scFv/VP2 fusion proteins.

An anti-CEA scFv was fused to the N-terminus of the GFP-VP2 fusion protein. Western blot analysis of vector purified particles revealed that the best aCEA-GFP-VP2 : VP1 ratio is achieved by using 10x more of the paCD30-GFP-VP2

plasmid (Figure 33 A, r-GFP-aCEA-A2-10). This vector was used in the following experiments and named r-GFP-aCEA-A2.

A)
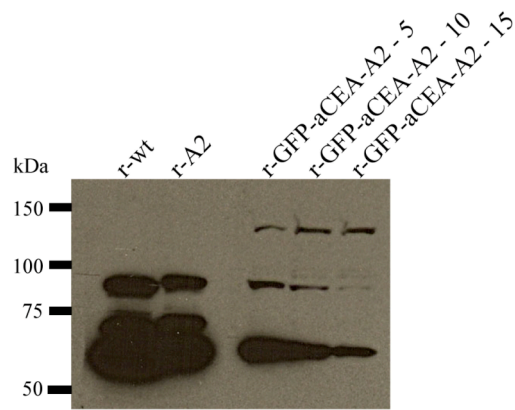
B)
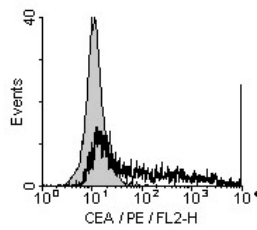
C)
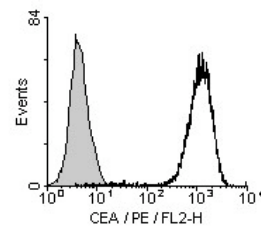
D)
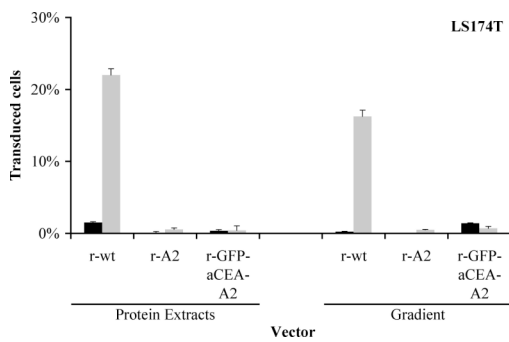
E)
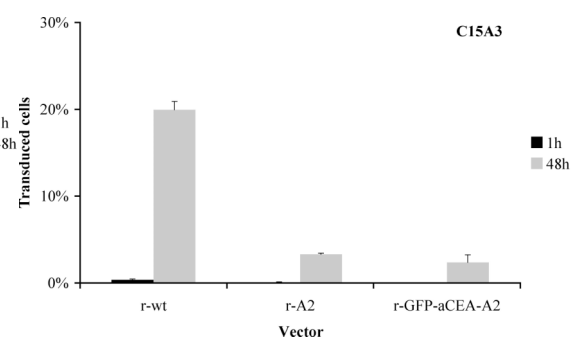
F)
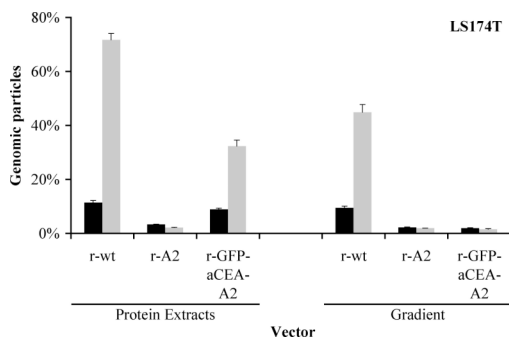
G)
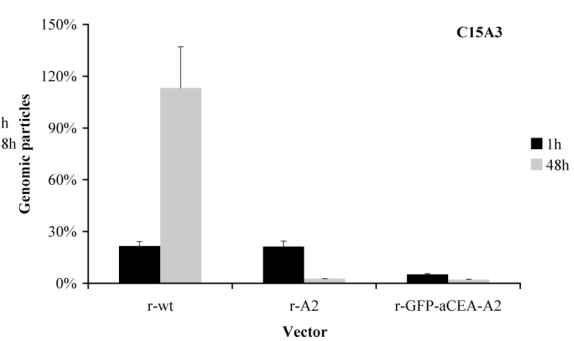
Figure 33. AAV-2-GFP-aCEA A) r-GFP-aCEA was packaged by increasing the amount of paCEA-GFP-VP2 VP2 supplied in trans 5 to 15x (r-GFP-aCEA-A2-5 to r-GFP-aCEA-15 respectively). After iodixanol gradient purification the different vectors were separated by SDS-PAGE, and analyzed by Western blotting using the B1 antibody (20 µl of r-wt, 20 µl of r-A2 and 40 µl of each of the remaining vectors). r-GFP-aCEA-A2-10 was used in the following experiments. B) The presence of the target molecule – CEA – on LS174T cells and C) C15A3 cells at the time of infection was determined by staining with an anti-CEA antibody (thicker black line) and analyzed by flow cytometry. D-G) The different vector preparations obtained either from protein extraction of vector producing cells or iodixanol gradient purification of the respective protein extracts were used to transduce D, E) LS174T cells and F, G) C15A3 cells – for the transduction of C15A3 cells only protein extracts were used - (MOI = 5,000 gen.p./cell). D, F) Amount of transgene expressing cells was determined by flow cytometry 1 h and 48 h p.t. E, G) Alternatively, cells were collected (C15A3 were first scraped out of the plates), washed three times in PBS, and used to perform DNA isolation. Amount of vector genomes found in the cells was determined by quantitative PCR. Show is the ratio between the amount of viral genomes used for transduction and the amount of viral genomes determined 1 h and 48 h p.t. Shown is the mean value of triplicate measurements. Error bars represent the standard error of the mean.

r-wt, r-A2, and r-GFP-aCEA-A2 preparations were obtained by protein extraction from vector producing cells and iodixanol gradient purification of the respective extractions. Only r-wt was able to transduce the CEA positive human colorectal carcinoma derived cell line LS174T (Figure 33 B; D, r-wt, 48 h, Protein Extracts and Gradients). Surprisingly, not only r-wt but also r-GFP-CEA-A2 (used after protein extraction) vector DNA was found with the cells (Figure 33, E, Protein Extracts, r-GFP-aCEA-A2, 48 h).

To clear this result as a r-GFP-aCEA-A2 specific interaction with the CEA antigen, preparations obtained from protein extraction were used to transduce a highly positive CEA cell line – C15A3 (Figure 33 C). Only r-wt was able to transduce C15A3 cells (Figure 33 F, r-wt, 48h). Furthermore, in contrast to the results obtained on LS174T cells, only r-wt vector DNA was found with C15A3 cells (Figure 33 G, r-wt, 48h).

In summary, it was not possible to detect full (capsids + transgene) AAV-2 mutants containing a scFv bound to their target cells. As a result, target cells were not transduced.

6. Discussion

A prerequisite for successful application of gene therapy is the achievement of efficient and selective gene transfer into target cells with little or no toxicity to non-target cells. Modification of vector tropism by non-genetic and genetic approaches aims to develop such vector systems.

Peptide insertion into the capsid of AAV vectors based on serotype 2 has been shown to enable transduction of cells refractory to AAV-2 infection (61, 62, 66, 128, 130, 139, 159, 172, 173, 192, 196, 197). Furthermore, improved specificity of gene transfer has been shown in small animal models after local (172) and systemic application (128, 192, 196). The most popular sites for insertion of small peptides into the AAV-2 capsid are 587 and 588. Here, by *in silico* analysis of the now available three dimensional structure of the AAV-2 capsid a more prominent position was identified. This analysis revealed that T454 is the less bulked residue in the outer surfaced of the capsid and at the same time one of the most distant residues from the virus center (Figure 9).

T454 like 587/588 maps to the GH loop which is the longest loop of the AAV-2 capsid (Figure 9). GH loops of two adjacent capsid subunits contribute to the 3-fold-proximal peaks, which cluster around the 3-fold symmetry axis and protrude from the capsid surface (203). 587/588 map to the second highest peak of this region and are located in a loop region connecting the anti-parallel β-sheets GH12 and GH13 (203). 453, instead, is found at the β-turn which connects the anti-parallel β-sheets GH2 and GH3 and which together contribute to the highest peak of the AAV-2 capsid (203). Thus, peptide insertions between G453 and T454 should be more protruding from the capsid surface than insertions at 587/588. Therefore, targeting peptides inserted at this position should be more accessible for the binding to their target receptor.

The β-sheets of the highest peak have been used for peptide insertion in previous attempts. Initially Girod and colleagues (62) inserted the β1 integrin binding peptide L14 (QAGTFAL<u>RGD</u>NPQG) at 447. This was followed by Grifman and colleagues (66), who successfully inserted a Myc epitope and the CD13 binding peptide NGR, respectively, at position 448. In two different approaches, Bartlett and colleagues (5, 171) used 459 to insert an AgeI restriction site, a 6 amino acid (aa) peptide from bovine papillomavirus (TPFYLK), a 10 aa peptide from human

luteinizing hormone (HCSTCYYHKS), and a 15 aa biotin acceptor peptide. Only one of the three positions, namely 447, was investigated for its usefulness in vector targeting. Interestingly, although the inserted L14 peptide conveyed cell binding, it failed to mediate target cell transduction (62).

Recently, also the β-turn was investigated for its ability to harbor peptide insertions (102). With the aim of identifying positions that tolerate a His_6-tag for vector purification by affinity chromatography, Koerber and colleagues generated a library of capsid mutants carrying a His_6-tag at various positions. Applying this library to a Ni-NTA-column selected a capsid mutant carrying the His_6-tag at 454. This result corroborates our hypothesis concerning the exposure of peptides inserted at this small loop. However, in contrast to r-RGD4C-453 and r-RGD4C-453-A2 for which we determined a genomic-to-infectious ratio of $\leq 3.0 \times 10^3$, their insertion mutant showed poor infectivity (genomic-to-infectious particle ratio of $>10^5$; determined on HeLa cells). One likely explanation for this discrepancy is that we inserted a peptide that unlike His_6-tag interacts with cellular receptors, as is the case for r-RGD4C-453-A2, or does not interfere with natural receptor interaction, as is the case for r-RGD4C-453. The latter may not be possible if a His_6-tag is inserted at 454. Taking into account that mutants displaying the His_6-tag in 587 remained infectious (102), these examples reveal the importance of the interplay between insertion site and the nature of the inserted peptide.

Neither insertion of RGD4C at 453 nor insertion combined with R585A and R588A substitution, interfered with viral packaging as indicated by the total-to-full capsid ratios which are comparable to r-wt. The same holds true for the transduction efficiencies, since capsid-to-infectious ratios of 6.3×10^3 and 6.0×10^3 were determined in HeLa cells for r-RGD4C-453 and r-RGD4C-453-A2, respectively. Thus insertion at 453 does not interfere with vector genome packaging or with essential viral functions.

Particles with R585A/R588A substitutions showed a decreased electrophoretic mobility (Figure 12, Figure 20, Figure 30 A, Figure 32 A and Figure 33 A). In a reducing SDS-page such lower protein mobility can only be the result of an increase in protein weight. Both VP1, VP2 and VP3 showed a 2-3 kDa increase in molecular weight. Although not commented, this has already been observed by others (135). Since substitution of one amino acid by a smaller one cannot result in a heavier protein, such change in molecular weight can only be the result of post-translation

modifications that do not occur in wt capsids but do occur in mutants with R585A and R588A substitutions (or vice versa). Interestingly, 2 residues N-terminally of R585 – S580 and T581 – are prone to phosphorylation. A previously published computer-simulated heparin-docking experiment involving the AAV-2 capsid surface showed that T581 is located at the top of the channel through which heparin enters and that T581 can indeed contribute to heparin binding via hydrogen bond stabilization (97). Thus, blocking this channel by modifying a residue situated at its entrance would leave almost no residues available for heparin binding. In summary, the absence of R585 and R588 may facilitate the phosphorylation of T581, which may result in the blocking of the HSPG binding channel. One other example is N496, which has polar contacts with R585 of an adjacent subunit. N496, part of an NxS motif (where x can be any amino acid except P), is a potential N-glycosilation site. Submission of one AAV-2 subunit to the GlyProt modeling tool resulted in a N496 connected N-Glycan that was modeled over the top of the R585/R588 loop of an adjacent subunit (data not shown; (60, 202)). Unfortunately this and other modeling tools are not able to process more than one subunit at once. Thus, it is possible that R585 and R588 prevent the glycosilation of N496 either by helping in the construction of such a sterically interfering loop or by establishing hydrogen bonds with N496. Although it is clear that capsid modifications can lead to new structures from which a new phenotype may result, further work must be done to prove the hypotheses described above. For this, the use of phosporylation or glycosilation deficient cell lines or chemical inhibitors could be of use.

The accessibility of RGD4C on the capsid surface was assessed by ELISA determining the amount of intact viral particles that were able to bind soluble $\alpha V\beta 3$ integrin. Interestingly, r-RGD4C-453 as well as r-RGD4C-587 showed only marginal receptor binding. The combination of peptide insertion with amino acid substitutions (R585A and R588A) dramatically improved the receptor binding capacity (Figure 13) revealing for the first time that modification of residues linearly distant from the insertion site can promote such effects. Although r-RGD4C-453&587, in contrast to the single insertion mutants, showed efficient interaction with $\alpha V\beta 3$ integrins, receptor binding was also enhanced when introducing the R585A and R588A substitutions. This enhancing effect of R585A and R588A substitutions may be the

result of a change in electrostatic interactions and/or structural conformation resulting in either better exposure of the inserted peptide or diminished sterical hindrance.

As demonstrated by many previous attempts (62, 128, 130, 139, 141, 196) and also in this study (Figure 14 A), peptides inserted at position 587 mediate cell infection by binding to their target receptor if primary receptor binding is prevented by the peptide insertion. The same holds true for peptides inserted at position 453 (Figure 14 A). r-RGD4C-453-A2 transduction of HeLa cells is inhibited by the addition of soluble RGD containing peptides and is not affected by the addition of heparin, which abolishes HSPG binding. In contrast, transduction by r-RGD4C-453 - containing an unmodified HSPG binding motif – was inhibited by the addition of heparin and not by soluble RGD peptides. This does not necessarily means that r-RGD4C-453 does not use RGD4C for cell entry. Thus, heparin binding to the capsid may result in an heparin coated capsid that is then shielded from the receptor by the bound heparin. Moreover, competitions with soluble RGD peptides may not be effective if a strong binding to the primary receptor – HSPG – is still possible.

Shi and colleagues created a double insertion mutant by inserting the RGD4C peptide simultaneously at positions 520 and 584 (173). When used to infect HeLa-C12, an AAV-2 rep- and cap-transfected HeLa derivative, the infectious titer was comparable to wild-type control. In our study, both of our double insertion mutants showed severely reduced transduction capacities even though they efficiently packaged vector genomes, bound soluble integrins and showed cell binding (Table 5, Figure 15 A, Figure 13 and Figure 14 B respectively). Both studies used the same peptide, but different insertion positions. We showed that RGD4C, displayed either at position 453 or 587 is able to mediate viral infection (Figure 14 A). Therefore, the non-infectious phenotype of our double insertion mutants may be the result of simultaneous receptor binding mediated by the peptides displayed by the two different peaks. This may result in either interference with structural rearrangements necessary to undergo the next steps in cell transduction (6) or with endosomal escape due to excessive receptor binding. Peptides in positions 520 and 585 show a different topological arrangement and may not face these problems.

Despite the differences observed *in vitro*, when compared *in vivo*, r-RGD4C-587 and r-RGD4C-453-A2 showed identical biodistributions. Thus, peptides inserted in 453 and 587 are equally efficient in re-directing AAV's tropism if primary receptor

binding is avoided. Furthermore, *in vivo* tropism was independent of the modification that led to an HSPG non-binding phenotype.

Assessment of RGD4C mutants particles stability was made by transduction of HSPG negative cells after consecutive freezing cycles. r-A2 and r-RGD4C-453&587 were to low in transduction efficiency to allow the visualization of any alteration. These low levels of transduction might as well be achieved by unspecific uptake bypassing the need for a stable functional particle. While the transduction efficiency of the analyzed capsid mutants dropped to half after 10 freezing cycles, the efficiency of unmodified particles remained unaffected.

Besides RGD4C also other (alternative) peptide insertions after G453 are tolerated. As with RGD4C, insertion of NGRI or GEN resulted in efficiently packaged particles that were able to transduce cells. Interestingly, while r-NGRI-453-A2 was not infectious, r-NGRI-453 was more infectious on HeLa cells and HUVEC than r-wt revealing that the inserted NGRI peptide may indeed contribute to cell transduction (Table 6, Figure 21). Despite its higher transduction efficiency r-NGRI-453 transduction was still inhibited by the addition of soluble heparin. The fact that a heparin covered mutant like r-NGRI-453 may not be able to efficiently bind to its target receptor (APN) - as a result of its heparin cover - and the high transduction efficiency of r-NGRI-453 shows that this vector may be able to bind HSPG and APN. Furthermore, r-NGRI-587 transduction was not inhibited by the addition of heparin and interestingly, the transduction efficiency of the double insertion mutant – r-NGRI-453&587 – was inferior to r-wt on HeLa cells but equal on HUVEC. Thus, it is possible, that also in this case both inserted peptides are able to bind their receptor. The insertion in 453 of an AAV display peptide that was selected in position 587 did not result in an improved vector. However, this could be expected since the selection protocol should lead to a peptide that best fits the position that was used during selection. Moreover, while the selection protocol was done using a single-stranded genome in this work a self-complementary genome was used for fast onset of gene expression – by overcoming the rate limiting step of second strand synthesis. Further competition experiments using GEN and cyclic NGR soluble peptides would be required for a better analysis of these insertions.

Submission of the AAV-2 capsid protein VP2 to the NCBI's Conserved Domain Database (CDD)(117) identified one major conserved domain (Figure 23). This domain, part of the Parvovirus coat protein superfamily (pfam00740, imported

from the Pfam database) includes G453 and N587. Analysis of the respective sequence alignments led to the identification of the AAV-2 G453 and N587 homologues in the other 8 *Parvovirinae*. Analysis of the complete capsid of CPV, B19, AAV-4 and MVM revealed that the G453 homologues were indeed located in the outer surface of the respective viral capsids (data not shown). Interestingly, while the most distant and less bulked (more separated from other residues) residue in the AAV-2 capsid is T454, in B19 it is K396, which is the AAV-2 587 homologue (Figure 23 C, D and E). Thus, G453 emerges as a position for insertion of small peptides in the capsid of *Parvovirinae*.

In summary, using rational design we have identified a new position for peptide insertions - 453. R585A and R588A mutations resulted in an improved target receptor binding of RGD4C inserted either at 453 or at 587. These are the first two examples showing that single point mutations of capsid residues can improve target receptor binding of AAV-2 based targeting vectors. All these results highlight the important relations between target receptor, inserted peptide, insertion site and neighboring regions for the design of specific and efficient targeting vectors. By using the recently developed AAV libraries (115, 128, 139, 140) and high-throughput selection protocols, tools are available to take this into account and identify the most suitable combination of target receptor, inserted peptide, insertion site, and modification of surrounding residues for the development of optimized targeting vectors.

Monoclonal antibodies have long been used as specific targeting reagents for the manipulation of the immune system in order to improve protection against tumors and pathogens (123). Fragments containing variable regions of the antibodies, such as the 100 and 50kDa F(ab')2 and Fab fragments have also been used in clinical trials (85). By genetic engineering, single-chain Fv recombinant proteins of approximately 28 kDa can be generated by connecting the gene encoding the heavy-chain and light chain variable regions by an oligonucleotide linker. These molecules retain the recognition ability of the whole immunoglobulin, and their small size and lack of carbohydrate groups allows them to be expressed in prokaryotic systems. To increase the functional affinity of the construct and improve targeting efficiency, bivalent or multivalent forms of scFv can also be generated by connecting subunits non-

covalently, covalently or with disulfide bonds. Thus, fusion of a scFv to an AAV should allow re-targeting of the viral vector.

The most suitable place for such fusions is the N-terminus of VP2. Insertions at the commom VP C-terminus are not tolerated (198). Insertion of peptides with more than 34 a.a. in non-terminal regions are not expected to result in the formation of viral particles (66, 128, 130, 139, 172, 192, 196, 197). The N-terminus of VP1 caries a phospholipase A2 domain that is essential for efficient transduction. The N-terminus of VP3 seems to be located in the inner part of the capsid and peptide insertions in this region are not tolerated (198). The viral protein VP2 is not necessary for capsid assembly and its presence is not required for a productive infection *in vitro* (113, 189). VP1 and probably VP2 N-terminal domains seem to translocate from the inside to the outside of the capsid during infection (105).

In the first ever genetic fusion of a ligand to an AAV capsid Yang and colleagues fused a scFv to the N-terminus of VP2 (208). The low expression of VP3 – probably as a result of the elimination of its Kozak consensus – did not allow the assembly of viral particles. It is now known that VP3 is essential for capsid assembly and that 10 VP3 particles are required per each VP1 and VP2. Not aware of this the authors supplied more wt VP2 and VP3 *in trans* to achieve capsid assembly. The resulting VP1 : scFv-VP2 : VP2 : VP3 chimeric particles were able to transduce their target cells with very low efficiency. Non-target cells were also efficiently transduced and *in vivo* experiments were not performed. In two recent reports, fusion of GFP (27 kDa) to the N-terminus of VP2 yielded GFP-tagged virus with 100% substitution of wt VP2 that were used to visualize the AAV infectious pathway. Thus, the unique N-terminal region of VP2 is the most appealing site for insertion of ~28 kDa molecules like the scFvs. Substitution of the wt VP2 by a scFv-VP2 fusion protein should result in a viral capsid with five scFv molecules. By comparison to other multivalent forms of scFv such pentavalente constructs should possess a good affinity to the target antigen.

The exact location of the N-terminus of VP2 is not known. The available three dimensional structure of AAV-2 does not include this region. The incapacity to resolve this region in crystallography studies is probably due to the fact that, as proposed by more recent models, this region is versatile, it can pass through the pores on the 5-fold symmetry axis being either in the inner or outer part of the capsid. For efficient targeting the ligand must be exposed on the outer surface of the capsid.

Using an anti-GFP antibody and an antibody against intact AAV-2 particles (A20), we were able to demonstrate that the recognized GFP epitope is located on the outer surface of intact capsids (Figure 24). However, this result can not exclude that other parts of the GFP molecule are not located on the inner part of the capsid. In an AAV-2 capsid with 100% substitution of the wt VP2 (72 kDa) per the GFP-VP2 fusion protein (99 kDa) five GFP proteins should be present per capsid. Having this and the small size of AAV-2 (diameter of 25nm) in account, it was indeed unlikely that this protein would be totally contained in the inner part of an intact capsid. This result is also in agreement with previous work where insertion of ligands on the VP2 N-terminus region led to an enlargement of the viral tropism (111, 198).

Not knowing the exact location of the N-terminus of VP2 but knowing that at least a part of the GFP molecule (on GFP-VP2 tagged AAV-2 particles) is located on the outer surface of intact capsids, we started by engineering a construct in which a scFv was fused to the N-terminus of GFP. Such particles would then be targeted and at the same time their infectious pathways could be followed.

As seen in Figure 25 A co-transfection of pGFP-VP2 and pRC VP2 KO (r-GFP) results in lower amounts of the VP1 and VP3 proteins when comparing to single transfections and wt plasmids. The GFP-VP2 ORF is under the control of a CMV promoter while VP1 and VP3 expression is controlled by the AAV-2 specific p40 promoter. Thus, while the expression of GFP-VP2 was expected to be superior to the expression of VP1 and VP3 (as seen on Figure 25 A), co-transfections were not expected to result in a decrease of the amounts of VP1 and VP3. Moreover, production of mutants with incorporated GFP-VP2 fusion proteins resulted in the recovery of approximately 100-fold less vector particles (by comparison with r-wt). Despite this, iodixanol gradient purification revealed that r-GFP particles contain the correct VP1 : GFP-VP2 : VP3 ratio (1:1:10). This did not hold true for all the r-GFP preparations made along this work. As it can be seen in Figure 30 in some r-GFP preparations there was an overrepresentation of the GFP-VP2 protein. The same was seen in previous reports where r-GFP vectors were produced (113, 189). Furthermore, as shown above it was possible to detect GFP on the outer surface of these capsids (Figure 24).

Very low amounts of the aCD30-GFP-VP2 protein were detected in cells transfected with paCD30-GFP-VP2 in comparison to GFP-VP2 in pGFP-VP2 transfect cells (Figure 25 A). As seen in the production of r-GFP, co-transfection of

paCD30-GFP-VP2 and pRC VP2 ko also led to lower amounts of VP1 and VP3. r-GFP-aCD30 purified vectors did not show any aCD30-GFP-VP2 protein (Figure 25 B). The same result was observed when using smaller constructs where the aCD30 scFv was fused to the N-terminus of VP2 either directly or by means of a small linker (Figure 26). Since such smaller constructs have approximately the same molecular weight as GFP-VP2, the differences observed in the incorporation of GFP-VP2 and aCD30-GFP-VP2 do not seem to be due to their different size.

The Kozak consensus translation initiation site, known to improve translation efficiency in eukaryotic cells, is present in the GFP-VP2 encoding plasmid. This site, not present in the remaining fusion proteins was cloned into the aCD30-VP2 encoding plasmid but no improvement in the amount of the fusion protein was visible before or after vector purification (Figure 27). pGFP-VP2 encodes a red-shifted variant of wild-type GFP which has been optimized for higher expression in mammalian cells. The coding sequence of GFP gene contains more than 190 silent base changes which correspond to human codon-usage preferences. Thus, since such optimization has not been done for the aCD30 coding sequence, it is reliable to say that the lower amount of aCD30-GFP-VP2 found in HEK293 cells after transfection is likely the result of non-favorable codons.

To overcome the low expression of aCD30-GFP-VP2, we increased the amount of the respective plasmid used for transfection. As expected, this increased the aCD30-GFP-VP2 : VP1 ratio (Figure 28). Surprisingly, this also resulted in the increase of the amount of VP1 and VP3. Although, after a threshold of 4 (4-fold increase in the amount of plasmid), increasing the amount of paCD30-GFP-VP2 resulted in a decrease in the protein amount of aCD30-GFP-VP2, VP1, and VP3. This was probably due to an increase in the amount of dying cells or slower proliferation due to the overload of DNA.

Particles containing total substitution of wt VP2 by aCD30-GFP-VP2, can still be obtained from the 40% fraction of an iodixanol gradient. A 10-fold decrease in the amount of recovered particles was seen in r-GFP-aCD30-4 (Table 8). Despite this, these particles remained infectious with a mere 1.9-fold reduction in infectivity (when compared to r-wt). Vector production using a paCD30-GFP-VP2 : pRC VP2 ko ratio of 4:1 did not always result in vector particles with an aCD30-GFP-VP2 : VP1 ratio of 1:1 (Figure 28 and Figure 30). Differences were seen when using different batches of cells, plasmid preparations, when up-scaling the transfection protocol and,

independently of this, from transfection to transfection. As discussed above, the same was seen when packaging r-GFP vectors along this work and in previous reports (113, 189). Thus, this is one of the major hurdles of supplying one plasmid *in trans*. Such hurdle might be overcome by designing a system were both XXX/VP2 (where XXX stands for any fused protein) and RC VP2 ko sequences are under the control of the same promoter (eg. p40). Although, the need to over express the XXX/VP2 fusion in relation to VP1 in order to have the fusion protein incorporated in the viral capsid could render this approach unsuccessful. Furthermore, having two gene sequences under the control of the same promotor may also decrease the overall expression of both ORFs. The sequence coding for the fused protein should be optimized for expression in mammalian cells. Alternatively, using the same approaches, construction of a pXXX-VP2/VP3 and a pVP1 plasmid could also be of use. Although, previous reports have shown that such constructs can result in the loss of VP3 expression (189). Moreover, both ORF could be included in one single plasmid. When establishing such systems one should keep in mind the need to achieve extremely high vector titers and the required protocol. This would be especially important when engineering scFv driven vectors. Separation of empty from full particles by ion exchange chromatography can also be of use.

Previous reports (189) have shown that complete absence of VP1 can lead to an 100-fold reduction in infectivity due to the lack of the PLA2 domain (presumably necessary during infection for endosomal escape). Despite this, the minor decrease in the amount of VP1 within our vector particles do not represent a serious obstacle to transduction as r-GFP-aCD30-6 only showed a 1.2-fold reduction in infectivity when compared to r-GFP-aCD30-4 (Table 8, Figure 28 and Figure 30). Thus, we were able to purify infectious AAV particles with an incorporated aCD30-GFP-VP2 fusion protein in substitution for the wt VP2.

Analysis of iodixanol purified and not purified r-GFP-aCD30 preparations revealed that the incorporated scFv was able to bind its antigen – determined using an anti-idiotypic antibody that recognizes the paratope (Figure 29 A and C). Unfortunately, it was not possible to make cross detection of such molecules with intact capsids (Figure 29 B). This may be a result of the low amount of scFv found in each capsid. Thus, while 60 A20 antibodies can bind each AAV-2 capsid, only 5 scFvs are available for anti-idiotypic binding. Sterical hindrance involving the 2 antibodies and the modified capsid may also be an hurdle.

Also, using an anti-GFP antibody it was possible to detect the GFP-aCD30 fusion after protein extraction of vector producing cells but not after iodixanol gradient purification (Figure 29 A). While in protein extracts there are incorporated and non-incorporated fusion proteins in solution, in the iodixanol gradient purified preparations all present fusion proteins are incorporated in the AAV capsid. It should be noticed that, in a western blot, for obtaining the correspondent fusion protein bands with the same signal intensity, about 10x more volume of the iodixanol purified preparation had to be used in relation to protein extracted from cell lysates.

To better differentiate between an AAV-2 wt phenotype and a scFv driven mutant, binding of AAV-2 to its primary receptor was abolished. For this, the known and above discussed R585A and R588A substitutions were added to our vectors (Figure 30 A and Figure 31 A). L540 cells, with a high expression of the target antigen – CD30 – were chosen as target cells (Figure 30 B). Anti-CD30 scFv driven vectors were not able to transduce the target cells (Figure 30 C and Figure 31 B). To discriminate between binding to the target cells and post-binding barriers amount of vector DNA was quantified 1 h and 48 h p.t. (Figure 30 D and Figure 31 C). Vector DNA was only detected in the target cells 48h p.t. when applying r-wt. The low permissibility of this cells did not allow the detection of vector DNA 1 h p.t.. Despite this, 1 h (at 37 ºC) should give enough time for the scFv to bind its target molecule. Immunological stainings can be done by incubating the antibodies and antigens for 30 min. Thus, our scFv targeting mutants, if bound but not internalized should be detectable by this assay (specially when the antigen is highly expressed on the cell surface). Indeed, it seems that the inability of the scFv targeting mutants to transduce their target cells is the result of their incapacity to bind the target antigen (Figure 30-33).

To increase the concentration of vector particles and cells in solution, cells were pelleted and ressuspended in viral solution (data not shown). Unfortunately, this has not resulted in detectable transduction. Comparison of performed transduction assays with immunophenotyping assays indicates that, indeed, the low titers of our vectors may not allow scFv / antigen binding events (Table 9). Although nearly the same particles-to-cell ratio is used, in immunophenotyping assays concentration of whole Ig molecules and cells is approximately 5.0×10^4 times higher. To perform transduction assays that would completely parallel immunophenotyping assays, vectors would have to be highly concentrated – 1.0×10^{15} genomic particles / ml.

Although one previous report has shown that wt AAV vectors can be produced with titers near the 1.0×10^{15} genomic particles/ml value, our mutants show a 10- to 100-fold decrease in packaging efficiency making it impossible to achieve such titers. Furthermore, the fact that whole Ig molecules have higher affinity to their antigens then scFvs indicates that even higher titers my be required.

	r-AAV-	
	aCEA (scFv)	anti-CEA (whole Ig)
Particles/Cell	1.00E+04	4.34E+04
Cells/ml	4.00E+04	6.67E+08
Particles/ml	4.00E+08	2.90E+13

Table 9. Transduction with AAV-scFv particles vs. Immunophenotyping with whole Ig molecules. Comparison of C15A3 cells transduction by an AAV/scFv targeting vector with immunophenotyping protocols using whole Ig molecules.

The inefficient targeting capacity of our anti-CD30 driven vectors is not idiotype specific. This is supported by the fact that vectors where the anti-CD30 scFv was substituted either by an anti-CA19.9 scFv or an anti-CEA scFv were also not able to bind and transduce their target cells (Figure 32 and Figure 33). Interestingly, assembly of r-GFP-aCEA-A2 particles with an aCEA-GFP-VP2 : VP1 ratio of 1:1 required a 10-fold increase in the amount of paCEA-GFP-VP2 plasmid used (while vectors with anti-CD30 and anti-CA19 scFvs only required a 4- and 5-fold increase in the amount of plasmid used in transfection).

Although surprising results could appear from *in vivo* assays, our preliminary *in vitro* data does not support such experiments.

In contrast to Yang and colleagues - 1998 - we were not able to generate targeting AAV-2 based particles by fusion of a scFv to the N-terminus of VP2 (208). One of the differences between this two works is the type of assays used for determination of the transduction efficiencies. Yang and colleagues used a *β*-galactosidase gene as a reporter gene and determined the transducing titers by counting under a microscope the amount of cells stained with X-Gal. In contrast, we used a GFP gene as a reporter gene and determined the transducing titers by fluorescent activated cell sorting (FACS) analysis. Also, while we used an adenovirus free production system for our vectors, Yang and colleagues did not. In their study, the best obtained titer was equal to 1.9×10^2 transducing units/mL. Furthermore, Yang and colleagues have not shown complete AAV particles with an incorporated scFv. One year after this report, another approach made use of antibody molecules. A bispecific antibody displaying affinities for αIIbβ3 integrin (AP-2 antibody part) and

the intact AAV-2 capsid (A20 antibody part) was used by Bartlett and colleagues to bind rAAV-2 to fibrinogen on MO7e and DAMI cells, which are not permissive for wild-type AAV-2 infection (12). The binding is likely to induce a receptor-mediated endocytosis and resulted in transduction efficiencies 70-fold above background (12). In 2002, Ried and colleagues inserted the immune globulin binding domain Z34C in position 587 (159). rAAV-2-Z34C vectors were coupled to antibodies and specifically transduced their target cells. Although they used a GFP gene as a reporter gene quantification of transduced cells was made by fluorescence microscopy. Transducing titers were also here extremely low. All mentioned reportrs failed to present *in vivo* results. Despite the large number of publications involving AAV targeting only the 3 reports mentioned above involved antibody molecules or antibody fragments. Although previous works have shown that insertion of peptide ligands in the VP2 unique region (VP1 + VP2) can lead to an increase in transduction efficiency, it is still to be shown that such result is due to the binding of the ligand to its receptor (111, 198). Moreover, the same group demonstrated that ligands as large as 146 amino acids can be exclusively inserted in the N-terminus of VP2, but no targeting or enlargement of tropism was shown until now (189). Furthermore, while one work showed success *in vitro* with scFv driven adenovirus type 5 vectors, others have failed to show targeted gene delivery (79, 187).

In summary, we were able to produce AAV-2-scFv infectious particles. Beside showing how such highly specific molecules can be fused to the vector capsid we demonstrate how proteins as big as the GFP-scFv can be fused to the N-terminus of VP2. The scFv-GFP fusion represents the biggest described fusion to the AAV-2 capsid. These particles had an incorporated scFv/VP2, whixh was recognized by an anti-idiotypic antibody directed against the paratope, re-enforcing the theory that the N-terminus of VP2 can indeed be displayed on the outer surface of the capsid. Unfortunately, these particles were not able to bind their target antigen when displayed on the surface of cells. Improved packaging systems and increased number of scFv molecules per capsid emerge as pre-requisites for the construction of scFv directed vectors. Despite this, in experimental designs where it is not necessary to have such high concentration of the fused protein, fusions to the N-terminus of VP2 can be of good use.

Abbreviations

a.a.	amino acid	p.i.	post-infection
AAV	adeno-associated virus, specifically adeno-associated virus type 2	p.t.	post-transduction
		PAGE	polyacrylamide gel electrophoresis
AAVS1	AAV integration site 1 (located in human chromosome 19)	r-AAV	recombinant AAV
		RBS	Rep binding site
Ab	antibody	Rep	viral regulatory protein
Ad	adenovirus	rpm	rounds per minute
B19	B19 human parvovirus	RT	room temperature
bp	base pair	scAAV	AAV containing self complementary DNA
BSA	bovine serum albumin		
Cap	capsid protein	SDS	sodium dodecyl sulfate
ch	chromosome	Stav	streptavidin
CMV	cytomegalovirus	ssAAV	AAV containing single stranded DNA
Da	Dalton		
DMEM	Dulbecco's Modified Eagle Medium	TRS	terminal resolution site
		VP	viral protein (AAV capsid protein)
DNA	Deoxyribonucleic Acid	wtAAV	wild-type AAV
e.g.	for example (Lat.: exempli gratia)		
ELISA	enzyme-linked immunosorbent assay		
FACS	fluorescence-activated cell sorting		
FCS	fetal calf serum		
FGFR	fibroblast growth factor receptor 1		
FITC	fluorescein isothiocyanate		
GFP	green fluorescence protein		
h	hour		
HSPG	heparan sulfate proteoglycan		
i.e.	that is (Lat.: id est)		
ITR	inverted terminal repeat		
kb	kilobases		
mAb	monoclonal antibody		
MHC	major histocompatibility complex		
min	minute		
MOI	multiplicity of infection		
NPC	nuclear pore complex		
nt	nucleotide		
ori	origin of replication		
ORF	open reading frame		

References

1. 2008. Gene Therapy Clinical Trials Worldwide. Journal of Gene Medicine, Wiley.
2. **Allen, J. M., C. L. Halbert, and A. D. Miller.** 2000. Improved adeno-associated virus vector production with transfection of a single helper adenovirus gene, E4orf6. Mol Ther **1:**88-95.
3. **Anderson, R., I. Macdonald, T. Corbett, A. Whiteway, and H. G. Prentice.** 2000. A method for the preparation of highly purified adeno-associated virus using affinity column chromatography, protease digestion and solvent extraction. J Virol Methods **85:**23-34.
4. **Arap, W., R. Pasqualini, and E. Ruoslahti.** 1998. Cancer treatment by targeted drug delivery to tumor vasculature in a mouse model. Science **279:**377-80.
5. **Arnold, G. S., A. K. Sasser, M. D. Stachler, and J. S. Bartlett.** 2006. Metabolic biotinylation provides a unique platform for the purification and targeting of multiple AAV vector serotypes. Mol Ther **14:**97-106.
6. **Asokan, A., J. B. Hamra, L. Govindasamy, M. Agbandje-McKenna, and R. J. Samulski.** 2006. Adeno-associated virus type 2 contains an integrin alpha5beta1 binding domain essential for viral cell entry. J Virol **80:**8961-9.
7. **Atchison, R. W., B. C. Casto, and W. M. Hammon.** 1965. Adenovirus-Associated Defective Virus Particles. Science **149:**754-6.
8. **Auricchio, A., M. Hildinger, E. O'Connor, G. P. Gao, and J. M. Wilson.** 2001. Isolation of highly infectious and pure adeno-associated virus type 2 vectors with a single-step gravity-flow column. Hum Gene Ther **12:**71-6.
9. **Balsinde, J., M. A. Balboa, P. A. Insel, and E. A. Dennis.** 1999. Regulation and inhibition of phospholipase A2. Annu Rev Pharmacol Toxicol **39:**175-89.
10. **Bantel-Schaal, U., B. Hub, and J. Kartenbeck.** 2002. Endocytosis of adeno-associated virus type 5 leads to accumulation of virus particles in the Golgi compartment. J Virol **76:**2340-9.
11. **Bantel-Schaal, U., and H. zur Hausen.** 1984. Characterization of the DNA of a defective human parvovirus isolated from a genital site. Virology **134:**52-63.
12. **Bartlett, J. S., J. Kleinschmidt, R. C. Boucher, and R. J. Samulski.** 1999. Targeted adeno-associated virus vector transduction of nonpermissive cells mediated by a bispecific F(ab'gamma)2 antibody. Nat Biotechnol **17:**181-6.
13. **Bartlett, J. S., R. Wilcher, and R. J. Samulski.** 2000. Infectious entry pathway of adeno-associated virus and adeno-associated virus vectors. J Virol **74:**2777-85.
14. **Becerra, S. P., F. Koczot, P. Fabisch, and J. A. Rose.** 1988. Synthesis of adeno-associated virus structural proteins requires both alternative mRNA splicing and alternative initiations from a single transcript. J Virol **62:**2745-54.
15. **Becerra, S. P., J. A. Rose, M. Hardy, B. M. Baroudy, and C. W. Anderson.** 1985. Direct mapping of adeno-associated virus capsid proteins B and C: a possible ACG initiation codon. Proc Natl Acad Sci U S A **82:**7919-23.
16. **Berns, K. I.** 1990. Parvovirus replication. Microbiol Rev **54:**316-29.
17. **Berns, K. I., and R. M. Linden.** 1995. The cryptic life style of adeno-associated virus. Bioessays **17:**237-45.
18. **Blackburn, S. D., R. A. Steadman, and F. B. Johnson.** 2006. Attachment of adeno-associated virus type 3H to fibroblast growth factor receptor 1. Arch Virol **151:**617-23.
19. **Blaese, R. M., K. W. Culver, A. D. Miller, C. S. Carter, T. Fleisher, M. Clerici, G. Shearer, L. Chang, Y. Chiang, P. Tolstoshev, J. J. Greenblatt, S. A. Rosenberg, H. Klein, M. Berger, C. A. Mullen, W. J. Ramsey, L. Muul, R. A. Morgan, and W. F. Anderson.** 1995. T lymphocyte-directed gene therapy for ADA- SCID: initial trial results after 4 years. Science **270:**475-80.
20. **Bomsel, M.** 1997. Transcytosis of infectious human immunodeficiency virus across a tight human epithelial cell line barrier. Nat Med **3:**42-7.
21. **Boyle, M. P., R. A. Enke, J. B. Reynolds, P. J. Mogayzel, Jr., W. B. Guggino, and P. L. Zeitlin.** 2006. Membrane-associated heparan sulfate is not required for rAAV-2 infection of human respiratory epithelia. Virol J **3:**29.
22. **Brister, J. R., and N. Muzyczka.** 2000. Mechanism of Rep-mediated adeno-associated virus origin nicking. J Virol **74:**7762-71.
23. **Brown, K. E.** 2000. Haematological consequences of parvovirus B19 infection. Baillieres Best Pract Res Clin Haematol **13:**245-59.

24.   **Carter, P. J., and R. J. Samulski.** 2000. Adeno-associated viral vectors as gene delivery vehicles. Int J Mol Med **6:**17-27.

25.   **Cassani, B., M. Mirolo, F. Cattaneo, U. Benninghoff, M. Hershfield, F. Carlucci, A. Tabucchi, C. Bordignon, M. G. Roncarolo, and A. Aiuti.** 2008. Altered intracellular and extracellular signaling leads to impaired T-cell functions in ADA-SCID patients. Blood **111:**4209-19.

26.   **Cavazzana-Calvo, M., S. Hacein-Bey, G. de Saint Basile, F. Gross, E. Yvon, P. Nusbaum, F. Selz, C. Hue, S. Certain, J. L. Casanova, P. Bousso, F. L. Deist, and A. Fischer.** 2000. Gene therapy of human severe combined immunodeficiency (SCID)-X1 disease. Science **288:**669-72.

27.   **Chejanovsky, N., and B. J. Carter.** 1989. Mutagenesis of an AUG codon in the adeno-associated virus rep gene: effects on viral DNA replication. Virology **173:**120-8.

28.   **Chignon, J. C., R. Distel, and J. Leclercq.** 1975. [Vectorcardiographic aspects of ventricular hypertrophy in the highly competitive athlete]. Ann Cardiol Angeiol (Paris) **24:**361-4.

29.   **Collaco, R. F., X. Cao, and J. P. Trempe.** 1999. A helper virus-free packaging system for recombinant adeno-associated virus vectors. Gene **238:**397-405.

30.   **Colombo, G., F. Curnis, G. M. De Mori, A. Gasparri, C. Longoni, A. Sacchi, R. Longhi, and A. Corti.** 2002. Structure-activity relationships of linear and cyclic peptides containing the NGR tumor-homing motif. J Biol Chem **277:**47891-7.

31.   **Cotrim, A. P., and B. J. Baum.** 2008. Gene therapy: some history, applications, problems, and prospects. Toxicol Pathol **36:**97-103.

32.   **Curnis, F., G. Arrigoni, A. Sacchi, L. Fischetti, W. Arap, R. Pasqualini, and A. Corti.** 2002. Differential binding of drugs containing the NGR motif to CD13 isoforms in tumor vessels, epithelia, and myeloid cells. Cancer Res **62:**867-74.

33.   **Daniel, T. O., D. F. Milfay, J. Escobedo, and L. T. Williams.** 1987. Biosynthetic and glycosylation studies of cell surface platelet-derived growth factor receptors. J Biol Chem **262:**9778-84.

34.   **de la Maza, L. M., and B. J. Carter.** 1981. Inhibition of adenovirus oncogenicity in hamsters by adeno-associated virus DNA. J Natl Cancer Inst **67:**1323-6.

35.   **DeLano, E. L. T.** 2002. The PyMOL Molecular Graphics System. DeLano Scientific, San Carlos, USA.

36.   **Dennis, E. A.** 1997. The growing phospholipase A2 superfamily of signal transduction enzymes. Trends Biochem Sci **22:**1-2.

37.   **Di Pasquale, G., and J. A. Chiorini.** 2006. AAV transcytosis through barrier epithelia and endothelium. Mol Ther **13:**506-16.

38.   **Di Pasquale, G., B. L. Davidson, C. S. Stein, I. Martins, D. Scudiero, A. Monks, and J. A. Chiorini.** 2003. Identification of PDGFR as a receptor for AAV-5 transduction. Nat Med **9:**1306-12.

39.   **Diehl, V., H. H. Kirchner, M. Schaadt, C. Fonatsch, H. Stein, J. Gerdes, and C. Boie.** 1981. Hodgkin's disease: establishment and characterization of four in vitro cell lies. J Cancer Res Clin Oncol **101:**111-24.

40.   **Ding, W., L. Zhang, Z. Yan, and J. F. Engelhardt.** 2005. Intracellular trafficking of adeno-associated viral vectors. Gene Ther **12:**873-80.

41.   **Ding, W., L. N. Zhang, C. Yeaman, and J. F. Engelhardt.** 2006. rAAV2 traffics through both the late and the recycling endosomes in a dose-dependent fashion. Mol Ther **13:**671-82.

42.   **Douar, A. M., K. Poulard, D. Stockholm, and O. Danos.** 2001. Intracellular trafficking of adeno-associated virus vectors: routing to the late endosomal compartment and proteasome degradation. J Virol **75:**1824-33.

43.   **Duan, D., Q. Li, A. W. Kao, Y. Yue, J. E. Pessin, and J. F. Engelhardt.** 1999. Dynamin is required for recombinant adeno-associated virus type 2 infection. J Virol **73:**10371-6.

44.   **Duan, D., Y. Yue, Z. Yan, J. Yang, and J. F. Engelhardt.** 2000. Endosomal processing limits gene transfer to polarized airway epithelia by adeno-associated virus. J Clin Invest **105:**1573-87.

45.   **Dubielzig, R., J. A. King, S. Weger, A. Kern, and J. A. Kleinschmidt.** 1999. Adeno-associated virus type 2 protein interactions: formation of pre-encapsidation complexes. J Virol **73:**8989-98.

46.   **Dutheil, N., F. Shi, T. Dupressoir, and R. M. Linden.** 2000. Adeno-associated virus site-specifically integrates into a muscle-specific DNA region. Proc Natl Acad Sci U S A **97:**4862-6.

47.   **Dyson, H., Wright, P.** 1993. Peptide conformation and protein folding. Curr Opin Struc Biol **3:**60-65.

48.   **Dyson, H. J., J. R. Sayre, G. Merutka, H. C. Shin, R. A. Lerner, and P. E. Wright.** 1992. Folding of peptide fragments comprising the complete sequence of proteins. Models for initiation of protein folding. II. Plastocyanin. J Mol Biol **226:**819-35.

49.   **Engert, A., G. Martin, M. Pfreundschuh, P. Amlot, S. M. Hsu, V. Diehl, and P. Thorpe.** 1990. Antitumor effects of ricin A chain immunotoxins prepared from intact antibodies and Fab' fragments on solid human Hodgkin's disease tumors in mice. Cancer Res **50:**2929-35.

50.   **ESGCT** 2008, posting date. European Society of Gene and Cell Therapy. [Online.]

51.   **Esko, J. D., T. E. Stewart, and W. H. Taylor.** 1985. Animal cell mutants defective in glycosaminoglycan biosynthesis. Proc Natl Acad Sci U S A **82:**3197-201.

52. **Fischer, H.** 2004. What made Hanno Buddenbrook sick? N Engl J Med **350:**419-20.

53. **Folkman, J.** 1971. Tumor angiogenesis: therapeutic implications. N Engl J Med **285:**1182-6.

54. **Forster-Horvath, C., L. Meszaros, E. Raso, B. Dome, A. Ladanyi, M. Morini, A. Albini, and J. Timar.** 2004. Expression of CD44v3 protein in human endothelial cells in vitro and in tumoral microvessels in vivo. Microvasc Res **68:**110-8.

55. **Gao, G., G. Qu, M. S. Burnham, J. Huang, N. Chirmule, B. Joshi, Q. C. Yu, J. A. Marsh, C. M. Conceicao, and J. M. Wilson.** 2000. Purification of recombinant adeno-associated virus vectors by column chromatography and its performance in vivo. Hum Gene Ther **11:**2079-91.

56. **Gao, G., L. H. Vandenberghe, M. R. Alvira, Y. Lu, R. Calcedo, X. Zhou, and J. M. Wilson.** 2004. Clades of Adeno-associated viruses are widely disseminated in human tissues. J Virol **78:**6381-8.

57. **Gao, G., L. H. Vandenberghe, and J. M. Wilson.** 2005. New recombinant serotypes of AAV vectors. Curr Gene Ther **5:**285-97.

58. **Gao, G. P., M. R. Alvira, L. Wang, R. Calcedo, J. Johnston, and J. M. Wilson.** 2002. Novel adeno-associated viruses from rhesus monkeys as vectors for human gene therapy. Proc Natl Acad Sci U S A **99:**11854-9.

59. **Gao, G. P., G. Qu, L. Z. Faust, R. K. Engdahl, W. Xiao, J. V. Hughes, P. W. Zoltick, and J. M. Wilson.** 1998. High-titer adeno-associated viral vectors from a Rep/Cap cell line and hybrid shuttle virus. Hum Gene Ther **9:**2353-62.

60. **German Cancer Research Center Heidelberg, C. S. D.** 2008, posting date. Glyprot. German Cancer Research Center Heidelberg, Central Spectroscopic Division. [Online.]

61. **Gigout, L., P. Rebollo, N. Clement, K. H. Warrington, Jr., N. Muzyczka, R. M. Linden, and T. Weber.** 2005. Altering AAV tropism with mosaic viral capsids. Mol Ther **11:**856-65.

62. **Girod, A., M. Ried, C. Wobus, H. Lahm, K. Leike, J. Kleinschmidt, G. Deleage, and M. Hallek.** 1999. Genetic capsid modifications allow efficient re-targeting of adeno-associated virus type 2. Nat Med **5:**1052-6.

63. **Girod, A., M. Ried, C. Wobus, H. Lahm, K. Leike, J. Kleinschmidt, G. Deleage, and M. Hallek.** 1999. Genetic capsid modifications allow efficient re-targeting of adeno-associated virus type 2. Nat Med **5:**1438.

64. **Girod, A., C. E. Wobus, Z. Zadori, M. Ried, K. Leike, P. Tijssen, J. A. Kleinschmidt, and M. Hallek.** 2002. The VP1 capsid protein of adeno-associated virus type 2 is carrying a phospholipase A2 domain required for virus infectivity. J Gen Virol **83:**973-8.

65. **Graham, F. L., J. Smiley, W. C. Russell, and R. Nairn.** 1977. Characteristics of a human cell line transformed by DNA from human adenovirus type 5. J Gen Virol **36:**59-74.

66. **Grifman, M., M. Trepel, P. Speece, L. B. Gilbert, W. Arap, R. Pasqualini, and M. D. Weitzman.** 2001. Incorporation of tumor-targeting peptides into recombinant adeno-associated virus capsids. Mol Ther **3:**964-75.

67. **Grimm, D., A. Kern, K. Rittner, and J. A. Kleinschmidt.** 1998. Novel tools for production and purification of recombinant adenoassociated virus vectors. Hum Gene Ther **9:**2745-60.

68. **Grimm, D., and J. A. Kleinschmidt.** 1999. Progress in adeno-associated virus type 2 vector production: promises and prospects for clinical use. Hum Gene Ther **10:**2445-50.

69. **Guex, N., and M. C. Peitsch.** 1997. SWISS-MODEL and the Swiss-PdbViewer: an environment for comparative protein modeling. Electrophoresis **18:**2714-23.

70. **Hacein-Bey-Abina, S., A. Garrigue, G. P. Wang, J. Soulier, A. Lim, E. Morillon, E. Clappier, L. Caccavelli, E. Delabesse, K. Beldjord, V. Asnafi, E. Macintyre, L. Dal Cortivo, I. Radford, N. Brousse, F. Sigaux, D. Moshous, J. Hauer, A. Borkhardt, B. H. Belohradsky, U. Wintergerst, M. C. Velez, L. Leiva, R. Sorensen, N. Wulffraat, S. Blanche, F. D. Bushman, A. Fischer, and M. Cavazzana-Calvo.** 2008. Insertional oncogenesis in 4 patients after retrovirus-mediated gene therapy of SCID-X1. J Clin Invest.

71. **Hacker, U. T., F. M. Gerner, H. Buning, M. Hutter, H. Reichenspurner, M. Stangl, and M. Hallek.** 2001. Standard heparin, low molecular weight heparin, low molecular weight heparinoid, and recombinant hirudin differ in their ability to inhibit transduction by recombinant adeno-associated virus type 2 vectors. Gene Ther **8:**966-8.

72. **Hacker, U. T., L. Wingenfeld, D. M. Kofler, N. K. Schuhmann, S. Lutz, T. Herold, S. B. King, F. M. Gerner, L. Perabo, J. Rabinowitz, D. M. McCarty, R. J. Samulski, M. Hallek, and H. Buning.** 2005. Adeno-associated virus serotypes 1 to 5 mediated tumor cell directed gene transfer and improvement of transduction efficiency. J Gene Med.

73. **Hacker, U. T., L. Wingenfeld, D. M. Kofler, N. K. Schuhmann, S. Lutz, T. Herold, S. B. King, F. M. Gerner, L. Perabo, J. Rabinowitz, D. M. McCarty, R. J. Samulski, M. Hallek, and H. Buning.** 2005. Adeno-associated virus serotypes 1 to 5 mediated tumor cell directed gene transfer and improvement of transduction efficiency. J Gene Med **7:**1429-38.

74. **Halbert, C. L., J. M. Allen, and A. D. Miller.** 2001. Adeno-associated virus type 6 (AAV6) vectors mediate efficient transduction of airway epithelial cells in mouse lungs compared to that of AAV2 vectors. J Virol **75:**6615-24.

75. **Hanahan, D.** 1983. Studies on transformation of Escherichia coli with plasmids. J Mol Biol **166:**557-80.

76. **Handa, A., S. Muramatsu, J. Qiu, H. Mizukami, and K. E. Brown.** 2000. Adeno-associated virus (AAV)-3-based vectors transduce haematopoietic cells not susceptible to transduction with AAV-2-based vectors. J Gen Virol **81:**2077-84.

77. **Hansen, J., K. Qing, and A. Srivastava.** 2001. Adeno-associated virus type 2-mediated gene transfer: altered endocytic processing enhances transduction efficiency in murine fibroblasts. J Virol **75:**4080-90.

78. **Hansen, J., K. Qing, and A. Srivastava.** 2001. Infection of purified nuclei by adeno-associated virus 2. Mol Ther **4:**289-96.

79. **Hedley, S. J., A. Auf der Maur, S. Hohn, D. Escher, A. Barberis, J. N. Glasgow, J. T. Douglas, N. Korokhov, and D. T. Curiel.** 2006. An adenovirus vector with a chimeric fiber incorporating stabilized single chain antibody achieves targeted gene delivery. Gene Ther **13:**88-94.

80. **Heilbronn, R., J. R. Schlehofer, A. O. Yalkinoglu, and H. Zur Hausen.** 1985. Selective DNA-amplification induced by carcinogens (initiators): evidence for a role of proteases and DNA polymerase alpha. Int J Cancer **36:**85-91.

81. **Hensley, S. E., and A. Amalfitano.** 2007. Toll-like receptors impact on safety and efficacy of gene transfer vectors. Mol Ther **15:**1417-22.

82. **Hermonat, P. L.** 1989. The adeno-associated virus Rep78 gene inhibits cellular transformation induced by bovine papillomavirus. Virology **172:**253-61.

83. **Heuser, C., A. Hombach, C. Losch, K. Manista, and H. Abken.** 2003. T-cell activation by recombinant immunoreceptors: impact of the intracellular signalling domain on the stability of receptor expression and antigen-specific activation of grafted T cells. Gene Ther **10:**1408-19.

84. **Hoffmann, P., N. Mueller, J. E. Shively, B. Fleischer, and M. Neumaier.** 2001. Fusion proteins of B7.1 and a carcinoembryonic antigen (CEA)-specific antibody fragment opsonize CEA-expressing tumor cells and coactivate T-cell immunity. Int J Cancer **92:**725-32.

85. **Holliger, P., and P. J. Hudson.** 2005. Engineered antibody fragments and the rise of single domains. Nat Biotechnol **23:**1126-36.

86. **Hombach, A., C. Pohl, U. Reinhold, and H. Abken.** 1999. Grafting T cells with tumor specificity: the chimeric receptor strategy for use in immunotherapy of malignant diseases. Hybridoma **18:**57-61.

87. **Hombach, A., C. Schneider, D. Sent, D. Koch, R. A. Willemsen, V. Diehl, W. Kruis, R. L. Bolhuis, C. Pohl, and H. Abken.** 2000. An entirely humanized CD3 zeta-chain signaling receptor that directs peripheral blood t cells to specific lysis of carcinoembryonic antigen-positive tumor cells. Int J Cancer **88:**115-20.

88. **Hoque, M., K. Ishizu, A. Matsumoto, S. I. Han, F. Arisaka, M. Takayama, K. Suzuki, K. Kato, T. Kanda, H. Watanabe, and H. Handa.** 1999. Nuclear transport of the major capsid protein is essential for adeno-associated virus capsid formation. J Virol **73:**7912-5.

89. **Huttner, N. A., A. Girod, L. Perabo, D. Edbauer, J. A. Kleinschmidt, H. Buning, and M. Hallek.** 2003. Genetic modifications of the adeno-associated virus type 2 capsid reduce the affinity and the neutralizing effects of human serum antibodies. Gene Ther **10:**2139-47.

90. **Im, D. S., and N. Muzyczka.** 1990. The AAV origin binding protein Rep68 is an ATP-dependent site-specific endonuclease with DNA helicase activity. Cell **61:**447-57.

91. **Inoue, N., and D. W. Russell.** 1998. Packaging cells based on inducible gene amplification for the production of adeno-associated virus vectors. J Virol **72:**7024-31.

92. **Kaludov, N., K. E. Brown, R. W. Walters, J. Zabner, and J. A. Chiorini.** 2001. Adeno-associated virus serotype 4 (AAV4) and AAV5 both require sialic acid binding for hemagglutination and efficient transduction but differ in sialic acid linkage specificity. J Virol **75:**6884-93.

93. **Kaludov, N., B. Handelman, and J. A. Chiorini.** 2002. Scalable purification of adeno-associated virus type 2, 4, or 5 using ion-exchange chromatography. Hum Gene Ther **13:**1235-43.

94. **Kapturczak, M. H., T. Flotte, and M. A. Atkinson.** 2001. Adeno-associated virus (AAV) as a vehicle for therapeutic gene delivery: improvements in vector design and viral production enhance potential to prolong graft survival in pancreatic islet cell transplantation for the reversal of type 1 diabetes. Curr Mol Med **1:**245-58.

95. **Kashiwakura, Y., K. Tamayose, K. Iwabuchi, Y. Hirai, T. Shimada, K. Matsumoto, T. Nakamura, M. Watanabe, K. Oshimi, and H. Daida.** 2005. Hepatocyte growth factor receptor is a coreceptor for adeno-associated virus type 2 infection. J Virol **79:**609-14.

96. **Kay, M. A., D. Liu, and P. M. Hoogerbrugge.** 1997. Gene therapy. Proc Natl Acad Sci U S A **94:**12744-6.

97. **Kern, A., K. Schmidt, C. Leder, O. J. Muller, C. E. Wobus, K. Bettinger, C. W. Von der Lieth, J. A. King, and J. A. Kleinschmidt.** 2003. Identification of a heparin-binding motif on adeno-associated virus type 2 capsids. J Virol **77:**11072-81.

98. **Khleif, S. N., T. Myers, B. J. Carter, and J. P. Trempe.** 1991. Inhibition of cellular transformation by the adeno-associated virus rep gene. Virology **181:**738-41.

99. **Kim, P. S., and R. L. Baldwin.** 1990. Intermediates in the folding reactions of small proteins. Annu Rev Biochem **59:**631-60.

100. **King, J. A., R. Dubielzig, D. Grimm, and J. A. Kleinschmidt.** 2001. DNA helicase-mediated packaging of adeno-associated virus type 2 genomes into preformed capsids. EMBO J **20:**3282-91.

101. **Knowles, B. B., C. C. Howe, and D. P. Aden.** 1980. Human hepatocellular carcinoma cell lines secrete the major plasma proteins and hepatitis B surface antigen. Science **209:**497-9.

102. **Koerber, J. T., J. H. Jang, J. H. Yu, R. S. Kane, and D. V. Schaffer.** 2007. Engineering adeno-associated virus for one-step purification via immobilized metal affinity chromatography. Hum Gene Ther **18:**367-78.

103. **Kotin, R. M., R. M. Linden, and K. I. Berns.** 1992. Characterization of a preferred site on human chromosome 19q for integration of adeno-associated virus DNA by non-homologous recombination. EMBO J **11:**5071-8.

104. **Kramer, R. M., and J. D. Sharp.** 1997. Structure, function and regulation of Ca2+-sensitive cytosolic phospholipase A2 (cPLA2). FEBS Lett **410:**49-53.

105. **Kronenberg, S., B. Bottcher, C. W. von der Lieth, S. Bleker, and J. A. Kleinschmidt.** 2005. A conformational change in the adeno-associated virus type 2 capsid leads to the exposure of hidden VP1 N termini. J Virol **79:**5296-303.

106. **Kyostio, S. R., R. A. Owens, M. D. Weitzman, B. A. Antoni, N. Chejanovsky, and B. J. Carter.** 1994. Analysis of adeno-associated virus (AAV) wild-type and mutant Rep proteins for their abilities to negatively regulate AAV p5 and p19 mRNA levels. J Virol **68:**2947-57.

107. **Labow, M. A., and K. I. Berns.** 1988. The adeno-associated virus rep gene inhibits replication of an adeno-associated virus/simian virus 40 hybrid genome in cos-7 cells. J Virol **62:**1705-12.

108. **Laughlin, C. A., J. D. Tratschin, H. Coon, and B. J. Carter.** 1983. Cloning of infectious adeno-associated virus genomes in bacterial plasmids. Gene **23:**65-73.

109. **Linden, R. M., P. Ward, C. Giraud, E. Winocour, and K. I. Berns.** 1996. Site-specific integration by adeno-associated virus. Proc Natl Acad Sci U S A **93:**11288-94.

110. **Liu, X. L., K. R. Clark, and P. R. Johnson.** 1999. Production of recombinant adeno-associated virus vectors using a packaging cell line and a hybrid recombinant adenovirus. Gene Ther **6:**293-9.

111. **Loiler, S. A., T. J. Conlon, S. Song, Q. Tang, K. H. Warrington, A. Agarwal, M. Kapturczak, C. Li, C. Ricordi, M. A. Atkinson, N. Muzyczka, and T. R. Flotte.** 2003. Targeting recombinant adeno-associated virus vectors to enhance gene transfer to pancreatic islets and liver. Gene Ther **10:**1551-8.

112. **Lusby, E. W., and K. I. Berns.** 1982. Mapping of the 5' termini of two adeno-associated virus 2 RNAs in the left half of the genome. J Virol **41:**518-26.

113. **Lux, K., N. Goerlitz, S. Schlemminger, L. Perabo, D. Goldnau, J. Endell, K. Leike, D. M. Kofler, S. Finke, M. Hallek, and H. Buning.** 2005. Green fluorescent protein-tagged adeno-associated virus particles allow the study of cytosolic and nuclear trafficking. J Virol **79:**11776-87.

114. **Maguire, A. M., F. Simonelli, E. A. Pierce, E. N. Pugh, Jr., F. Mingozzi, J. Bennicelli, S. Banfi, K. A. Marshall, F. Testa, E. M. Surace, S. Rossi, A. Lyubarsky, V. R. Arruda, B. Konkle, E. Stone, J. Sun, J. Jacobs, L. Dell'osso, R. Hertle, J. X. Ma, T. M. Redmond, X. Zhu, B. Hauck, O. Zelenaia, K. S. Shindler, M. G. Maguire, J. F. Wright, N. J. Volpe, J. W. McDonnell, A. Auricchio, K. A. High, and J. Bennett.** 2008. Safety and Efficacy of Gene Transfer for Leber's Congenital Amaurosis. N Engl J Med.

115. **Maheshri, N., J. T. Koerber, B. K. Kaspar, and D. V. Schaffer.** 2006. Directed evolution of adeno-associated virus yields enhanced gene delivery vectors. Nat Biotechnol **24:**198-204.

116. **Manno, C. S., G. F. Pierce, V. R. Arruda, B. Glader, M. Ragni, J. J. Rasko, M. C. Ozelo, K. Hoots, P. Blatt, B. Konkle, M. Dake, R. Kaye, M. Razavi, A. Zajko, J. Zehnder, P. K. Rustagi, H. Nakai, A. Chew, D. Leonard, J. F. Wright, R. R. Lessard, J. M. Sommer, M. Tigges, D. Sabatino, A. Luk, H. Jiang, F. Mingozzi, L. Couto, H. C. Ertl, K. A. High, and M. A. Kay.** 2006. Successful transduction of liver in hemophilia by AAV-Factor IX and limitations imposed by the host immune response. Nat Med **12:**342-7.

117. **Marchler-Bauer, A., J. B. Anderson, P. F. Cherukuri, C. DeWeese-Scott, L. Y. Geer, M. Gwadz, S. He, D. I. Hurwitz, J. D. Jackson, Z. Ke, C. J. Lanczycki, C. A. Liebert, C. Liu, F. Lu, G. H. Marchler, M. Mullokandov, B. A. Shoemaker, V. Simonyan, J. S. Song, P. A. Thiessen, R. A. Yamashita, J. J. Yin, D. Zhang, and S. H. Bryant.** 2005. CDD: a Conserved Domain Database for protein classification. Nucleic Acids Res **33:**D192-6.

118. **Mayor, H. D., G. S. Houlditch, and D. M. Mumford.** 1973. Influence of adeno-associated satellite virus on adenovirus-induced tumours in hamsters. Nat New Biol **241:**44-6.

119. **Mayor, H. D., R. M. Jamison, L. E. Jordan, and J. L. Melnick.** 1965. Structure and Composition of a Small Particle Prepared from a Simian Adenovirus. J Bacteriol **90:**235-42.

120. **McCarty, D. M., D. J. Pereira, I. Zolotukhin, X. Zhou, J. H. Ryan, and N. Muzyczka.** 1994. Identification of linear DNA sequences that specifically bind the adeno-associated virus Rep protein. J Virol **68:**4988-97.

121. **McIntyre, M. C.** 2007. ASGT 10th Annual Meeting, Early-Bird Session 001 - Process Development for Gene Therapy Products: Who, What, When, Where and How?, Seattle.

122. **McLaughlin, S. K., P. Collis, P. L. Hermonat, and N. Muzyczka.** 1988. Adeno-associated virus general transduction vectors: analysis of proviral structures. J Virol **62:**1963-73.

123. **Molnar, E., J. Prechl, A. Isaak, and A. Erdei.** 2003. Targeting with scFv: immune modulation by complement receptor specific constructs. J Mol Recognit **16:**318-23.

124. **Monahan, P. E., and R. J. Samulski.** 2000. AAV vectors: is clinical success on the horizon? Gene Ther **7:**24-30.

125. **Monahan, P. E., and R. J. Samulski.** 2000. Adeno-associated virus vectors for gene therapy: more pros than cons? Mol Med Today **6:**433-40.

126. **Mori, S., L. Wang, T. Takeuchi, and T. Kanda.** 2004. Two novel adeno-associated viruses from cynomolgus monkey: pseudotyping characterization of capsid protein. Virology **330:**375-83.

127. **Moskalenko, M., L. Chen, M. van Roey, B. A. Donahue, R. O. Snyder, J. G. McArthur, and S. D. Patel.** 2000. Epitope mapping of human anti-adeno-associated virus type 2 neutralizing antibodies: implications for gene therapy and virus structure. J Virol **74:**1761-6.

128. **Muller, O. J., F. Kaul, M. D. Weitzman, R. Pasqualini, W. Arap, J. A. Kleinschmidt, and M. Trepel.** 2003. Random peptide libraries displayed on adeno-associated virus to select for targeted gene therapy vectors. Nat Biotechnol **21:**1040-6.

129. **Muzyczka, N.** 1992. Use of adeno-associated virus as a general transduction vector for mammalian cells. Curr Top Microbiol Immunol **158:**97-129.

130. **Nicklin, S. A., H. Buening, K. L. Dishart, M. de Alwis, A. Girod, U. Hacker, A. J. Thrasher, R. R. Ali, M. Hallek, and A. H. Baker.** 2001. Efficient and selective AAV2-mediated gene transfer directed to human vascular endothelial cells. Mol Ther **4:**174-81.

131. **NIH.** 2007. RAC meeting on June 19-21.

132. **O'Connell, P. J., V. Gerkis, and A. J. d'Apice.** 1991. Variable O-glycosylation of CD13 (aminopeptidase N). J Biol Chem **266:**4593-7.

133. **Ohno, K., and D. Meruelo.** 1997. Retrovirus vectors displaying the IgG-binding domain of protein A. Biochem Mol Med **62:**123-7.

134. **Ohno, K., K. Sawai, Y. Iijima, B. Levin, and D. Meruelo.** 1997. Cell-specific targeting of Sindbis virus vectors displaying IgG-binding domains of protein A. Nat Biotechnol **15:**763-7.

135. **Opie, S. R., K. H. Warrington, Jr., M. Agbandje-McKenna, S. Zolotukhin, and N. Muzyczka.** 2003. Identification of amino acid residues in the capsid proteins of adeno-associated virus type 2 that contribute to heparan sulfate proteoglycan binding. J Virol **77:**6995-7006.

136. **Ouzilou, L., E. Caliot, I. Pelletier, M. C. Prevost, E. Pringault, and F. Colbere-Garapin.** 2002. Poliovirus transcytosis through M-like cells. J Gen Virol **83:**2177-82.

137. **Pajusola, K., M. Gruchala, H. Joch, T. F. Luscher, S. Yla-Herttuala, and H. Bueler.** 2002. Cell-type-specific characteristics modulate the transduction efficiency of adeno-associated virus type 2 and restrain infection of endothelial cells. J Virol **76:**11530-40.

138. **Peitsch, M. C.** 1995. Protein modeling by e-mail. Nat Biotechnol **13:**658-660.

139. **Perabo, L., H. Buning, D. M. Kofler, M. U. Ried, A. Girod, C. M. Wendtner, J. Enssle, and M. Hallek.** 2003. In vitro selection of viral vectors with modified tropism: the adeno-associated virus display. Mol Ther **8:**151-7.

140. **Perabo, L., J. Endell, S. King, K. Lux, D. Goldnau, M. Hallek, and H. Buning.** 2006. Combinatorial engineering of a gene therapy vector: directed evolution of adeno-associated virus. J Gene Med **8:**155-62.

141. **Perabo, L., D. Goldnau, K. White, J. Endell, J. Boucas, S. Humme, L. M. Work, H. Janicki, M. Hallek, A. H. Baker, and H. Buning.** 2006. Heparan sulfate proteoglycan binding properties of adeno-associated virus retargeting mutants and consequences for their in vivo tropism. J Virol **80:**7265-9.

142. **Pereira, D. J., D. M. McCarty, and N. Muzyczka.** 1997. The adeno-associated virus (AAV) Rep protein acts as both a repressor and an activator to regulate AAV transcription during a productive infection. J Virol **71:**1079-88.

143. **Philpott, N. J., C. Giraud-Wali, C. Dupuis, J. Gomos, H. Hamilton, K. I. Berns, and E. Falck-Pedersen.** 2002. Efficient integration of recombinant adeno-associated virus DNA vectors requires a p5-rep sequence in cis. J Virol **76:**5411-21.

144.	**Philpott, N. J., J. Gomos, K. I. Berns, and E. Falck-Pedersen.** 2002. A p5 integration efficiency element mediates Rep-dependent integration into AAVS1 at chromosome 19. Proc Natl Acad Sci U S A **99:**12381-5.

145.	**Pohl, C., C. Renner, M. Schwonzen, I. Schobert, V. Liebenberg, W. Jung, J. Wolf, M. Pfreundschuh, and V. Diehl.** 1993. CD30-specific AB1-AB2-AB3 internal image antibody network: potential use as anti-idiotype vaccine against Hodgkin's lymphoma. Int J Cancer **54:**418-25.

146.	**Ponnazhagan, S., G. Mahendra, S. Kumar, J. A. Thompson, and M. Castillas, Jr.** 2002. Conjugate-based targeting of recombinant adeno-associated virus type 2 vectors by using avidin-linked ligands. J Virol **76:**12900-7.

147.	**Promochem, A.-L.** 2005, posting date. ATCC-LGC Promochem Partnership [Online.]

148.	**Puck, T. T., S. J. Cieciura, and A. Robinson.** 1958. Genetics of somatic mammalian cells. III. Long-term cultivation of euploid cells from human and animal subjects. J Exp Med **108:**945-56.

149.	**Qing, K., C. Mah, J. Hansen, S. Zhou, V. Dwarki, and A. Srivastava.** 1999. Human fibroblast growth factor receptor 1 is a co-receptor for infection by adeno-associated virus 2. Nat Med **5:**71-7.

150.	**Qiu, J., and K. E. Brown.** 1999. A 110-kDa nuclear shuttle protein, nucleolin, specifically binds to adeno-associated virus type 2 (AAV-2) capsid. Virology **257:**373-82.

151.	**Qu, G., J. Bahr-Davidson, J. Prado, A. Tai, F. Cataniag, J. McDonnell, J. Zhou, B. Hauck, J. Luna, J. M. Sommer, P. Smith, S. Zhou, P. Colosi, K. A. High, G. F. Pierce, and J. F. Wright.** 2007. Separation of adeno-associated virus type 2 empty particles from genome containing vectors by anion-exchange column chromatography. J Virol Methods **140:**183-92.

152.	**Rabinowitz, J. E., D. E. Bowles, S. M. Faust, J. G. Ledford, S. E. Cunningham, and R. J. Samulski.** 2004. Cross-dressing the virion: the transcapsidation of adeno-associated virus serotypes functionally defines subgroups. J Virol **78:**4421-32.

153.	**Rabinowitz, J. E., F. Rolling, C. Li, H. Conrath, W. Xiao, X. Xiao, and R. J. Samulski.** 2002. Cross-packaging of a single adeno-associated virus (AAV) type 2 vector genome into multiple AAV serotypes enables transduction with broad specificity. J Virol **76:**791-801.

154.	**Raj, K., P. Ogston, and P. Beard.** 2001. Virus-mediated killing of cells that lack p53 activity. Nature **412:**914-7.

155.	**Raper, S. E., N. Chirmule, F. S. Lee, N. A. Wivel, A. Bagg, G. P. Gao, J. M. Wilson, and M. L. Batshaw.** 2003. Fatal systemic inflammatory response syndrome in a ornithine transcarbamylase deficient patient following adenoviral gene transfer. Mol Genet Metab **80:**148-58.

156.	**Reddy, V. S., P. Natarajan, B. Okerberg, K. Li, K. V. Damodaran, R. T. Morton, C. L. Brooks, 3rd, and J. E. Johnson.** 2001. Virus Particle Explorer (VIPER), a website for virus capsid structures and their computational analyses. J Virol **75:**11943-7.

157.	**Redemann, B. E., E. Mendelson, and B. J. Carter.** 1989. Adeno-associated virus rep protein synthesis during productive infection. J Virol **63:**873-82.

158.	**Ren, M., G. Xu, J. Zeng, C. De Lemos-Chiarandini, M. Adesnik, and D. D. Sabatini.** 1998. Hydrolysis of GTP on rab11 is required for the direct delivery of transferrin from the pericentriolar recycling compartment to the cell surface but not from sorting endosomes. Proc Natl Acad Sci U S A **95:**6187-92.

159.	**Ried, M. U., A. Girod, K. Leike, H. Buning, and M. Hallek.** 2002. Adeno-associated virus capsids displaying immunoglobulin-binding domains permit antibody-mediated vector retargeting to specific cell surface receptors. J Virol **76:**4559-66.

160.	**Rolling, F., and R. J. Samulski.** 1995. AAV as a viral vector for human gene therapy. Generation of recombinant virus. Mol Biotechnol **3:**9-15.

161.	**Rubanyi, G. M.** 2001. The future of human gene therapy. Mol Aspects Med **22:**113-42.

162.	**Sambrook J, R. D.** 2001. Cesium chloride and chesium chloride equilibrium density gradients., p. 1.154-155, Molecular cloning: A laboratory manual. , 3rd ed. Cold Spring Harbor Laboratory Press, New York.

163.	**Samulski, R. J., K. I. Berns, M. Tan, and N. Muzyczka.** 1982. Cloning of adeno-associated virus into pBR322: rescue of intact virus from the recombinant plasmid in human cells. Proc Natl Acad Sci U S A **79:**2077-81.

164.	**Samulski, R. J., L. S. Chang, and T. Shenk.** 1987. A recombinant plasmid from which an infectious adeno-associated virus genome can be excised in vitro and its use to study viral replication. J Virol **61:**3096-101.

165.	**Sanlioglu, S., P. K. Benson, J. Yang, E. M. Atkinson, T. Reynolds, and J. F. Engelhardt.** 2000. Endocytosis and nuclear trafficking of adeno-associated virus type 2 are controlled by rac1 and phosphatidylinositol-3 kinase activation. J Virol **74:**9184-96.

166.	**Scherer, W. F., J. T. Syverton, and G. O. Gey.** 1953. Studies on the propagation in vitro of poliomyelitis viruses. IV. Viral multiplication in a stable strain of human malignant epithelial cells (strain HeLa) derived from an epidermoid carcinoma of the cervix. J Exp Med **97:**695-710.

167.   **Schmidt, M., A. Voutetakis, S. Afione, C. Zheng, D. Mandikian, and J. A. Chiorini.** 2008. Adeno-associated virus type 12 (AAV12): a novel AAV serotype with sialic acid- and heparan sulfate proteoglycan-independent transduction activity. J Virol **82:**1399-406.

168.   **Schwede, T., J. Kopp, N. Guex, and M. C. Peitsch.** 2003. SWISS-MODEL: An automated protein homology-modeling server. Nucleic Acids Res **31:**3381-5.

169.   **Seiler, M. P., A. D. Miller, J. Zabner, and C. L. Halbert.** 2006. Adeno-associated virus types 5 and 6 use distinct receptors for cell entry. Hum Gene Ther **17:**10-9.

170.   **Seisenberger, G., M. U. Ried, T. Endress, H. Buning, M. Hallek, and C. Brauchle.** 2001. Real-time single-molecule imaging of the infection pathway of an adeno-associated virus. Science **294:**1929-32.

171.   **Shi, W., G. S. Arnold, and J. S. Bartlett.** 2001. Insertional mutagenesis of the adeno-associated virus type 2 (AAV2) capsid gene and generation of AAV2 vectors targeted to alternative cell-surface receptors. Hum Gene Ther **12:**1697-711.

172.   **Shi, W., and J. S. Bartlett.** 2003. RGD inclusion in VP3 provides adeno-associated virus type 2 (AAV2)-based vectors with a heparan sulfate-independent cell entry mechanism. Mol Ther **7:**515-25.

173.   **Shi, X., G. Fang, and W. Shi.** 2006. Insertional mutagenesis at positions 520 and 584 of adeno-associated virus type 2 (AAV2) capsid gene and generation of AAV2 vectors with eliminated heparin-binding ability and introduced novel tropism. Hum Gene Ther **17:**353-61.

174.   **Shi, X., G. Fang, W. Shi, and J. S. Bartlett.** 2006. Insertional mutagenesis at positions 520 and 584 of adeno-associated virus type 2 (AAV2) capsid gene and generation of AAV2 vectors with eliminated heparin- binding ability and introduced novel tropism. Hum Gene Ther **17:**353-61.

175.   **Shipp, M. A., and A. T. Look.** 1993. Hematopoietic differentiation antigens that are membrane-associated enzymes: cutting is the key! Blood **82:**1052-70.

176.   **Snyder, R. O., D. S. Im, and N. Muzyczka.** 1990. Evidence for covalent attachment of the adeno-associated virus (AAV) rep protein to the ends of the AAV genome. J Virol **64:**6204-13.

177.   **Sonnichsen, B., S. De Renzis, E. Nielsen, J. Rietdorf, and M. Zerial.** 2000. Distinct membrane domains on endosomes in the recycling pathway visualized by multicolor imaging of Rab4, Rab5, and Rab11. J Cell Biol **149:**901-14.

178.   **Srivastava, A., E. W. Lusby, and K. I. Berns.** 1983. Nucleotide sequence and organization of the adeno-associated virus 2 genome. J Virol **45:**555-64.

179.   **Stachler, M. D., and J. S. Bartlett.** 2006. Mosaic vectors comprised of modified AAV1 capsid proteins for efficient vector purification and targeting to vascular endothelial cells. Gene Ther **13:**926-31.

180.   **Starovasnik, M. A., A. C. Braisted, and J. A. Wells.** 1997. Structural mimicry of a native protein by a minimized binding domain. Proc Natl Acad Sci U S A **94:**10080-5.

181.   **Summerford, C., J. S. Bartlett, and R. J. Samulski.** 1999. AlphaVbeta5 integrin: a co-receptor for adeno-associated virus type 2 infection. Nat Med **5:**78-82.

182.   **Summerford, C., and R. J. Samulski.** 1998. Membrane-associated heparan sulfate proteoglycan is a receptor for adeno-associated virus type 2 virions. J Virol **72:**1438-45.

183.   **Tal, J.** 2000. Adeno-associated virus-based vectors in gene therapy. J Biomed Sci **7:**279-91.

184.   **Tamayose, K., Y. Hirai, and T. Shimada.** 1996. A new strategy for large-scale preparation of high-titer recombinant adeno-associated virus vectors by using packaging cell lines and sulfonated cellulose column chromatography. Hum Gene Ther **7:**507-13.

185.   **Vafaie, J., and R. A. Schwartz.** 2004. Parvovirus B19 infections. Int J Dermatol **43:**747-9.

186.   **Vandenberghe, L. H., and J. M. Wilson.** 2007. AAV as an immunogen. Curr Gene Ther **7:**325-33.

187.   **Vellinga, J., J. de Vrij, S. Myhre, T. Uil, P. Martineau, L. Lindholm, and R. C. Hoeben.** 2007. Efficient incorporation of a functional hyper-stable single-chain antibody fragment protein-IX fusion in the adenovirus capsid. Gene Ther **14:**664-70.

188.   **Vincent, K. A., S. T. Piraino, and S. C. Wadsworth.** 1997. Analysis of recombinant adeno-associated virus packaging and requirements for rep and cap gene products. J Virol **71:**1897-905.

189.   **Warrington, K. H., Jr., O. S. Gorbatyuk, J. K. Harrison, S. R. Opie, S. Zolotukhin, and N. Muzyczka.** 2004. Adeno-associated virus type 2 VP2 capsid protein is nonessential and can tolerate large peptide insertions at its N terminus. J Virol **78:**6595-609.

190.   **Watson, J. D.** 1990. The human genome project: past, present, and future. Science **248:**44-9.

191.   **Weitzman, M. D., S. R. Kyostio, R. M. Kotin, and R. A. Owens.** 1994. Adeno-associated virus (AAV) Rep proteins mediate complex formation between AAV DNA and its integration site in human DNA. Proc Natl Acad Sci U S A **91:**5808-12.

192.   **White, S. J., S. A. Nicklin, H. Buning, M. J. Brosnan, K. Leike, E. D. Papadakis, M. Hallek, and A. H. Baker.** 2004. Targeted gene delivery to vascular tissue in vivo by tropism-modified adeno-associated virus vectors. Circulation **109:**513-9.

193.   **Wistuba, A., A. Kern, S. Weger, D. Grimm, and J. A. Kleinschmidt.** 1997. Subcellular compartmentalization of adeno-associated virus type 2 assembly. J Virol **71:**1341-52.

194. **Wistuba, A., S. Weger, A. Kern, and J. A. Kleinschmidt.** 1995. Intermediates of adeno-associated virus type 2 assembly: identification of soluble complexes containing Rep and Cap proteins. J Virol **69:**5311-9.
195. **Wolf, J. L., D. H. Rubin, R. Finberg, R. S. Kauffman, A. H. Sharpe, J. S. Trier, and B. N. Fields.** 1981. Intestinal M cells: a pathway for entry of reovirus into the host. Science **212:**471-2.
196. **Work, L. M., H. Buning, E. Hunt, S. A. Nicklin, L. Denby, N. Britton, K. Leike, M. Odenthal, U. Drebber, M. Hallek, and A. H. Baker.** 2006. Vascular bed-targeted in vivo gene delivery using tropism-modified adeno-associated viruses. Mol Ther **13:**683-93.
197. **Work, L. M., S. A. Nicklin, N. J. Brain, K. L. Dishart, D. J. Von Seggern, M. Hallek, H. Buning, and A. H. Baker.** 2004. Development of efficient viral vectors selective for vascular smooth muscle cells. Mol Ther **9:**198-208.
198. **Wu, P., W. Xiao, T. Conlon, J. Hughes, M. Agbandje-McKenna, T. Ferkol, T. Flotte, and N. Muzyczka.** 2000. Mutational analysis of the adeno-associated virus type 2 (AAV2) capsid gene and construction of AAV2 vectors with altered tropism. J Virol **74:**8635-47.
199. **Xiao, W., N. Chirmule, S. C. Berta, B. McCullough, G. Gao, and J. M. Wilson.** 1999. Gene therapy vectors based on adeno-associated virus type 1. J Virol **73:**3994-4003.
200. **Xiao, W., K. H. Warrington, Jr., P. Hearing, J. Hughes, and N. Muzyczka.** 2002. Adenovirus-facilitated nuclear translocation of adeno-associated virus type 2. J Virol **76:**11505-17.
201. **Xiao, X., J. Li, and R. J. Samulski.** 1998. Production of high-titer recombinant adeno-associated virus vectors in the absence of helper adenovirus. J Virol **72:**2224-32.
202. **Xie, Q., W. Bu, S. Bhatia, J. Hare, T. Somasundaram, A. Azzi, and M. S. Chapman.** 2002. The atomic structure of adeno-associated virus (AAV-2), a vector for human gene therapy. Proc Natl Acad Sci U S A **99:**10405-10.
203. **Xie, Q., T. Somasundaram, S. Bhatia, W. Bu, and M. S. Chapman.** 2003. Structure determination of adeno-associated virus 2: three complete virus particles per asymmetric unit. Acta Crystallogr D Biol Crystallogr **59:**959-70.
204. **Yakobson, B., T. A. Hrynko, M. J. Peak, and E. Winocour.** 1989. Replication of adeno-associated virus in cells irradiated with UV light at 254 nm. J Virol **63:**1023-30.
205. **Yakobson, B., T. Koch, and E. Winocour.** 1987. Replication of adeno-associated virus in synchronized cells without the addition of a helper virus. J Virol **61:**972-81.
206. **Yalkinoglu, A. O., H. Zentgraf, and U. Hubscher.** 1991. Origin of adeno-associated virus DNA replication is a target of carcinogen-inducible DNA amplification. J Virol **65:**3175-84.
207. **Yan, Z., R. Zak, G. W. Luxton, T. C. Ritchie, U. Bantel-Schaal, and J. F. Engelhardt.** 2002. Ubiquitination of both adeno-associated virus type 2 and 5 capsid proteins affects the transduction efficiency of recombinant vectors. J Virol **76:**2043-53.
208. **Yang, Q., M. Mamounas, G. Yu, S. Kennedy, B. Leaker, J. Merson, F. Wong-Staal, M. Yu, and J. R. Barber.** 1998. Development of novel cell surface CD34-targeted recombinant adenoassociated virus vectors for gene therapy. Hum Gene Ther **9:**1929-37.
209. **Zadori, Z., J. Szelei, M. C. Lacoste, Y. Li, S. Gariepy, P. Raymond, M. Allaire, I. R. Nabi, and P. Tijssen.** 2001. A viral phospholipase A2 is required for parvovirus infectivity. Dev Cell **1:**291-302.
210. **Zaiss, A. K., Q. Liu, G. P. Bowen, N. C. Wong, J. S. Bartlett, and D. A. Muruve.** 2002. Differential activation of innate immune responses by adenovirus and adeno-associated virus vectors. J Virol **76:**4580-90.
211. **Zolotukhin, S., B. J. Byrne, E. Mason, I. Zolotukhin, M. Potter, K. Chesnut, C. Summerford, R. J. Samulski, and N. Muzyczka.** 1999. Recombinant adeno-associated virus purification using novel methods improves infectious titer and yield. Gene Ther **6:**973-85.

Curriculum Vitae

Jorge Miguel Martins Boucas

Born on the 1st of June of 1982 in Lisbon, Portugal

Kuenstr. 42
50733 Koeln
Germany
Tel.: +49-178-1835002
E-Mail: mail@JorgeBoucas.com

Education

2005-2008	**Ph.D. Student** AAV-Vector Development Group, Internal Medicine I, University Hospital of Cologne, Germany PD Dr. Hildegard Buening Engineering AAV-2 Targeting Vectors: A New Insertion Site and scFv Driven Vectors Defense in October 2008
2004-2005	**Diploma student** AAV-Vector Development Group, Internal Medicine I, University Hospital of Cologne, Germany PD Dr. Hildegard Buening Anti-proliferative properties of Adeno-associated virus: Potential uses in cancer therapy Grade: 20
2000-2005	**Diploma in Biochemistry** Department of Chemistry and Biochemistry, Faculty of Sciences, University of Lisbon, Portugal Grade: 16
1997-2000	**High school, Natural Sciences** Escola Selecta Prof. Doutor Amadeu Andres, Lisbon, Portugal Grade: 18

Publications

Boucas J., Hombach A., Hallek M., Abken H. and Buning H. (2008). Construction of scFv-VP2 directed AAV-2 vectors. *Manuscript in preparation.*

Boucas J., Lux K., Huber A., Schievenbusch S., Perabo L., Quadt-Humme S., Odenthal M., Hallek M., Buning H. (2008). Engineering AAV-2 based targeting vectors using a new insertion site – 453 – and single point mutations. *J Gene Med, under review.*

Perabo L., **Boucas J.**, Coutelle O., Hallek M. and Buning H. 2008. Engineering of viral capsids to evade the host immune system. *In* R. Herzog (ed.), Immunology of Gene Therapy. John Wiley & Sons. *In press.*

Perabo L. Goldnau D., White K., Endell J., **Boucas J.**, Humme S., Work L.M., Janicki H., Hallek M., Backer A.H. and Buning H. (2006). Heparan sulfate proteoglycan binding properties of adeno-associated virus retargeting mutants and consequences for their in vivo tropism. *J Virol* 80(14), 7265-9.

Patents

PCT/EP2008/004368; Buening H., Lux K., Nieland J., **Boucas J.**, Ritter M., Hoerer M., (2008) Mutated structural protein of a parvovirus. World Intellectual Property Organization

Presentations at meetings

German Society of Gene Therapy 14th annual meeting, Heidelberg, Germany (2007)
> **Poster presentation**: Targeting of angiogenic endothelial cells using a new AAV-2 insertion site

American Society of Gene Therapy 10th annual meeting, Seattle, USA (2007)
> **Poster presentation**: Targeting of angiogenic endothelial cells using a new AAV-2 insertion site

Training
Basic research in Flow Cytometry, 3 days course at Becton Dickinson, Heidelberg, Germany (2007)

Languages

Portuguese	Mother tongue
English	Fluent in speaking and writing
German	Good in speaking, basic in writing

Other professional experiences

2003   Data operator and treatment of statistic data; control and identification of logistic related issues.
Reckitt Benckiser Portugal Lda

2003   Auditor, 3rd secretary; control of customer contracts and national stock of gas cylinders.
ESSO Portuguesa Lda

Other qualifications / hobbies
Professor of Kung-Fu TOA
Painting (12.7 x 8.9 cm, postcards)

References

Prof. Dr. Michael Hallek   *Department director*
Director of the German CLL Study Group; Director of the Center for Integrated Oncology and Director of the Department of Internal Medicine I, University Hospital of Cologne, Germany
Tel.: +49-221-4784400
michael.hallek@uk-koeln.de

PD Dr. Hildegard Buening   *Lab head*
AAV-Vector Development Group, Internal Medicine I, University Hospital of Cologne, Germany
Tel.: +49-221-4784448
hildegard.buening@uk-koeln.de

Prof. Dr. Margarida Amaral   *Former professor (2000-05)*
Centre of Human Genetics, Center for Biodiversity, Functional & Integrative Genomics, Portuguese National Institute of Health; Department of Chemistry and Biochemistry, Faculty of Sciences, University of Lisbon, Portugal
Tel.: +351-21-7508155 (am); +351-21-7500861 (pm)
mdamaral@fc.ul.pt

Prof. Dr. Ulrike Protzer   *Head of collaborator group*
Director of the Institute of Virology, Technical University Munich / Helmholtz Center Munich, Germany
Tel.: +49-89-41406821
protzer@helmholtz-muenchen.de

Jorge Boucas

Cologne, 19th of August 2008